NASA Technical Memorandum 81331

A Comparison of Theoretical and Experimental Pressure Distributions for Two Advanced Fighter Wings

H. P. Haney and R. M. Hicks

October 1981

NASA
National Aeronautics and
Space Administration

NASA Technical Memorandum 81331

A Comparison of Theoretical and Experimental Pressure Distributions for Two Advanced Fighter Wings

H. P. Haney, Vought Corporation, Dallas, Texas
R. M. Hicks, Ames Research Center, Moffett Field, California

NASA
National Aeronautics and
Space Administration

Ames Research Center
Moffett Field, California 94035

NOMENCLATURE

c	chord, m
C_p	pressure coefficient, $\frac{P_l - P_\infty}{q_\infty}$
C_L	wing lift coefficint
CLL	section lift coefficient
M	Mach number
P	pressure, N/m^2
q	dynamic pressure, N/m^2
Re	Reynolds number
X	chordwise distance, m
ALPHA	angle of attack, deg
ETA	nondimensional spanwise distance

Subscripts:

l	local
∞	free stream

A COMPARISON OF THEORETICAL AND EXPERIMENTAL PRESSURE DISTRIBUTIONS FOR TWO ADVANCED FIGHTER WINGS

H. P. Haney
Vought Corporation, Dallas, Texas

and

R. M. Hicks
Ames Research Center, NASA

SUMMARY

A comparison was made between experimental pressure distributions measured during testing of the Vought A-7 fighter and the theoretical predictions of four transonic potential flow codes. Isolated wing and three wing-body codes were used for comparison. All comparisons are for transonic Mach numbers and include both attached and separate flows.

In general, the wing-body codes gave better agreement with the experiment than did the isolated wing code but, because of the greater complexity of the geometry, were found to be considerably more expensive and less reliable.

INTRODUCTION

The past 10 years has seen the development of numerous transonic-flow analysis codes based on finite difference solutions of the exact potential and small disturbance equations. The most widely used of these codes are those developed by Jameson and Caughey (refs. 1 and 2); FL022, the most reliable of these codes, computes the flow about an isolated wing on a wall. FL022 has been used extensively in the design of advanced wings for transonic aircraft. Data from two such wings designed for the Vought A-7 fighter are compared with theoretical calculations from four different transonic codes to show the strengths and weaknesses of each code. The two wings were designed during a cooperative study involving the Vought Corp., the David Taylor Naval Ship Research and Development Center, and the Ames Research Center. During the cooperative study a wing design code was developed by coupling FL022 with a numerical optimization algorithm (ref. 3). This report will demonstrate that wing design for transonic aircraft by use of isolated wing codes may lead to unsatisfactory results if the aircraft has a low fineness ratio fuselage.

FL022 COMPARISON WITH EXPERIMENT

FL022 is a full potential, non-conservative, transonic analysis code which uses an explicit, square root transformation to map an isolated wing to a "bump" on a plane.

Theoretically predicted pressure distributions from FL022 disagreed significantly from test data at the wing design condition, 0.85 Mach number and $0.30C_L$ (fig. 1). The

wing performed satisfactorily; but when compared with the original A-7, underprediction of shock strength may have resulted in premature drag divergence. Possible causes of this disagreement were identified as code approximations, isolated wing limitations, boundary layer analysis approximations, and test inaccuracies.

A strip boundary layer displacement thickness computed for the design pressure distribution was added to the wing geometry during both design and analysis which introduced an error into the theoretical calculations because the experimental spanwise pressures differ from the design pressures which resulted in an improper displacement thickness. In order to assess this error, FL022NM predictions were compared with the experiment (fig. 2). FL022NM combines Jameson's FL022 code with a Nash-McDonald boundary layer analysis. Displacement thicknesses were computed for each spanwise strip and updated as the solution converged. FL022NM predictions were somewhat closer to the experiment than FL022 pressures, but the strong experimental shock was still not predicted. A comparison of FL022 and FL022NM pressures is shown in figure 3.

FL028 COMPARISON WITH EXPERIMENT

FL028 is a full potential, fully conservative, transonic analysis code developed by Jameson (ref. 3). The code uses the finite volume approach and solves for the flow about a wing in the presence of a finite body. The body is mapped to a vertical slit by use of a generalized Joukowsky transformation.

The A-7 body with a 12% thick supercritical wing was analyzed using FL028 on the NASA Ames CDC 7600 computer. Initial solutions were remarkably bad. Wing pressures were characterized by chordwise oscillations. Comparable irregularities and discontinuities were seen in the wing mapped surface coordinates at the root and tip. Since the correctly input wing-body geometry caused unsmooth transformed coordinates, it was obvious that some compromise in the geometric representation would be required. The body was modified because of its incompatibility with the code approximations. The Joukowsky transformation had difficulty mapping the A-7 body which has a nearly rectangular fuselage. Progressive rounding of the body corners had a smoothing effect on the root and tip mapped coordinates and on the resultant pressures. A slight lowering of the A-7 high wing was required by this body modification. These geometry changes smoothed wing pressures, but oscillations were still so bad that it was impossible to compare the theory with experiment.

It seems illogical that smoothing the mapped surface coordinates had not caused a more pronounced improvement in the wing pressures. The code was modified to plot mapped coordinates at every computational station instead of only the root and tip. While the earlier changes had smoothed the root and tip, intermediate span stations were still very irregular – particularly in the 30%-40% semi-span region. While the use of a circular fuselage model seemed the easiest fix, wing height changes were tried first. It was found that even a slight lowering of the wing relative to the body made dramatic improvements in smoothing the mapped coordinates. The best results were achieved with a mid-wing position on the fuselage with slightly rounded corners. Adjusting input geometry to achieve a criteria of smooth mapped coordinates may lack mathematical rigor, but it does produce improved results. Further, it is a relatively easy to use criterion and is not dependent upon agreement of theory with a particular set of test data.

FL022 and early FL028 comparisons with experiment showed better agreement if the theory was run at a slightly higher Mach number than the test data. Other investigators had reached this conclusion. The best agreement with 0.85 Mach number experimental pressures was achieved with theoretical data run at 0.86 Mach number. It was hypothesized that this relatively large Mach shift might indicate a small experimental calibration error. In retrospect, after making comparisons with other codes, this reasoning appears specious.

Once a satisfactory input geometry was achieved, analyses were run at experimental lift conditions. The theory was run at approximately one degree higher angle-of-attack in order to match the test lift. Each analysis was run 50 iterations on the crude and medium grids, and 250 iterations on a fine grid of 160 × 16 × 28. A typical average residual was converged to 2×10^{-6}. Each run required approximately 1700 sec of CDC 7600 time. A few runs were executed an additional 250 iterations on the fine grid, doubling the run time and reducing the average residual to 0.6×10^{-6}, while having little effect on the pressures. The tip shock was strengthened and moved aft very slightly, but pressures over most of the wing were unchanged.

FL028 wing pressure predictions are compared with the experiment at 0.34 C_L, the wing design condition (fig. 4). Some mild upper surface pressure oscillations are evident from the wing root to mid-span. Agreement of shock strength and position is very good. At 0.515 C_L, agreement is equally good except near the tip where the experimental shock has shifted forward (fig. 5). Oil flow photographs indicate that there is probably some trailing-edge separation outboard of 90% semi-span at this lift. Shock induced separation has spread to mid-span at the next higher lift coefficient 0.63 (fig. 6). It is interesting to note that small oscillations in experimental upper surface pressures appear to have a correspondence with theoretical oscillations.

FL028 wing-body predictions show much closer agreement with the experiment than do FL022 isolated wing predictions. Is this difference caused by body effects or by differences in the two codes? FL028 was run with an isolated wing in order to investigate this question. Isolated wing pressures are compared with test data for 0.34 C_L and 0.515 C_L in figures 7 and 8. Notice that pressure oscillations are no longer present. Both FL028 and FL022 predict similar pressure distribution for an isolated wing although FL028 predicts a slightly stronger shock. It appears that the improved experiment-theory correlation observed with FL028 is due to the inclusion of body effects rather than code differences.

FL030 COMPARISON WITH EXPERIMENT

FL030 is a finite volume wing-body transonic analysis code developed by Caughey (ref. 2). This code uses body oriented coordinates instead of the Joukowsky transformation of FL028. Geometry input for the 12% wing was identical to FL028 input except the nose was not closed and the wing was raised back to its original high position on the fuselage (fig. 9). A 9% thick supercritical wing was also investigated.

No geometry problems were encountered in running FL030. Most analyses were run 200 iterations on a crude grid and 200 iterations on a moderate grid of 80 × 12 × 16 points. One solution was run an additional 200 iterations on a fine grid, 160 × 24 × 32. The fine grid solution showed very little pressure change over the moderate grid solution except at the leading edge (fig. 10) yet required four

times the computer time (3720 sec vs 950 sec). A pressure spike approximately two chord lengths aft of the wing root trailing edge was evident on all runs. While it is not clear that this anomaly degraded pressures on the wing, there is an obvious error in the code.

Theory and experiment are compared for the 9% thick wing-body configuration in figures 11 through 13 for 0.28 C_L, 0.416 C_L, and 0.57 C_L. Agreement is generally good prior to separation except near the tip. Model manufacturing errors may account for pressure differences at the tip and at the leading-edge near mid-span. The effect of a 0.01 Mach number change on FL030 wing pressures is shown in figure 14. The differences are concentrated in the vicinity of the shock and are largest near the tip.

Comparison of theory with experiment for the 12% thick wing is presented in figure 15 for the design condition. Agreement is good, with the largest errors being in the predicted shock strength at 0.4 semi-span and shock position at 0.88 semi-span. Results at 0.52 C_L are shown in figure 16. As discussed earlier, some trailing-edge separation exists for this condition at the wing tip.

Although both FL028 and FL030 show good agreement with the experiment, significant differences exist between predicted pressures (fig. 17). The wing input geometry was identical for both codes. FL030 was easier to use for the configurations investigated and did not require angle-of-attack adjustments to match experimental lift.

WIBCO COMPARISON WITH EXPERIMENT

WIBCO is a small perturbation transonic wing-body analysis code written by Boppe (ref. 4). A two-dimensional boundary layer subroutine is linked to this code which adds a displacement thickness to the wing geometry and updates it at specified intervals. The 12% thick supercritical wing was analyzed using WIBCO on NASA Langley's CYBER 175 computer. In order to save time, the wing was run on a circular fuselage in a mid-wing position.

Predicted pressures are compared with the experiment at 0.34 C_L and 0.52 C_L in figures 18 and 19. Theory was run at the test angles-of-attack. Agreement is surprisingly good considering the geometric and code approximations.

Isolated wing and wing-body predictions are compared in figure 20. Relatively little difference is seen between isolated wing and wing-body predicted pressures except at the root. Significant differences were predicted by FL028 across the entire span.

CONCLUSIONS

Three wing-body analysis codes have been evaluated by comparing predicted wing pressure distributions with experiment. All three codes show significant improvement over the isolated wing code, FL022. FL028 was very difficult to use for the particular fuselage analyzed. FL030 was much easier to use than FL028 but was more expensive. The simplest method evaluated, WIBCO, gave very good results without excessive

run times. Unfortunately, all codes investigated are too expensive to be used for extensive design perturbations.

ACKNOWLEDGMENT

Contract monitor for this study was Mr. Paul Scheurich, DTNSRDC. Dr. Jerry South, Theoretical Aerodynamics Branch of NASA Langley Research Center, made computer time available for WIBCO analyses. Mr. Ed Waggoner assisted in running the WIBCO code.

1. Jameson, Antony; and Caughey, D. A.: Numerical Calculation of the Flow Past a Swept Wing. ERDA Report COO-3077-140, June 1977.

2. Caughey, D. A.; and Jameson, A.: Recent Progress in Finite-Volume Calculations for Wing-Fuselage Combinations. AIAA Paper 79-2523, 23th Fluid and Plasma Dynamics Conference, July 1979.

3. Haney, H. P.; and Johnson, R. R.: Application of Numerical Optimization to the Design of Wings with Specified Pressure Distributions. NASA CR-3238, February 1980.

4. Boppe, C. W.: Calculation of Transonic Wing Flows by Grid Embedding. AIAA Paper 77-207, January 1977.

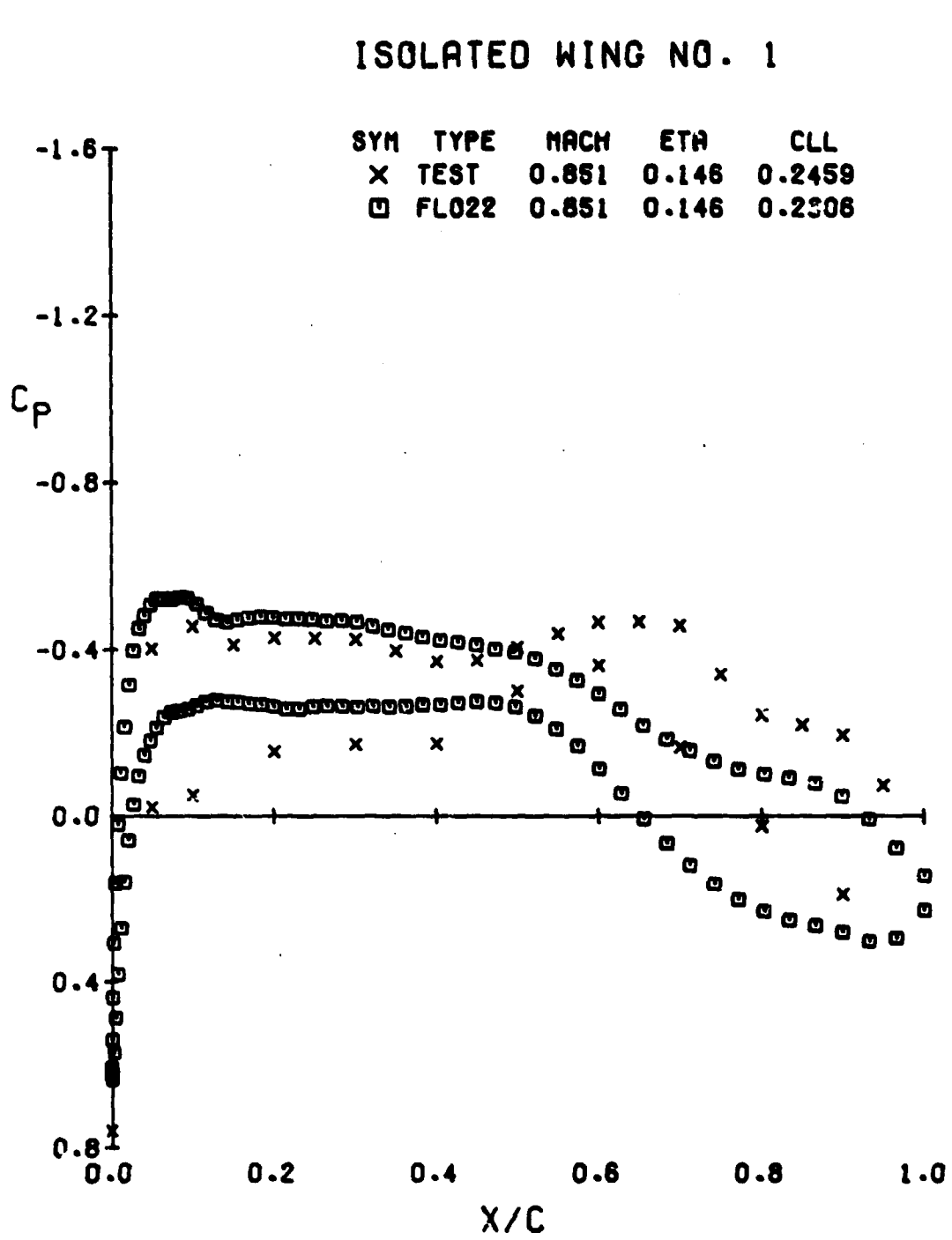

(A) ETA = 0.146

FIGURE 1.- COMPARISON OF FLO22 WING PRESSURES WITH EXPERIMENT

ALPHA = 4.68 CL = .34

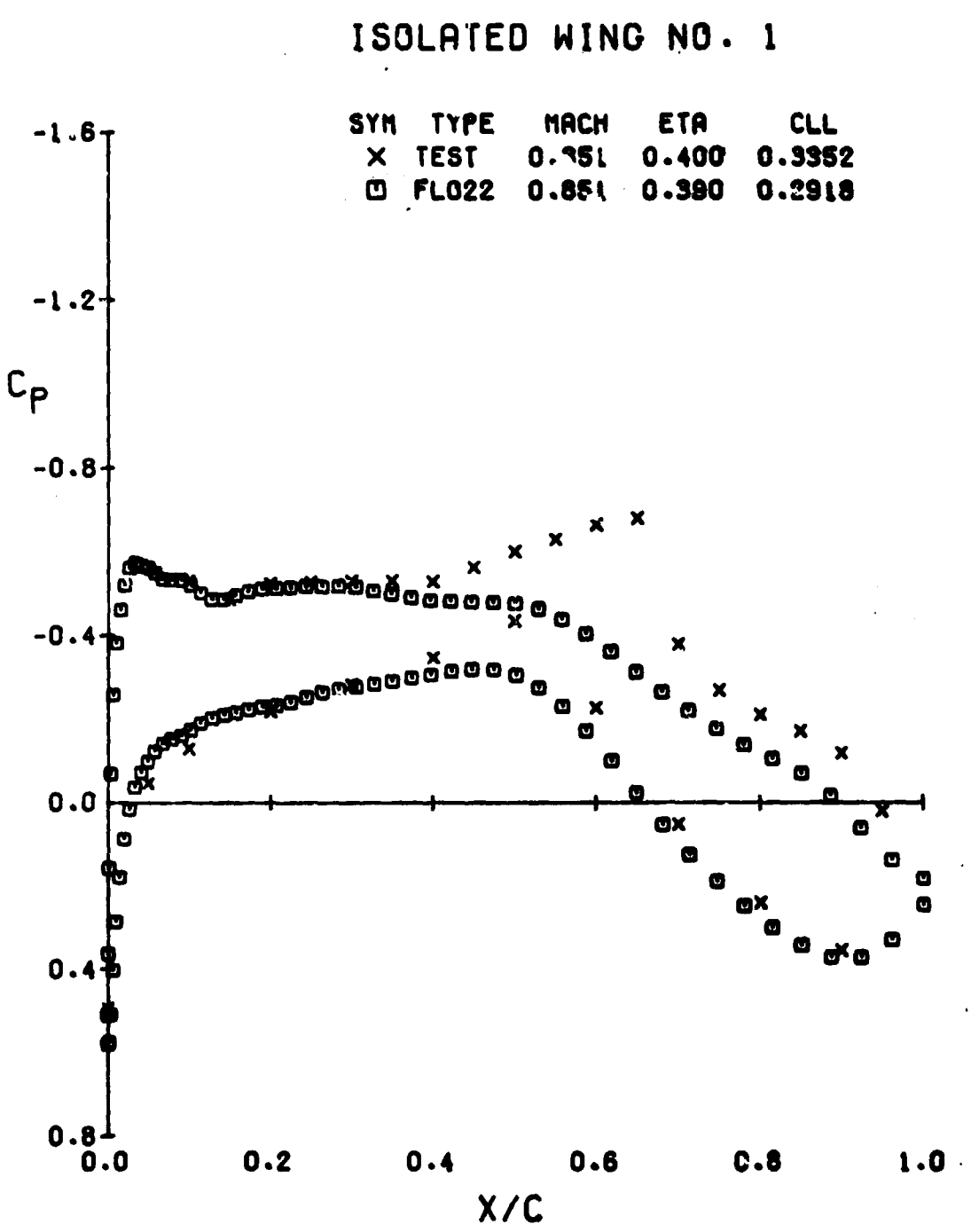

(B) ETA = 0.400

FIGURE 1.- CONTINUED

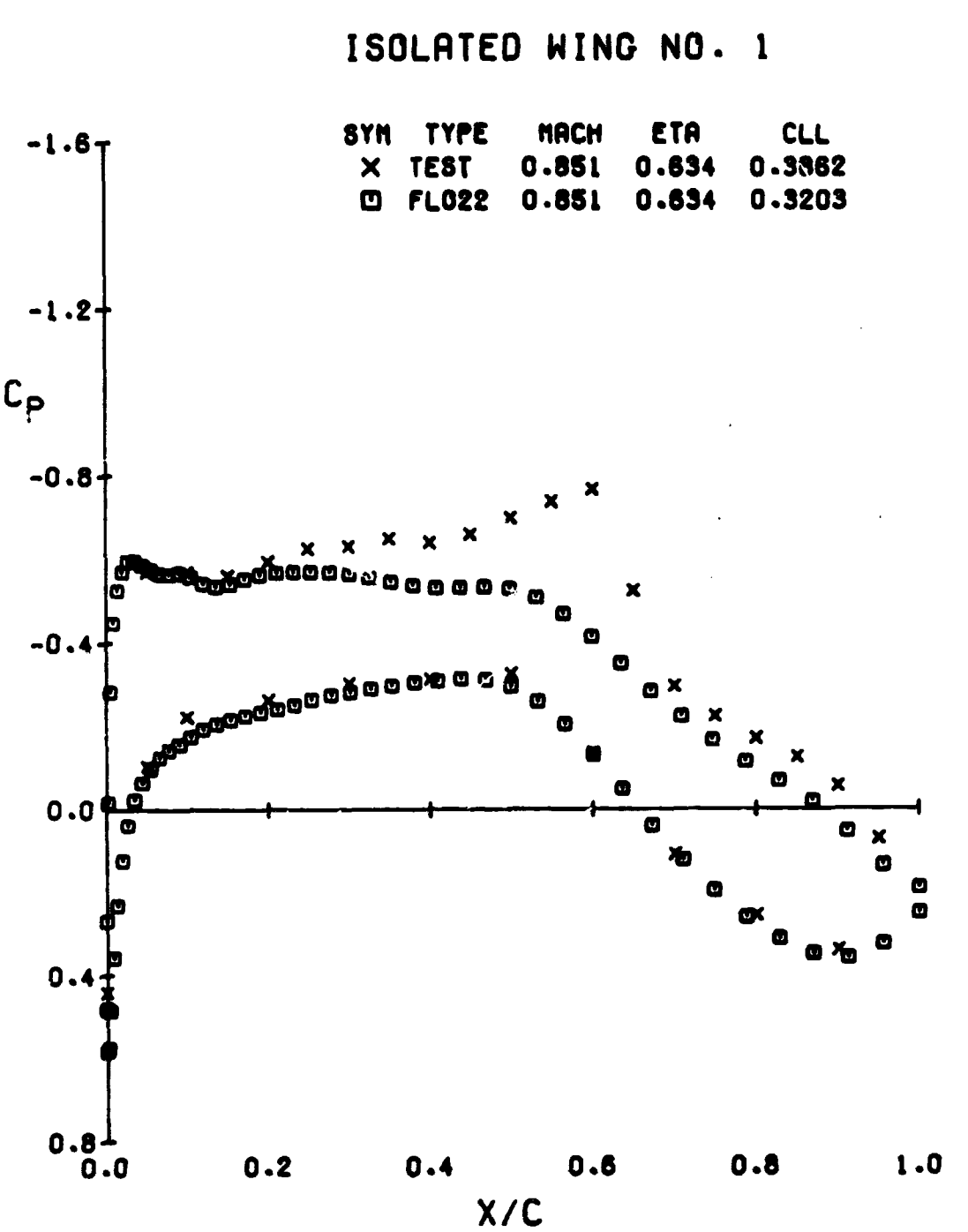

(C) ETA = 0.634

FIGURE 1.- CONTINUED

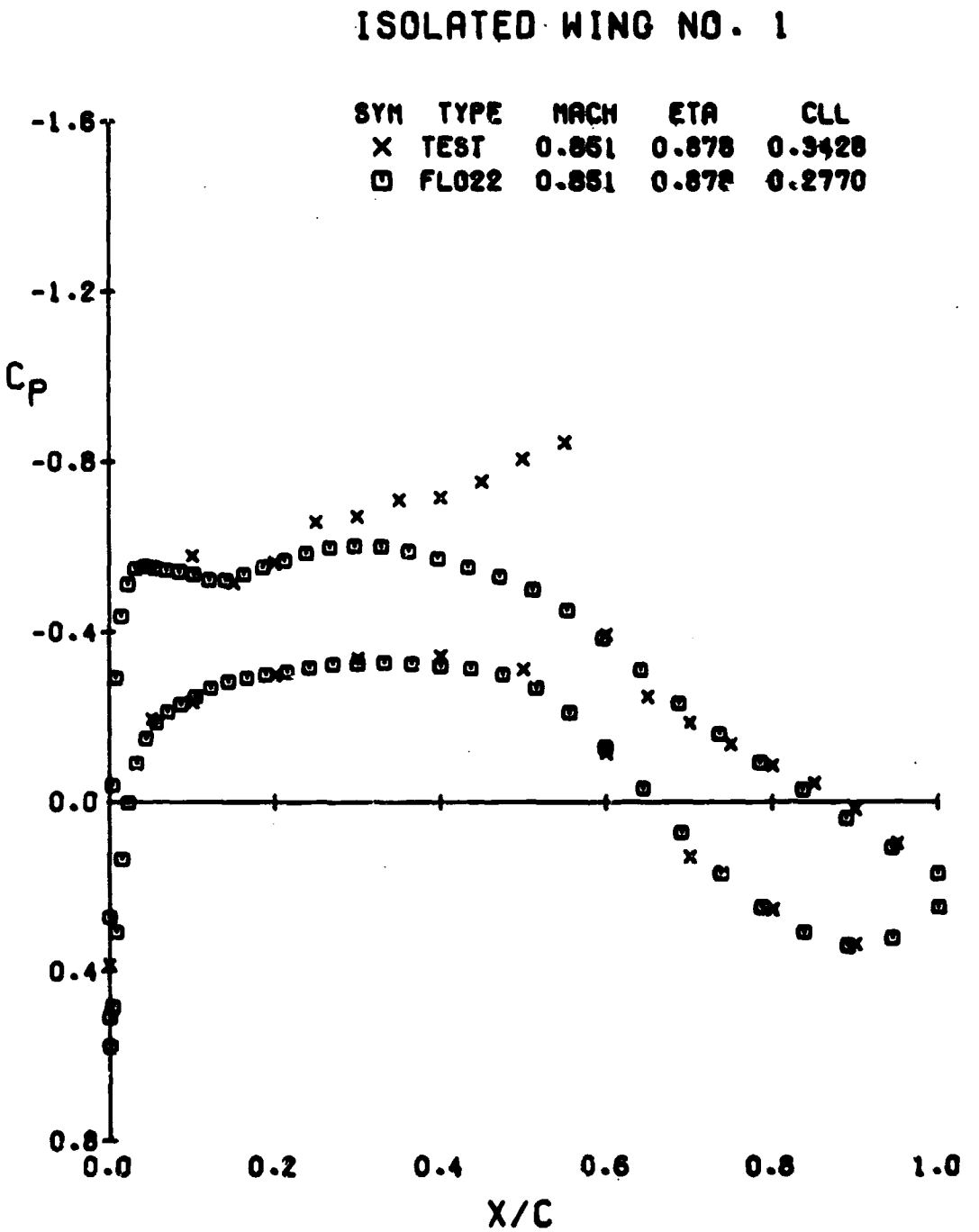

(D) ETA = 0.878

FIGURE 1.- CONCLUDED

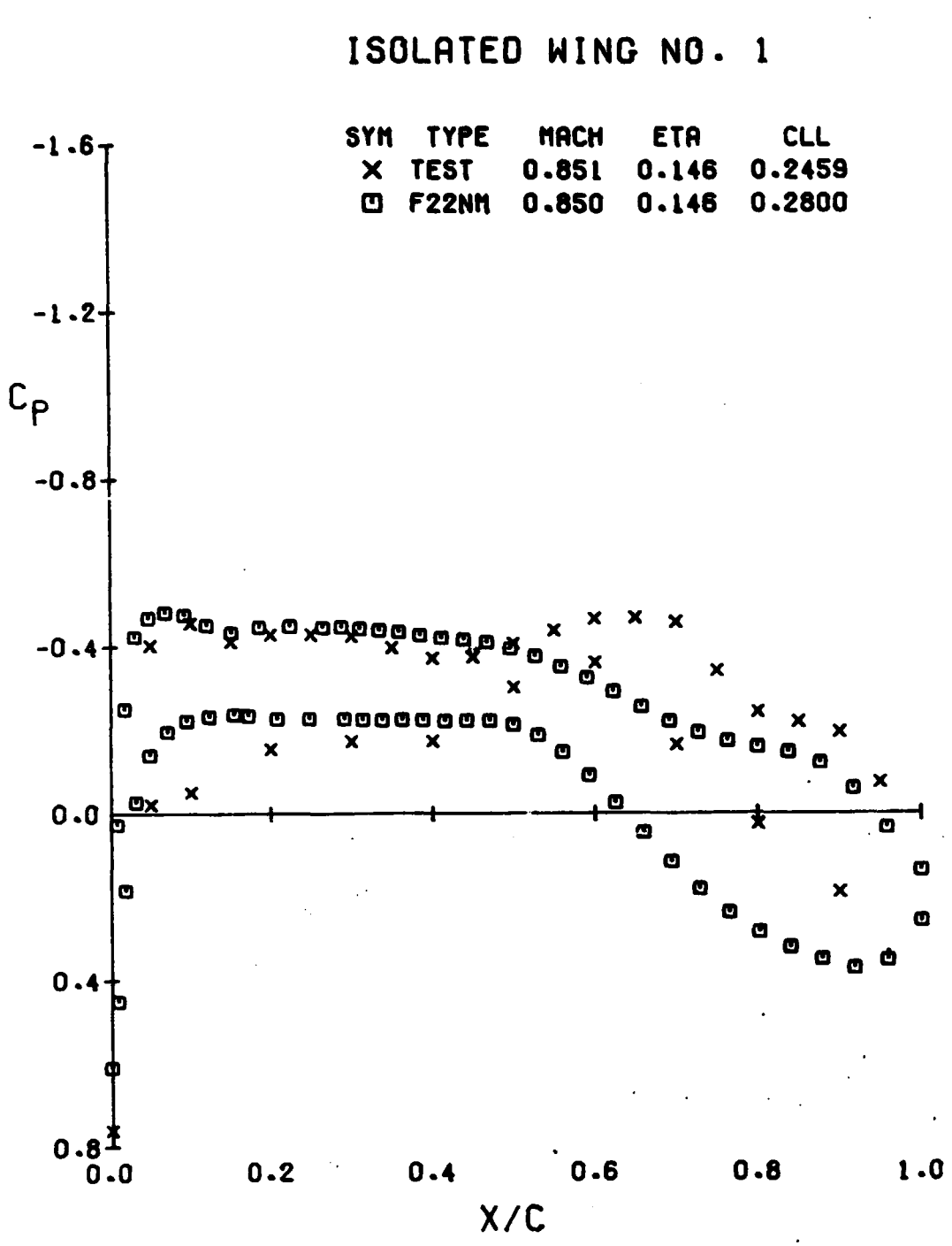

(A) ETA = 0.14S

FIGURE 2.- COMPARISON OF FL022NM WING PRESSURES WITH EXPERIMENT

ALPHA = 4.68 CL(EXP) = .34

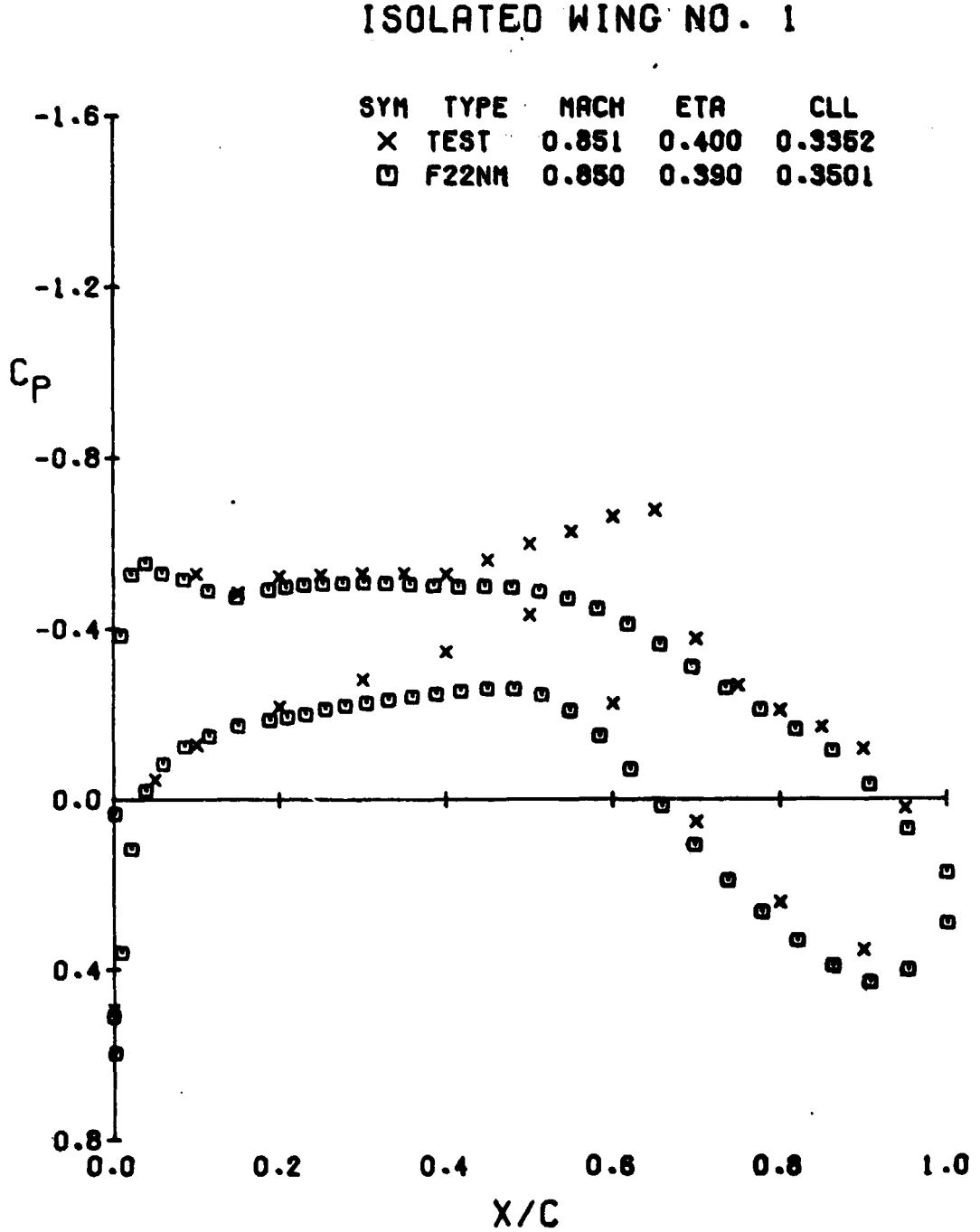

(B) ETA = 0.400

FIGURE 2.- CONTINUED

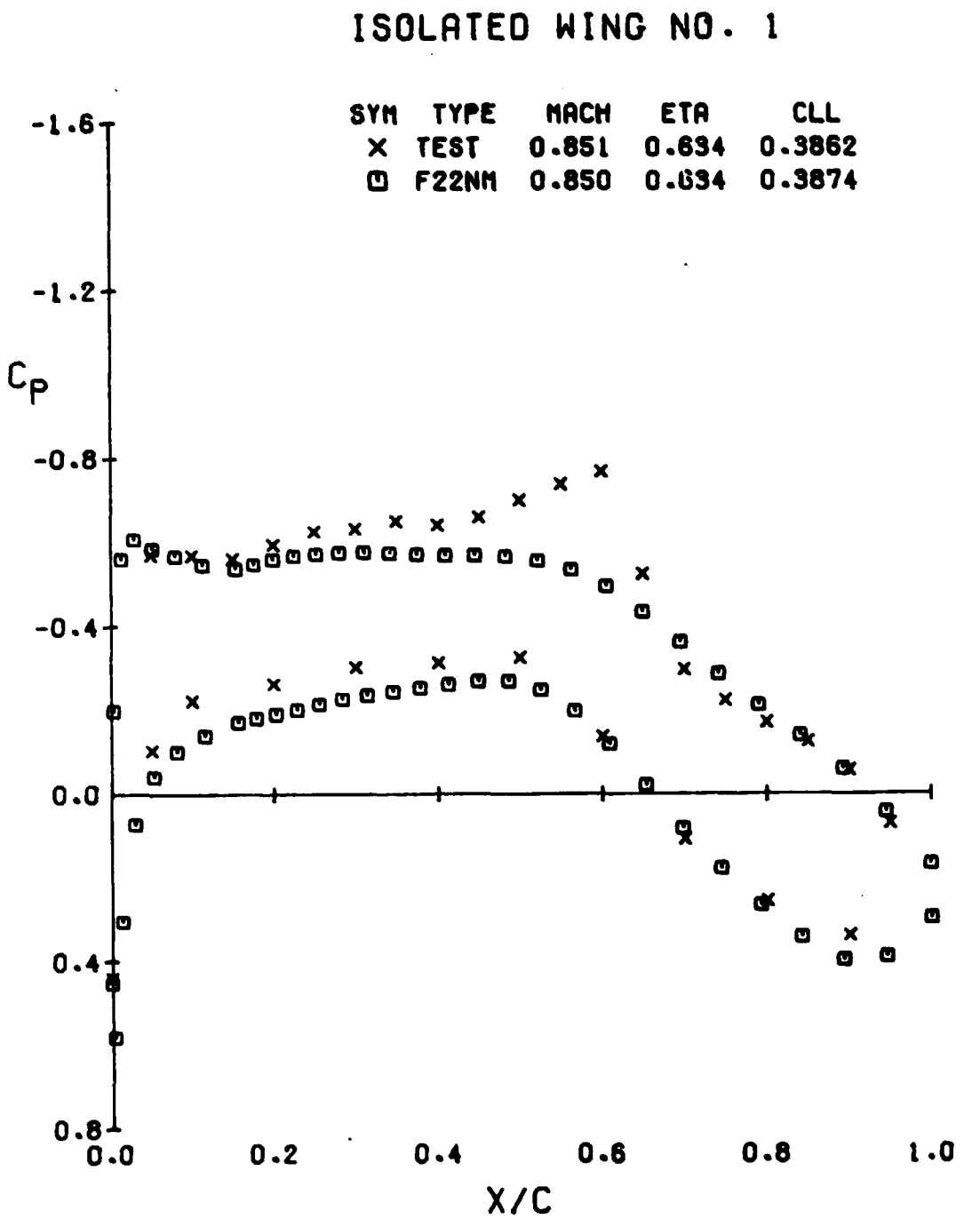

(C) ETA = 0.634

FIGURE 2.- CONTINUED

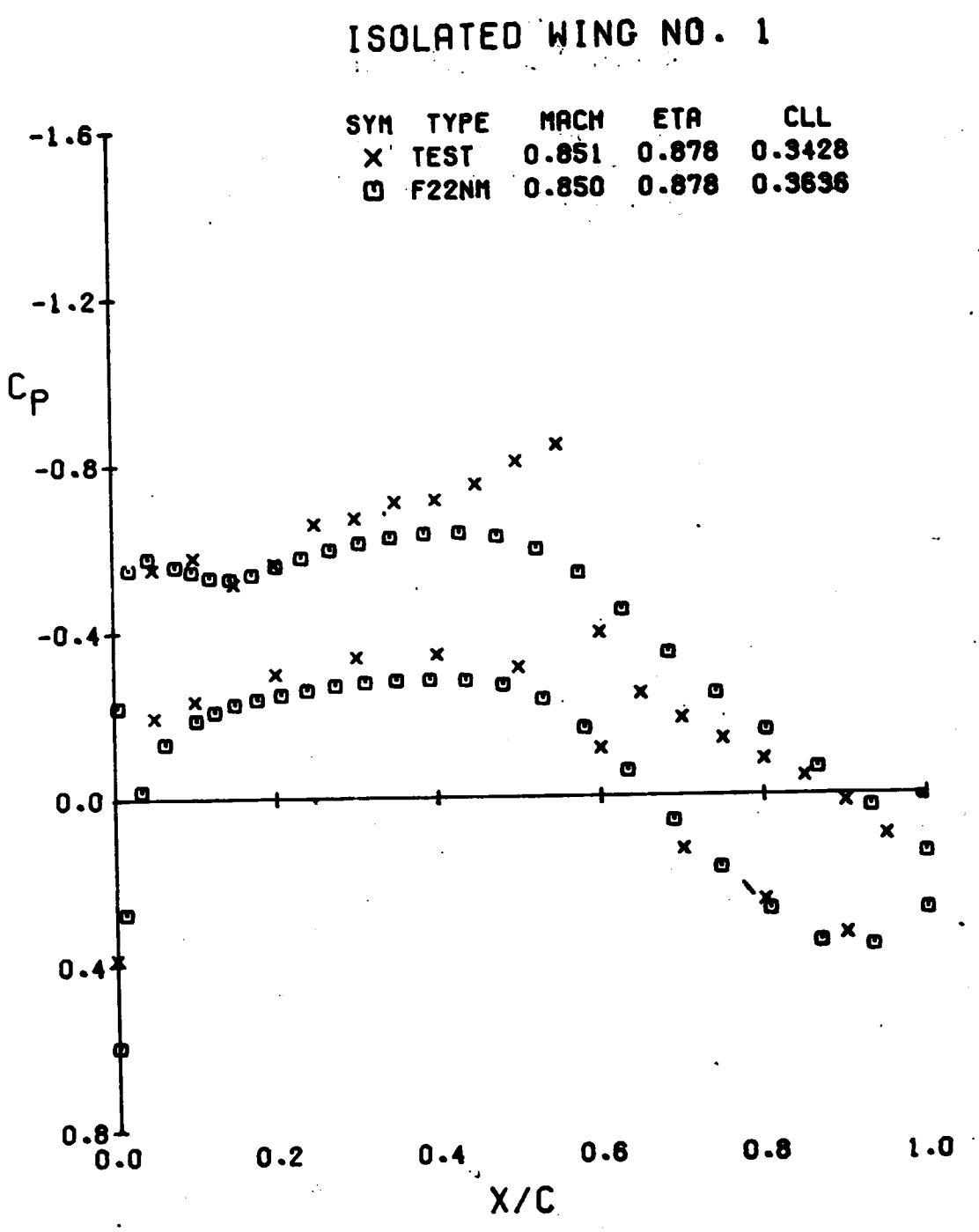

(D) ETA = 0.878

FIGURE 2.- CONCLUDED

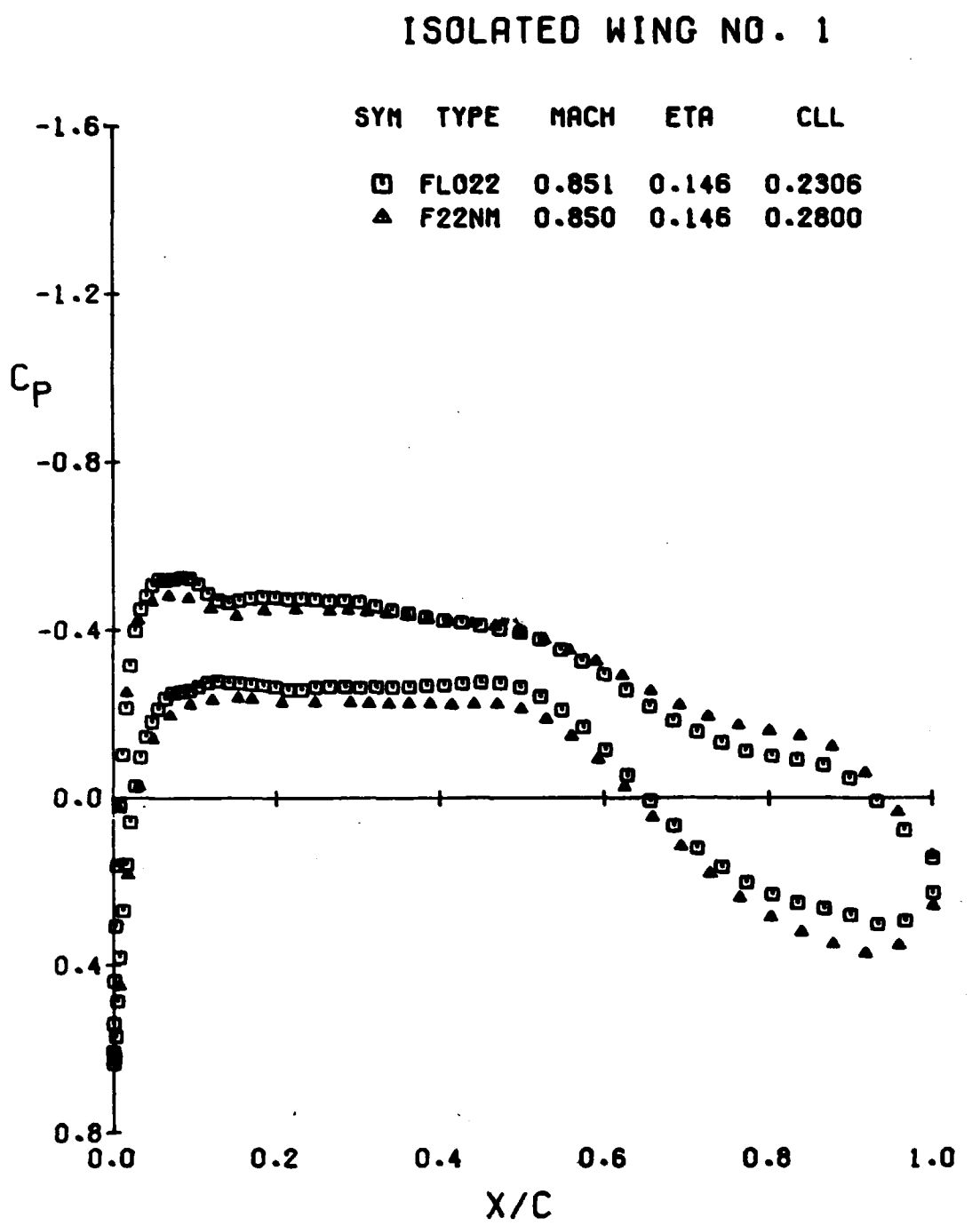

(A) ETA = 0.146

FIGURE 3.- COMPARISON OF FL022 AND FL022NM PRESSURE PREDICTIONS

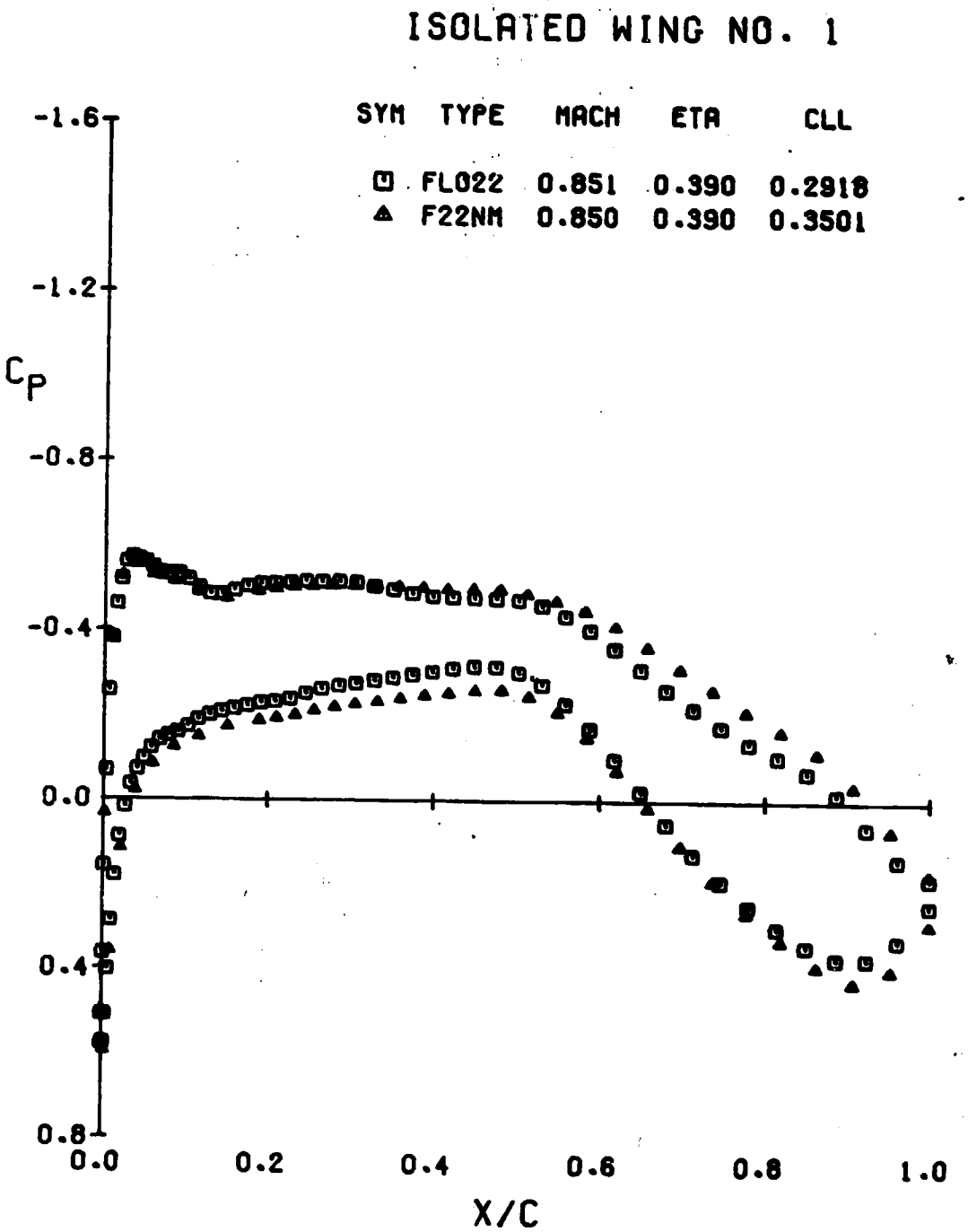

(B) ETA = 0.390

FIGURE 3.- CONTINUED

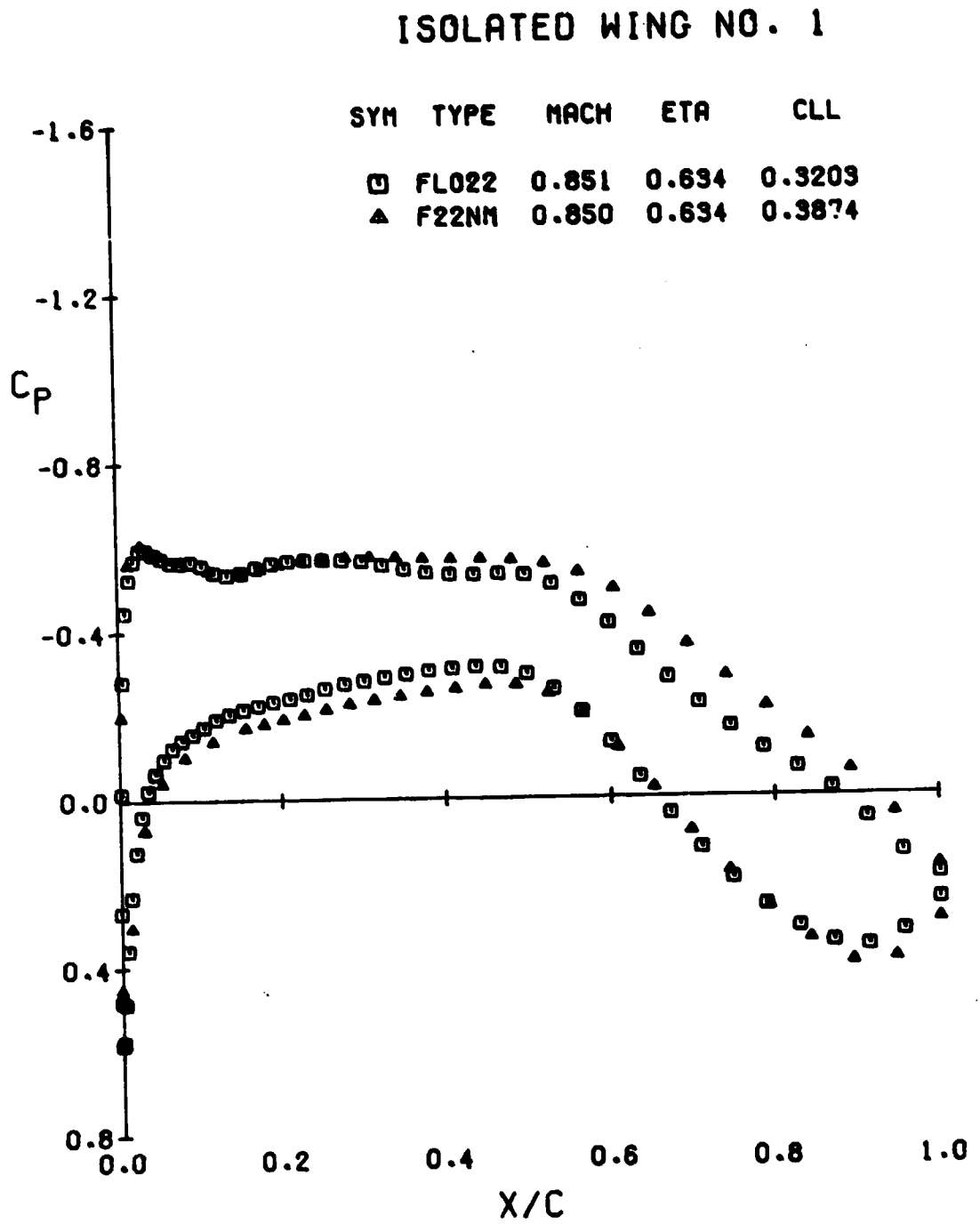

(C) ETA = 0.634

FIGURE 3.- CONTINUED

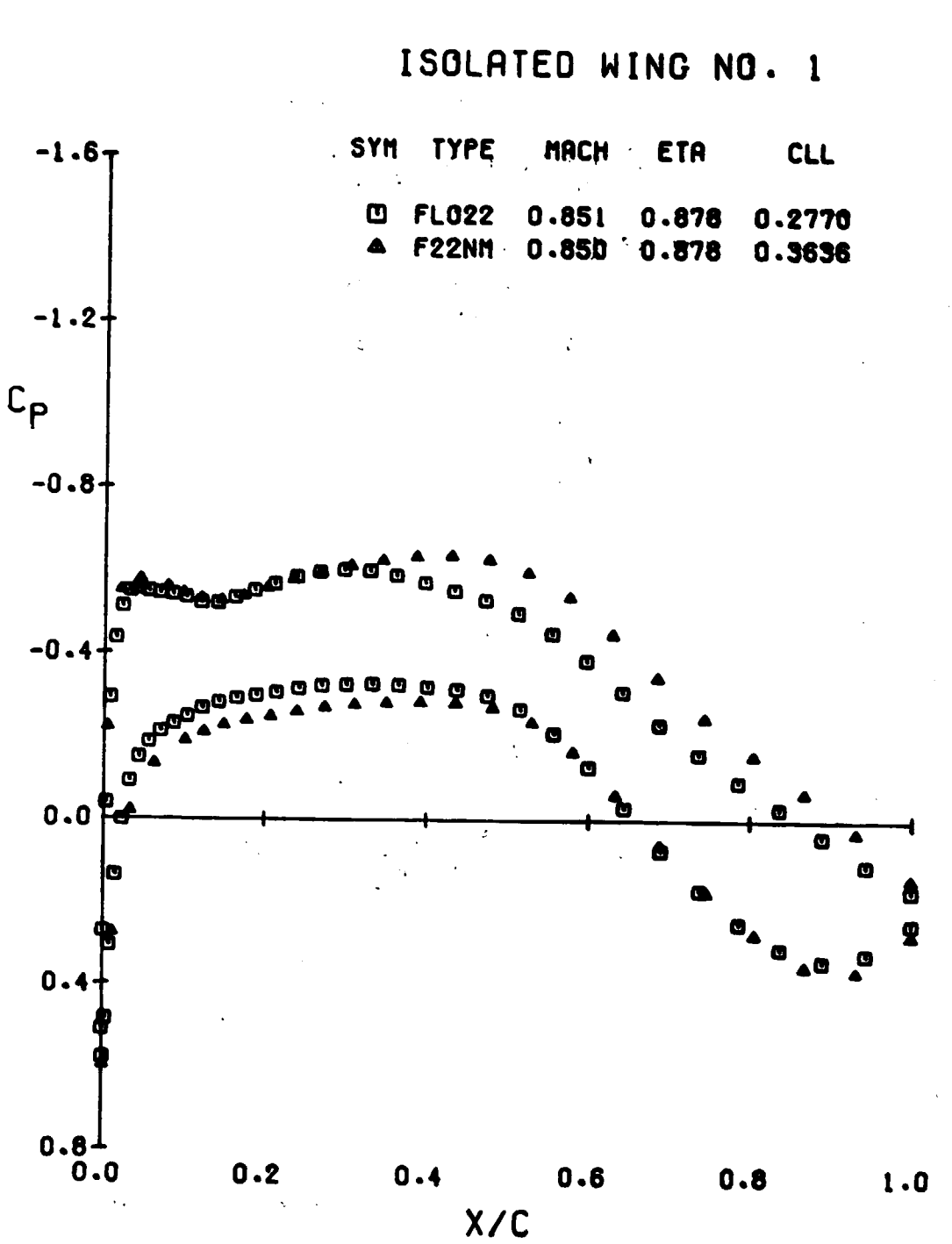

(D) ETA = 0.878

FIGURE 3.- CONCLUDED

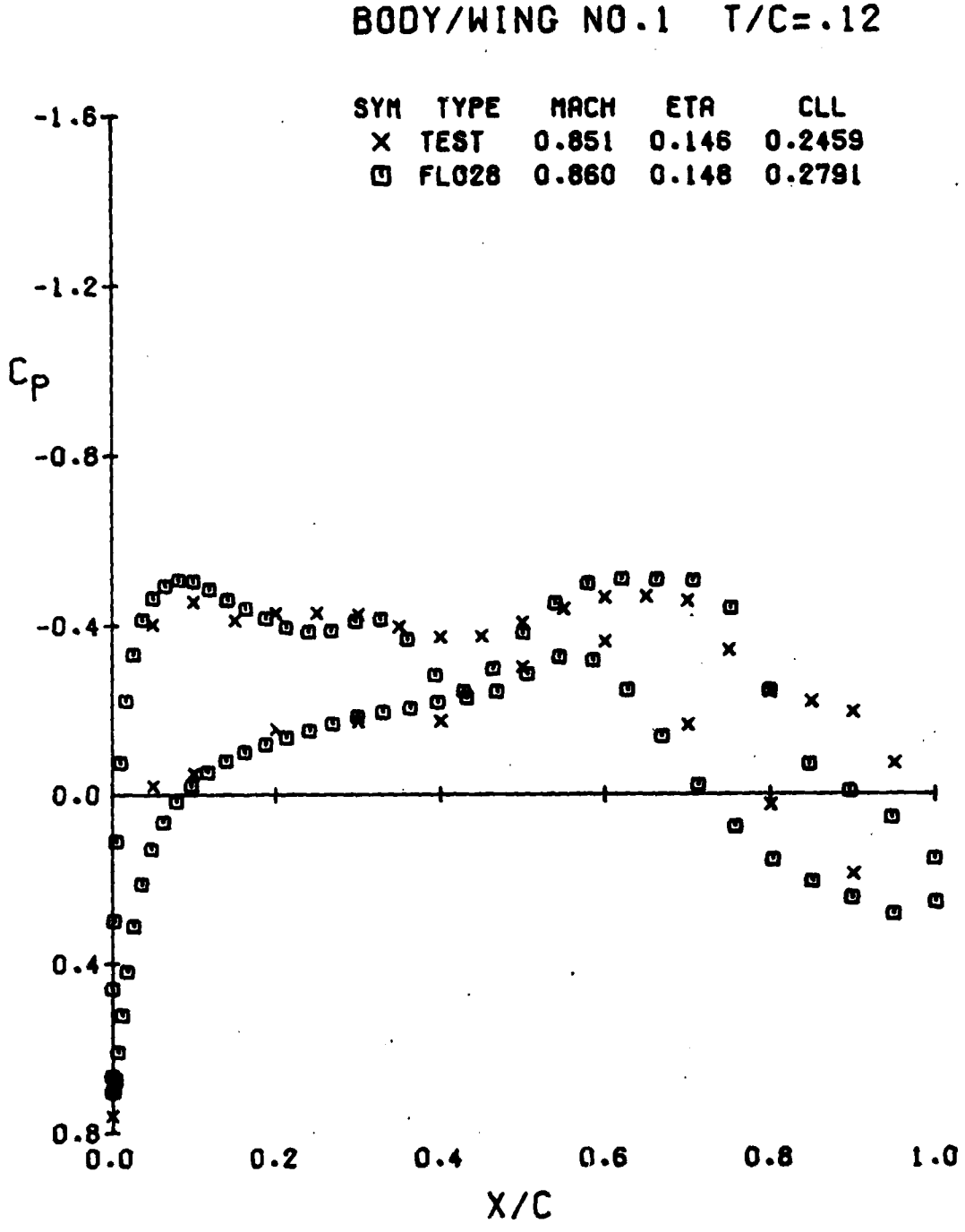

(A) ETA = 0.146

FIGURE 4.- COMPARISON OF FLO28 WING/BODY PRESSURES WITH EXPERIMENT

ALPHA = 4.68 CL(EXP) = .34

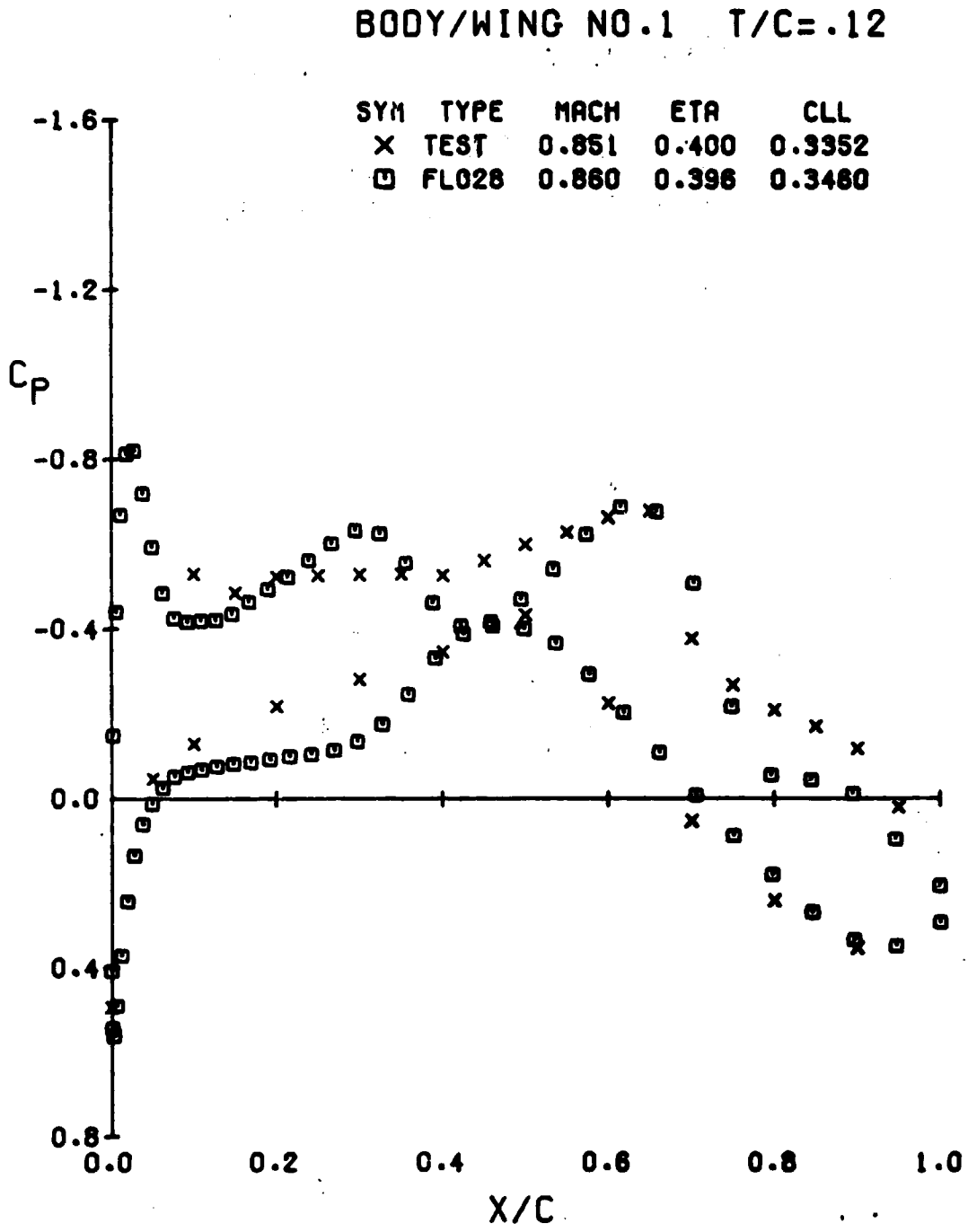

(B) ETA = 0.400

FIGURE 4.- CONTINUED

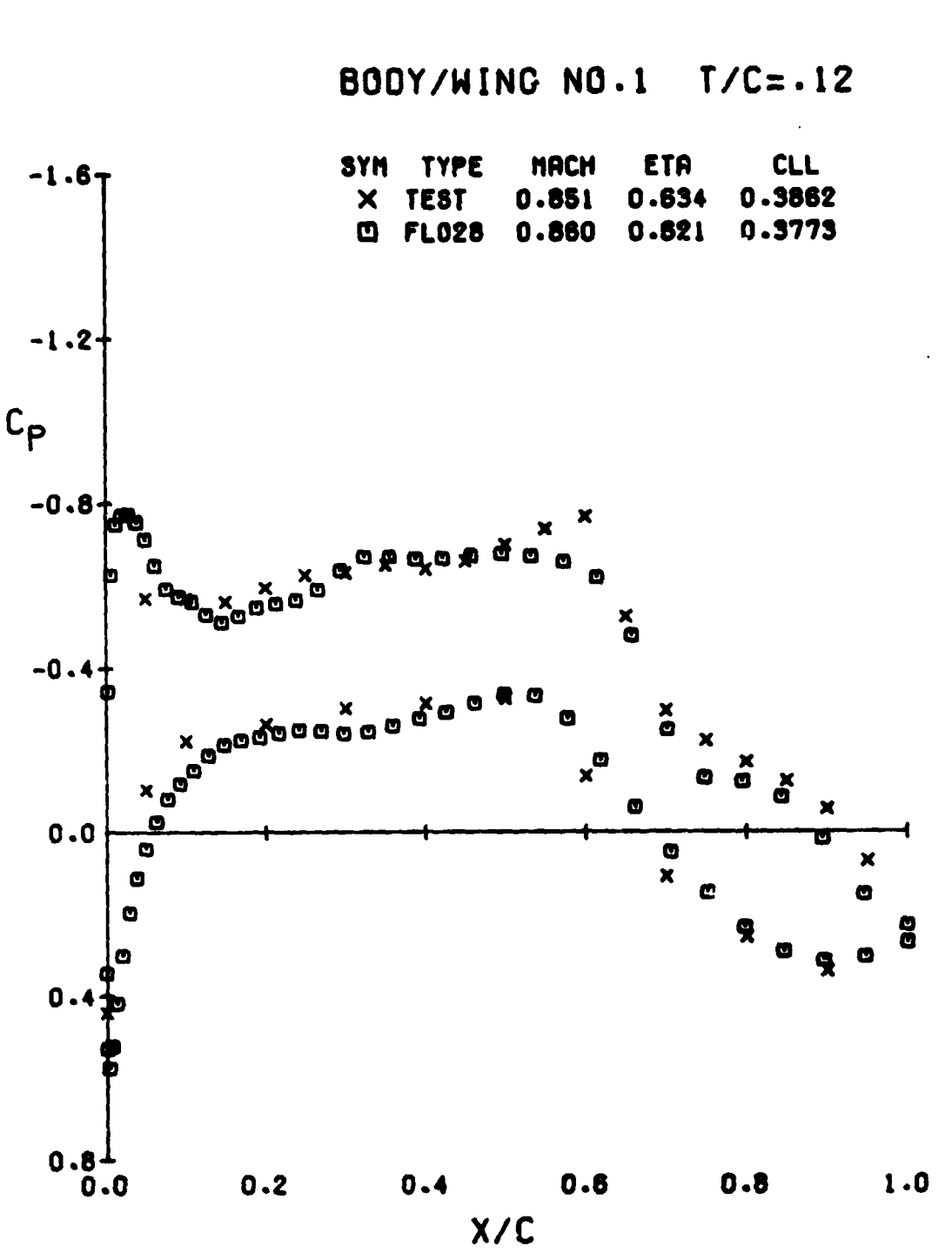

(C) ETA = 0.634

FIGURE 4.- CONTINUED

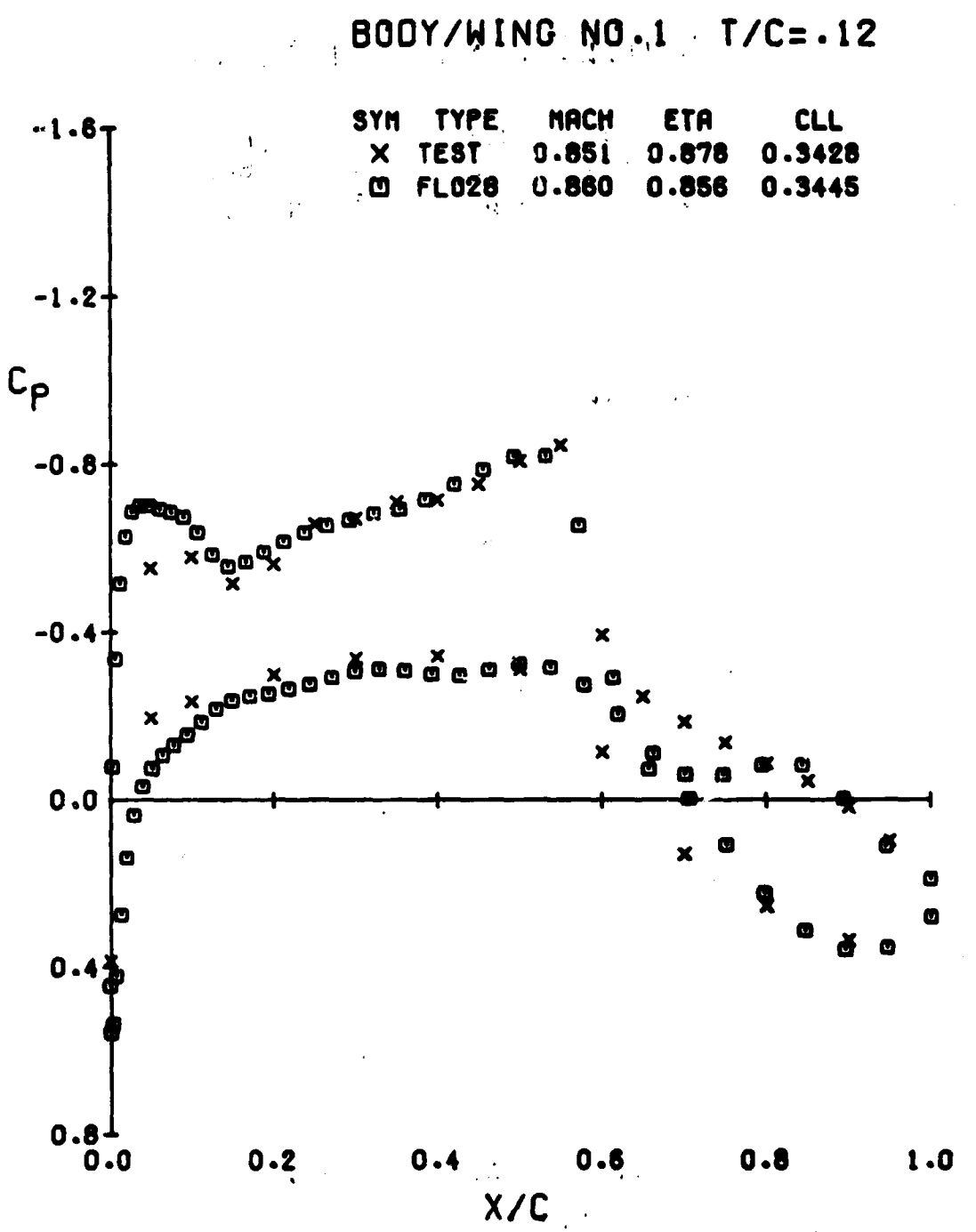

(D) ETA = 0.878

FIGURE 4.- CONCLUDED

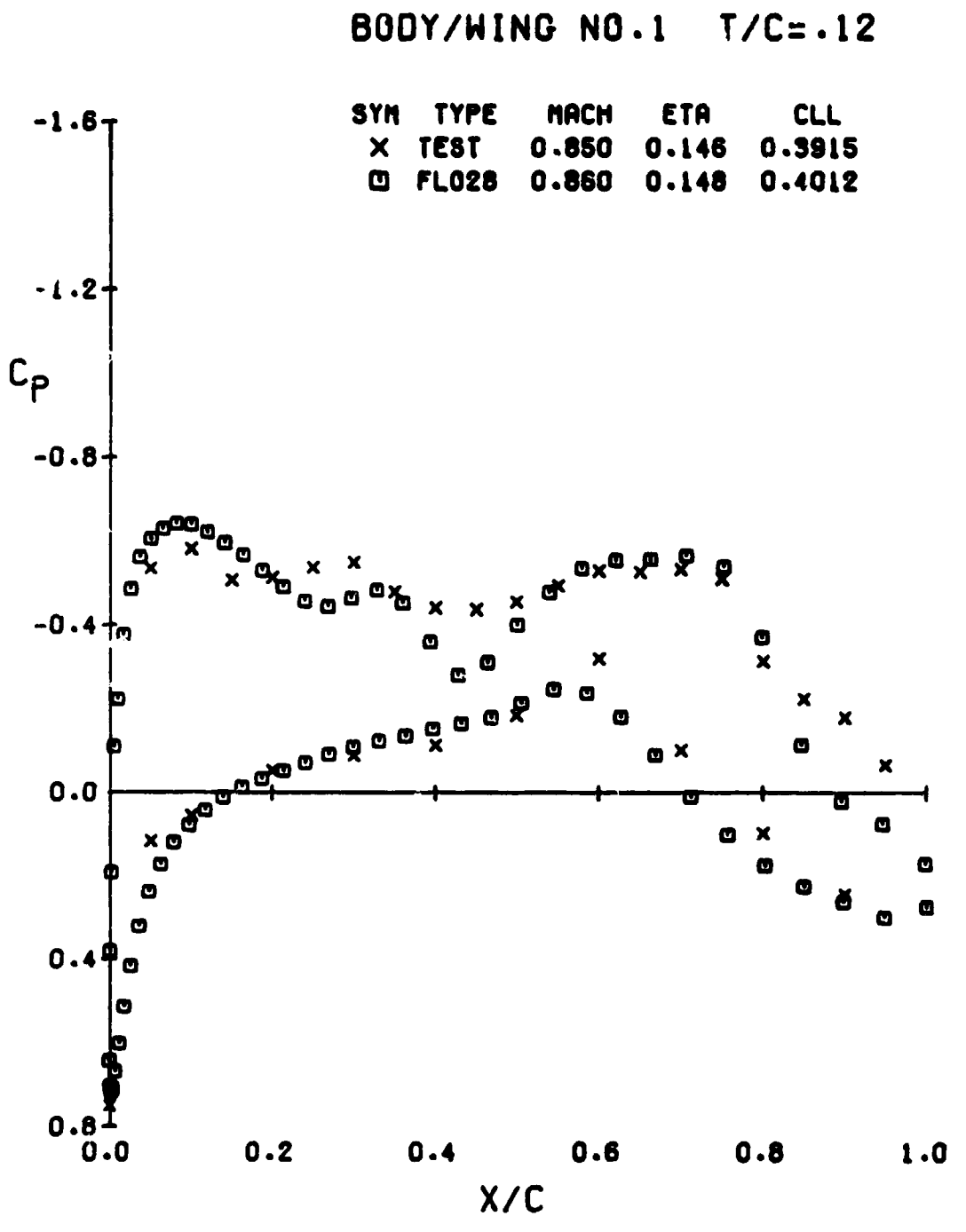

(A) ETA = 0.146

FIGURE 5.- COMPARISON OF FL028 WING/BODY PRESSURES WITH EXPERIMENT

ALPHA = 6.52 CL(EXP) = .515

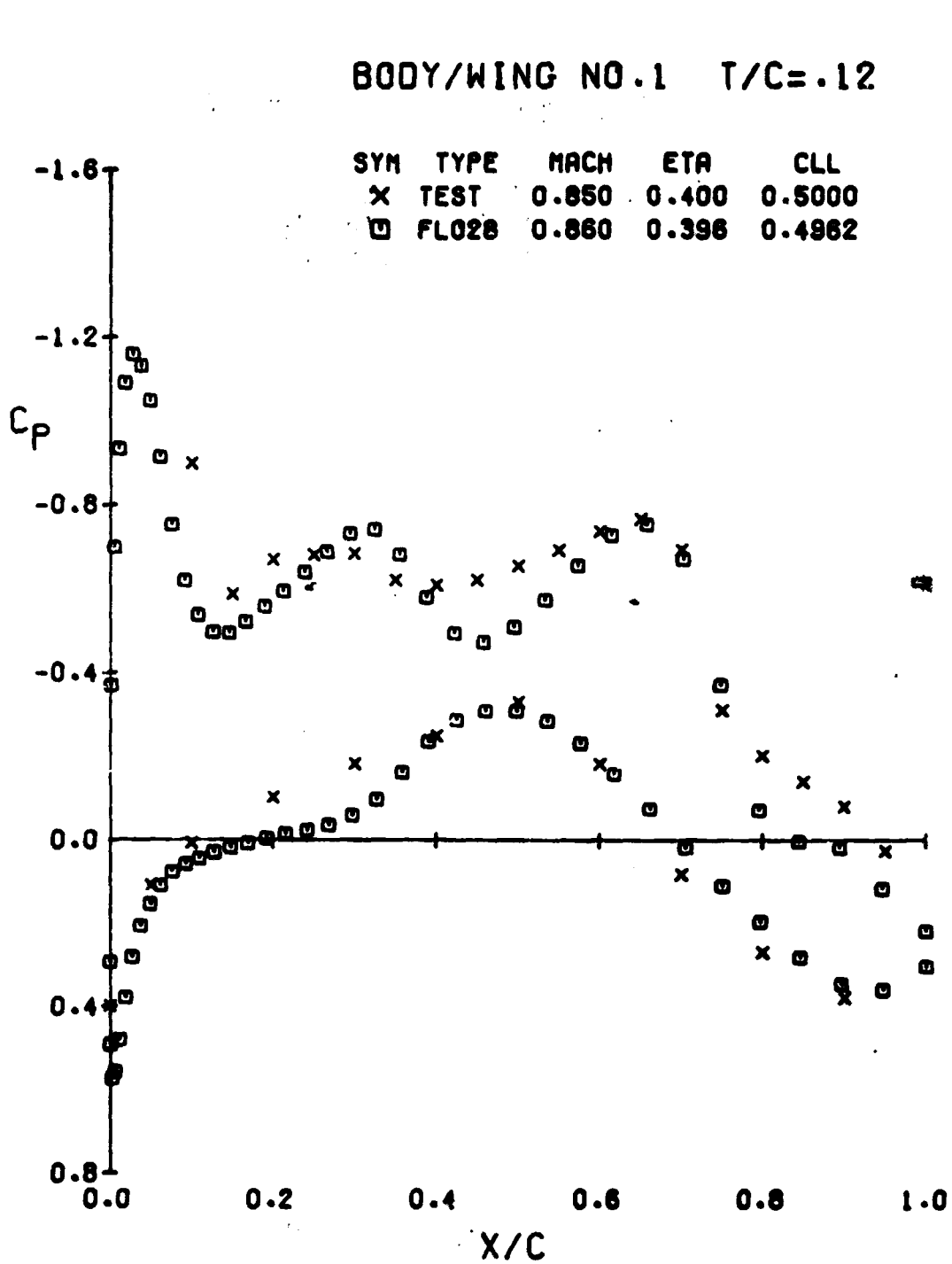

(B) ETA = 0.400

FIGURE 5.- CONTINUED

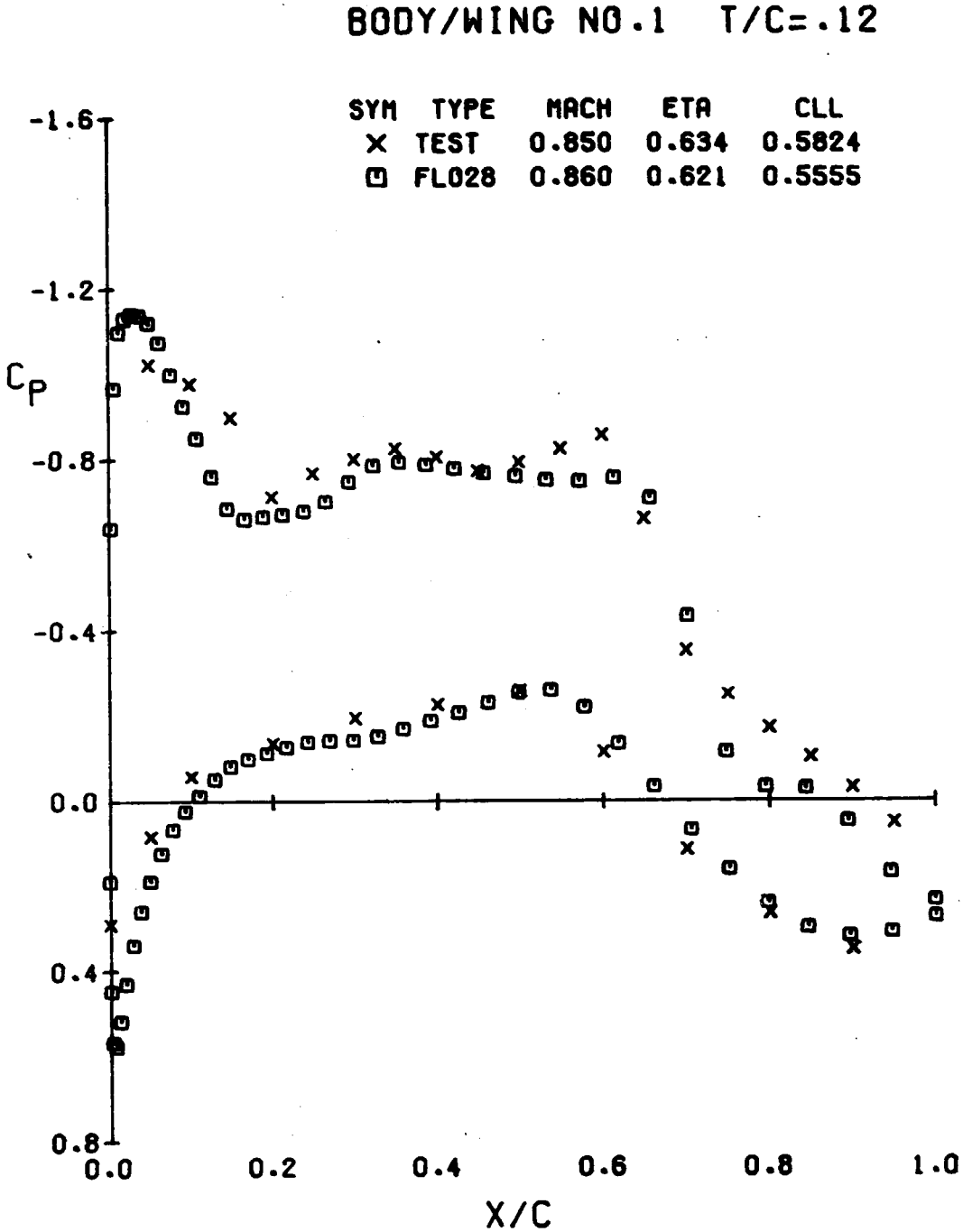

(C) ETA = 0.634

FIGURE 5.- CONTINUED

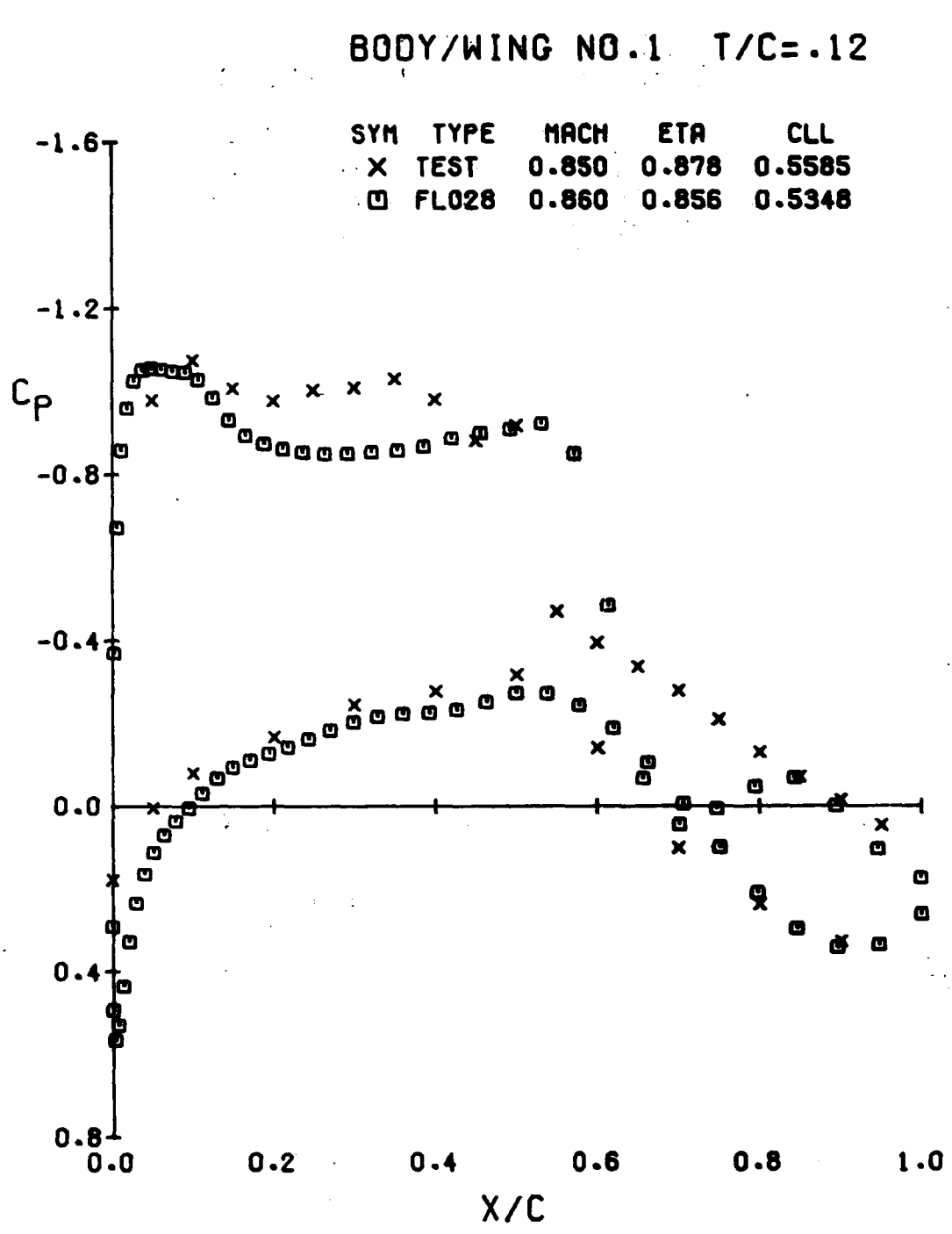

(D) ETA = 0.878

FIGURE 5.- CONCLUDED

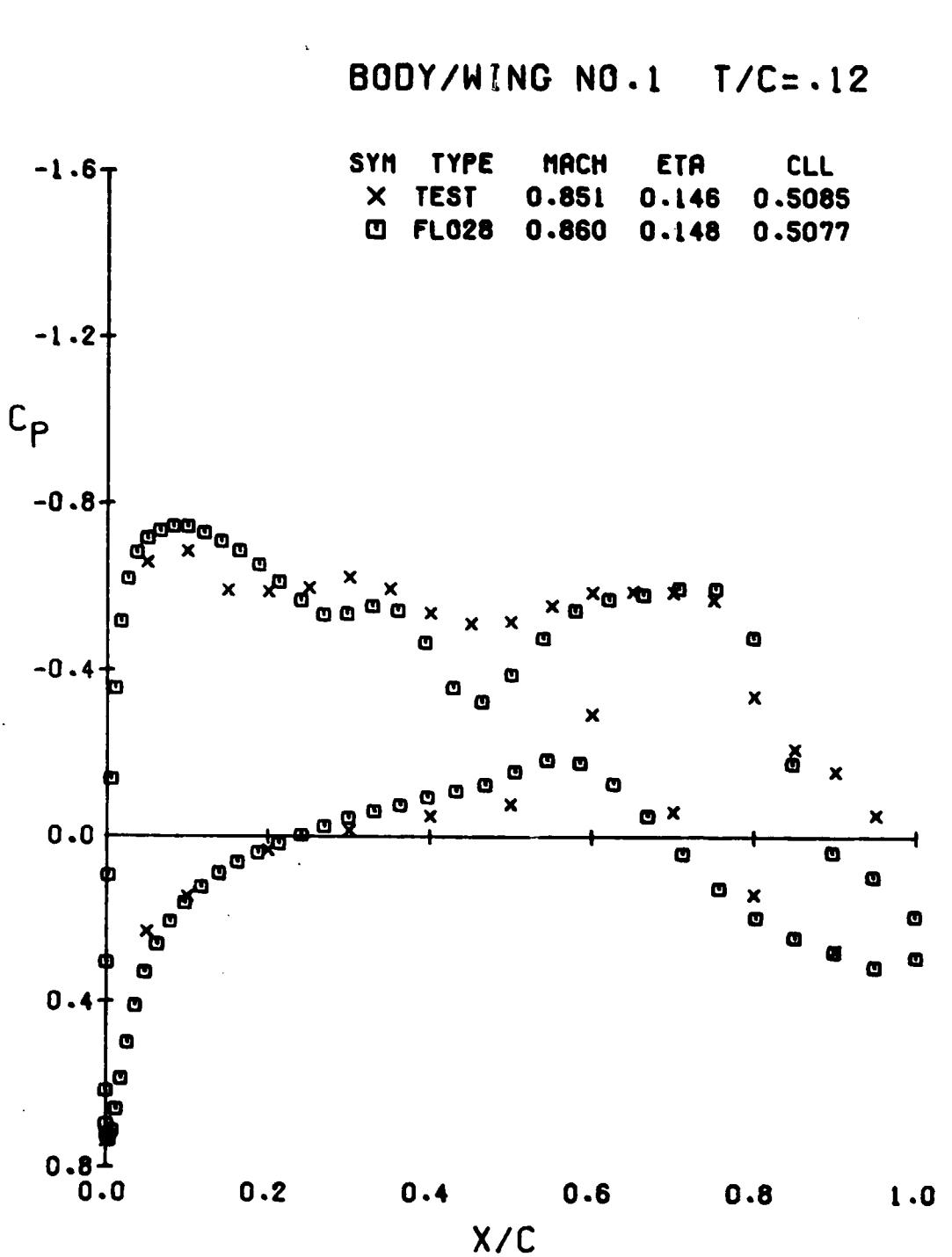

(A) ETA = 0.146

FIGURE 6.- COMPARISON OF FL028 WING/BODY PRESSURES WITH EXPERIMENT

ALPHA = 8.14 CL(EXP) = .63

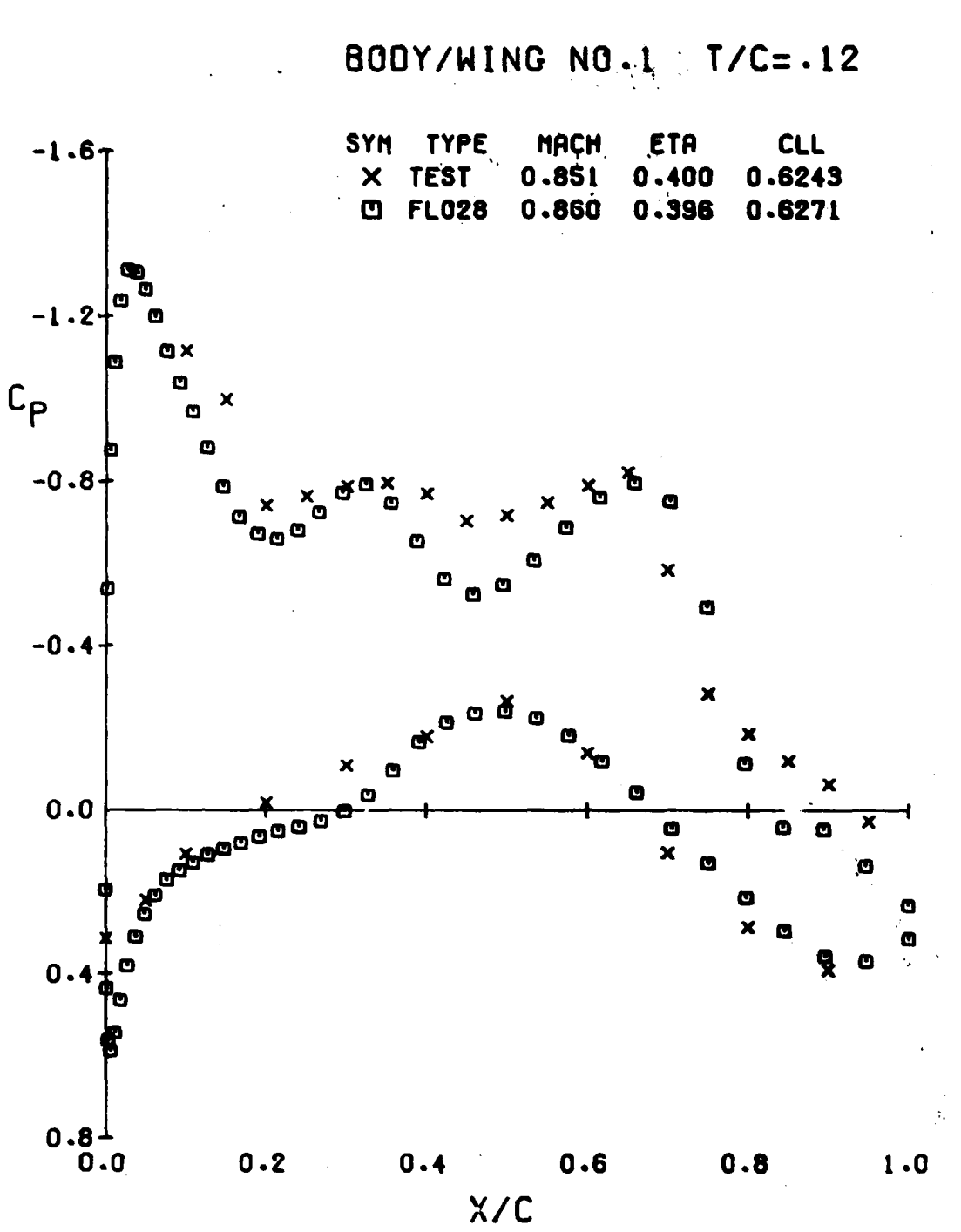

(B) ETA = 0.400

FIGURE 6.- CONTINUED

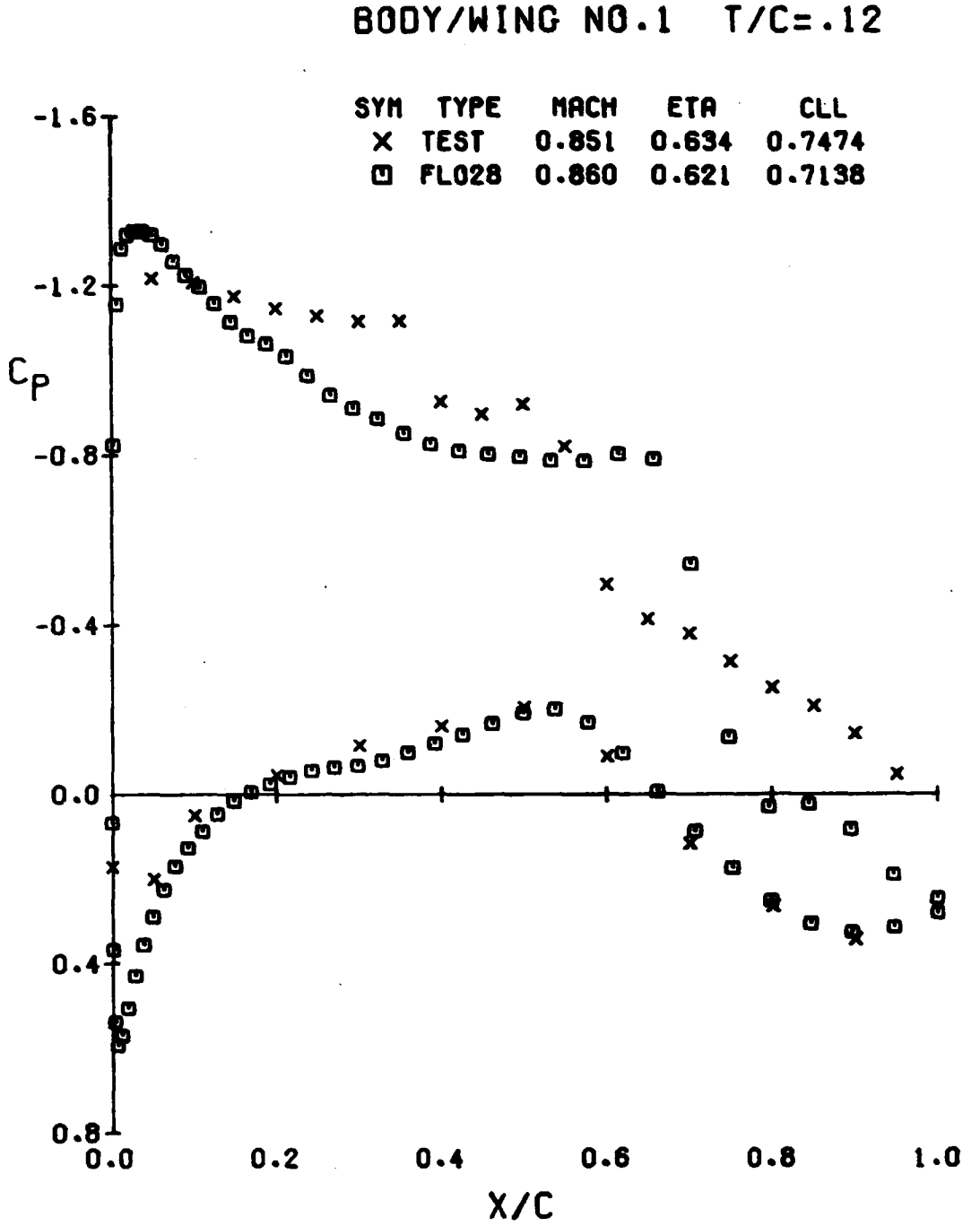

(C) ETA = 0.634

FIGURE 6.- CONTINUED

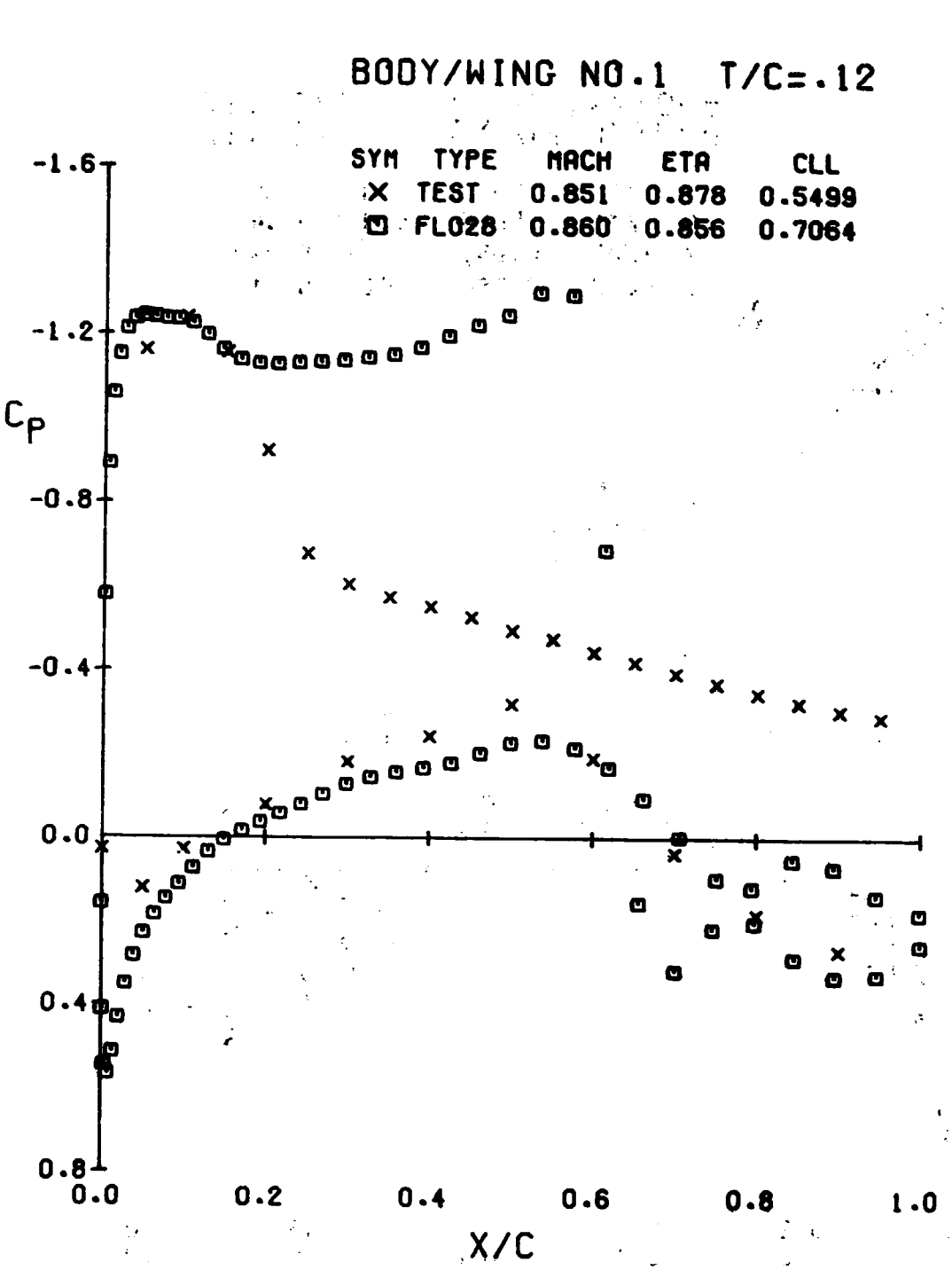

(D) ETA = 0.878

FIGURE 6.- CONCLUDED

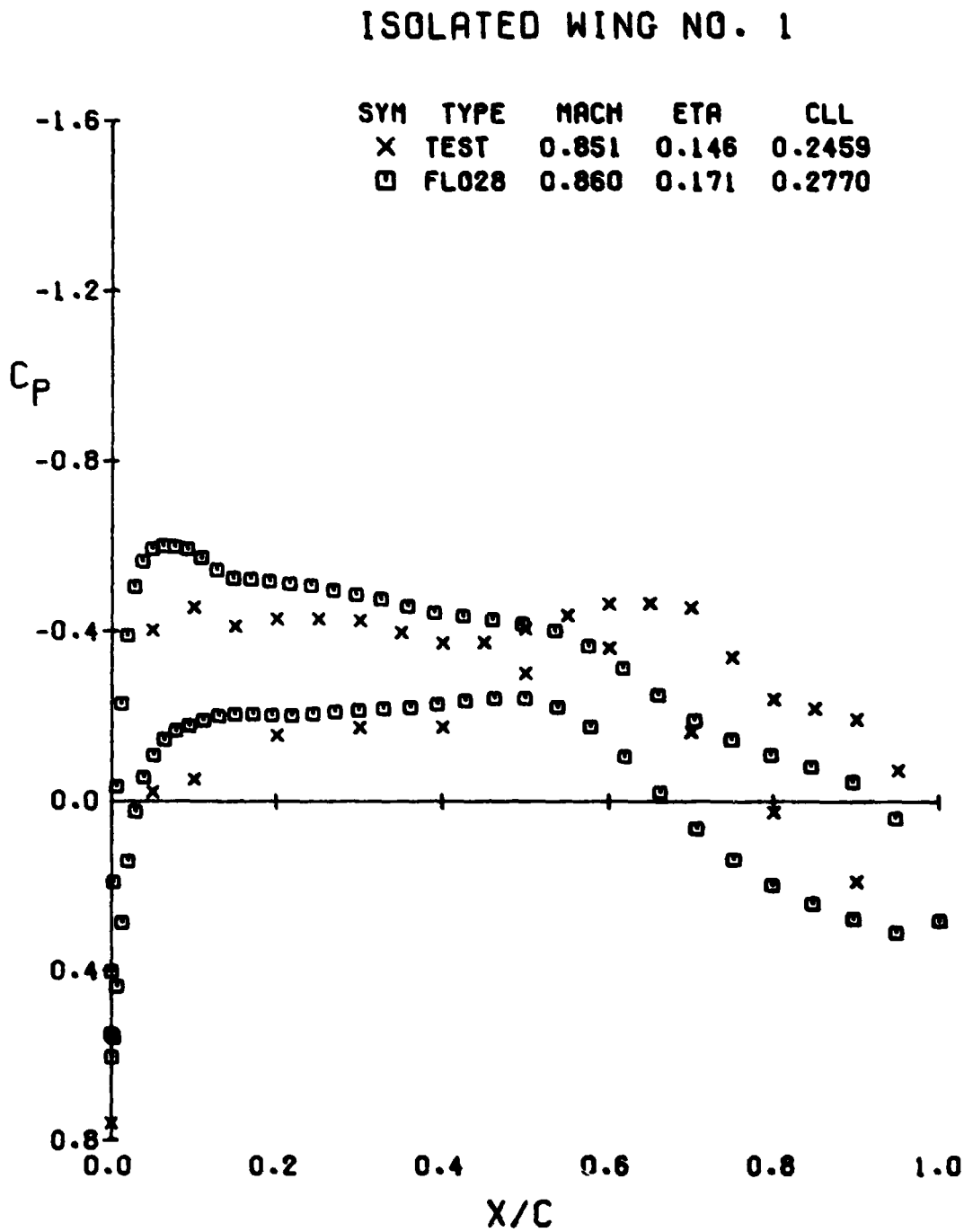

(A) ETA = 0.146

FIGURE 7.- COMPARISON OF FLO28 WING PRESSURES WITH EXPERIMENT

ALPHA = 4.68 CL(EXP) = .94

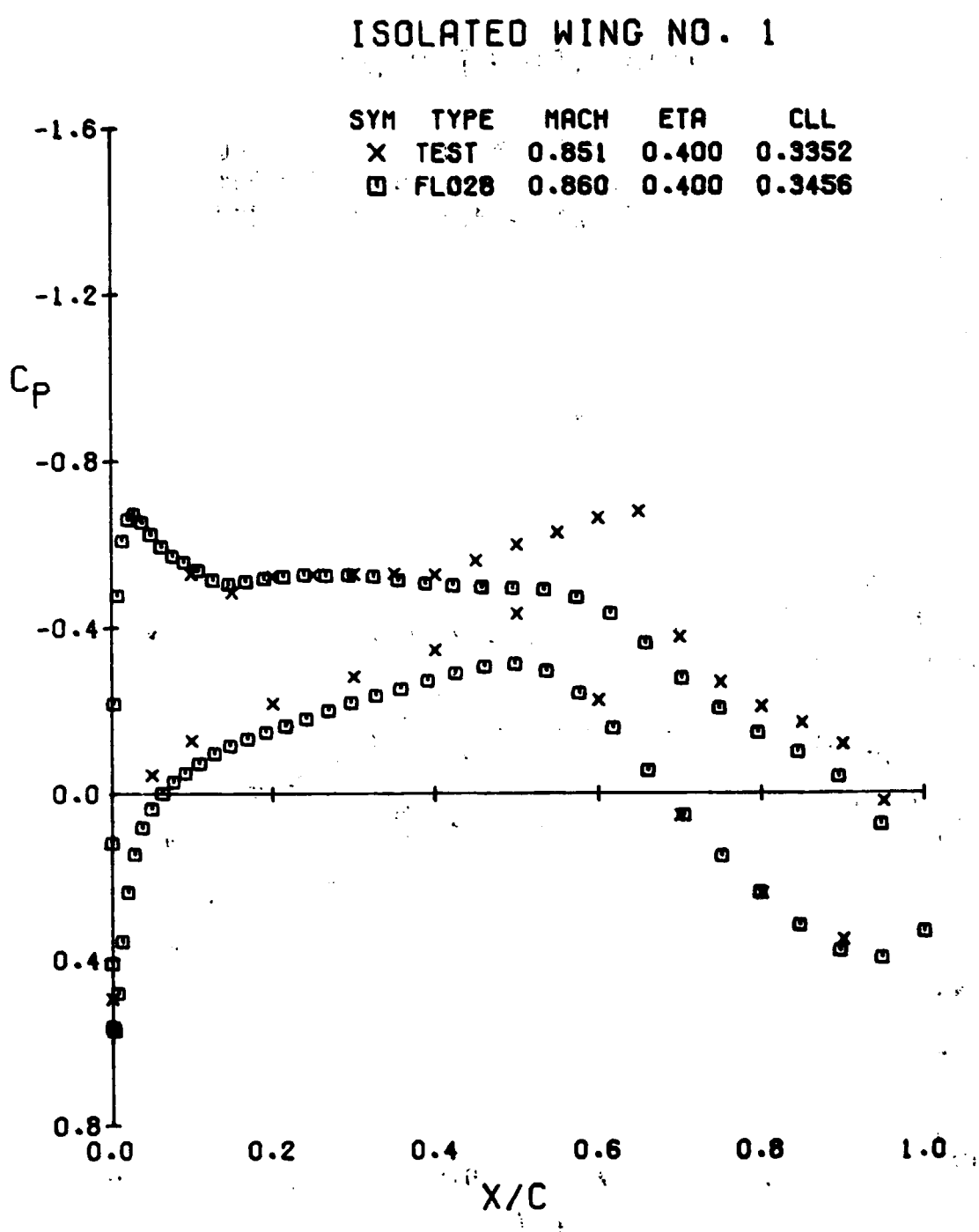

(B) ETA = 0.400

FIGURE 7.- CONTINUED

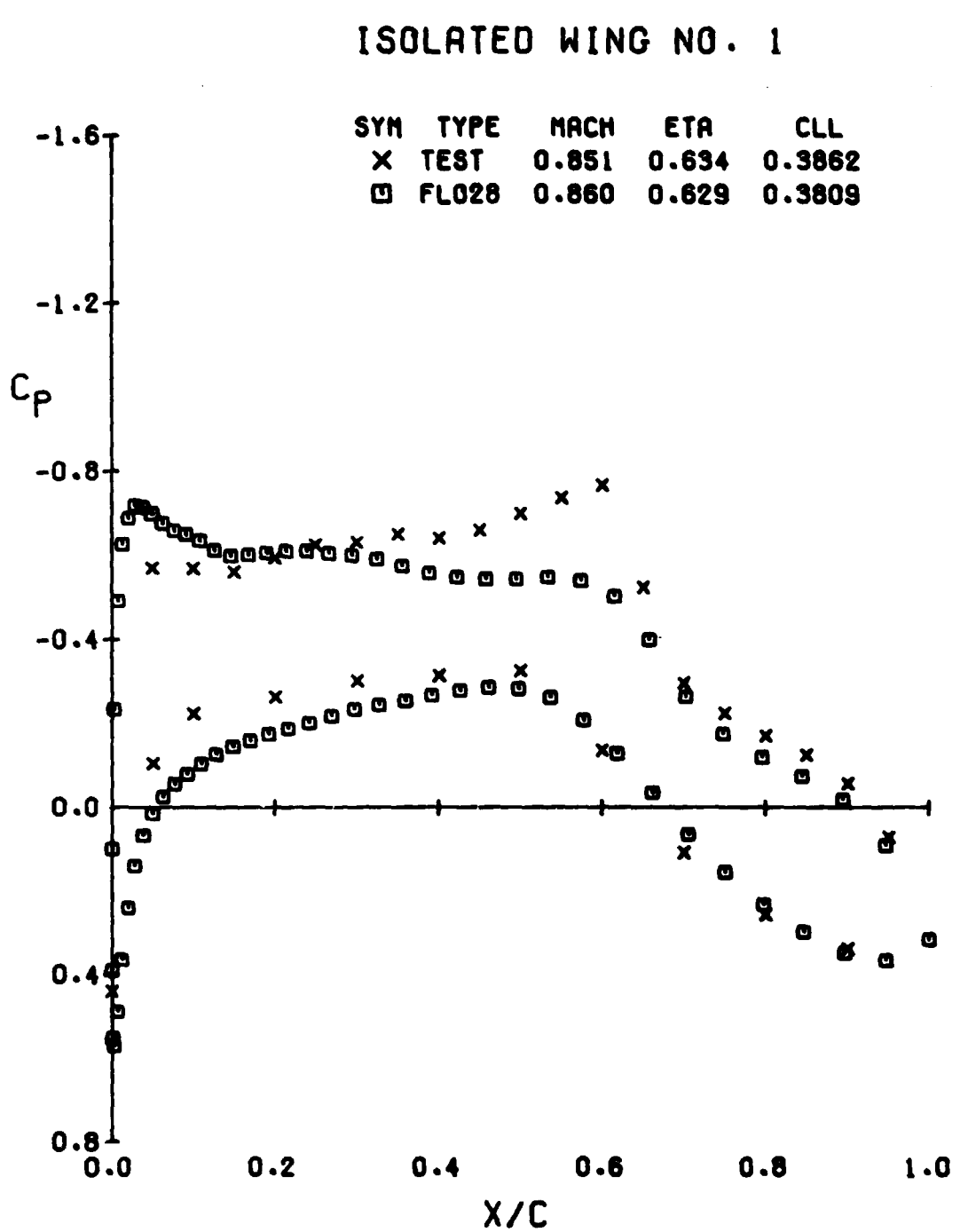

(C) ETA = 0.634

FIGURE 7.- CONTINUED

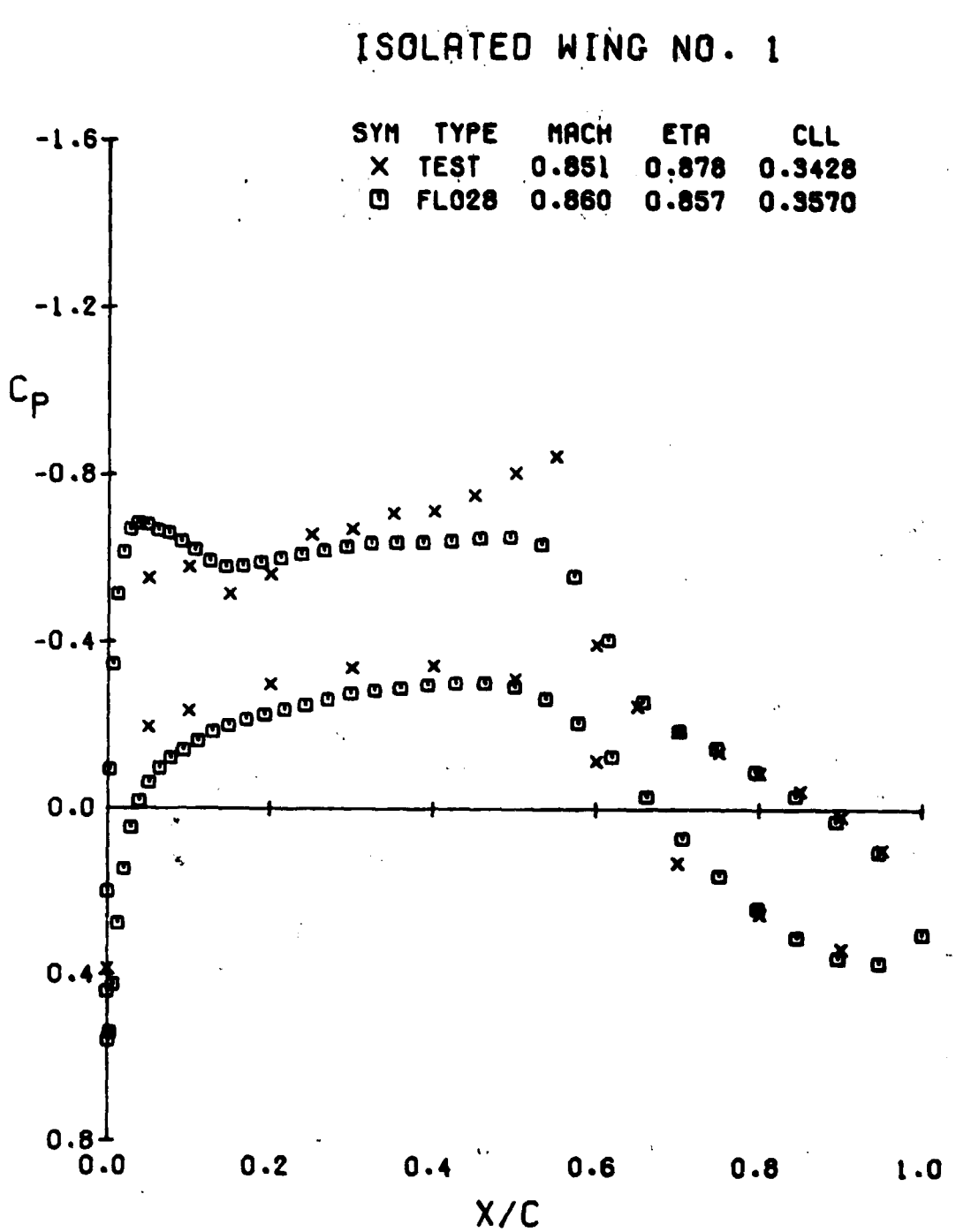

(D) ETA = 0.878

FIGURE 7.- CONCLUDED

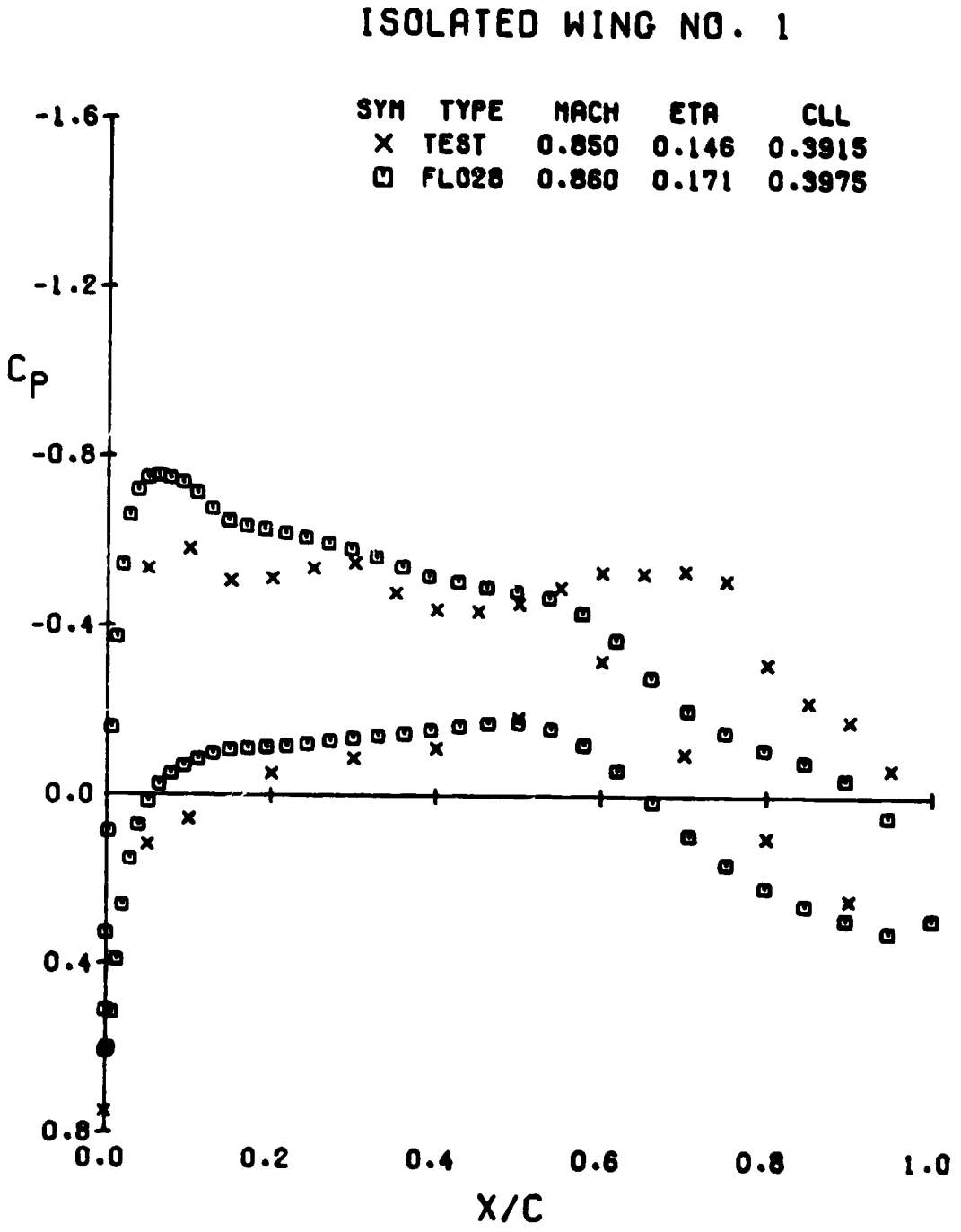

(A) ETA = 0.146

FIGURE 8.- COMPARISON OF FL028 WING PRESSURES WITH EXPERIMENT
ALPHA = 6.52 CL(EXP) = .515

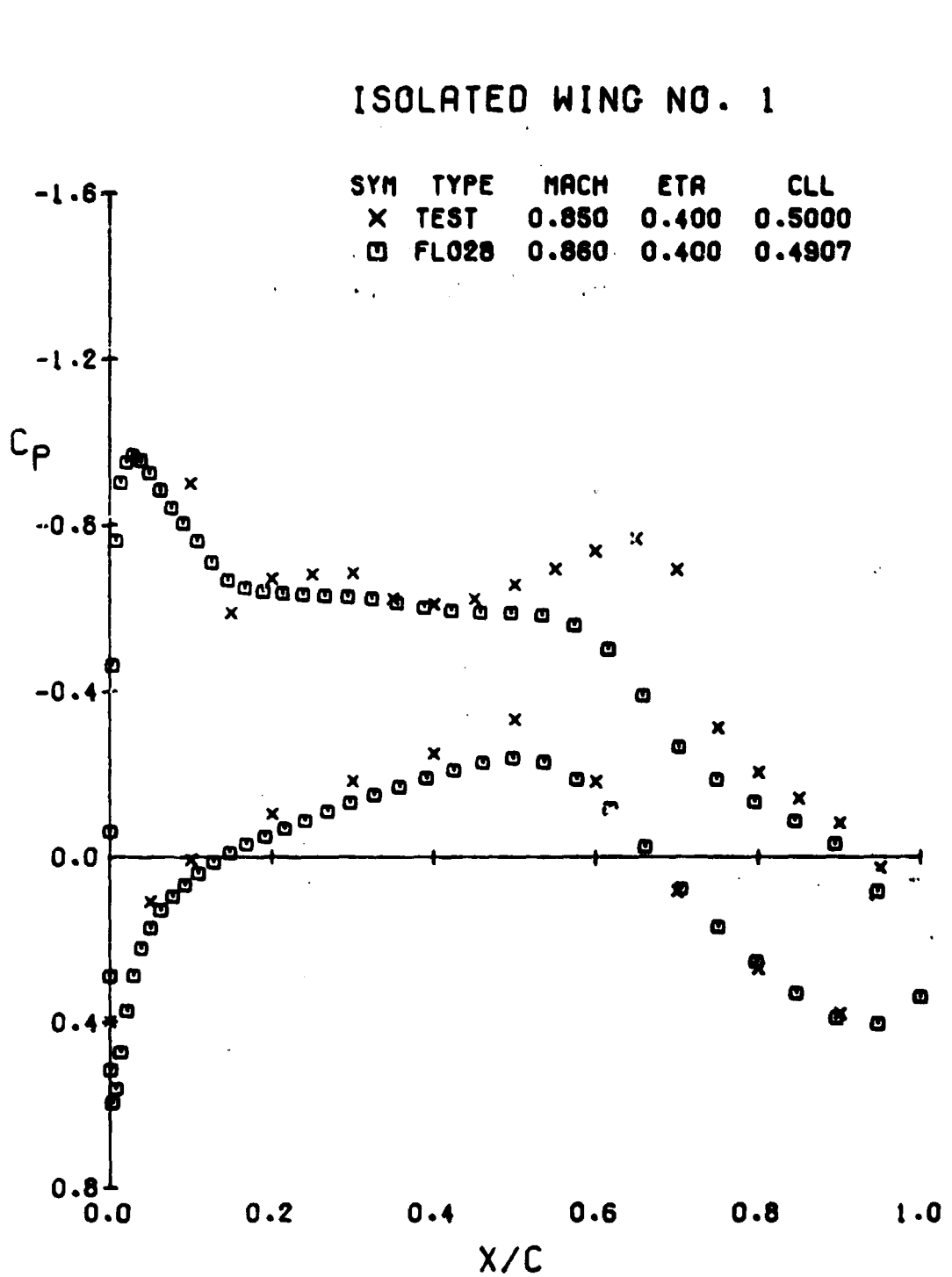

(B) ETA = 0.400

FIGURE 8.- CONTINUED

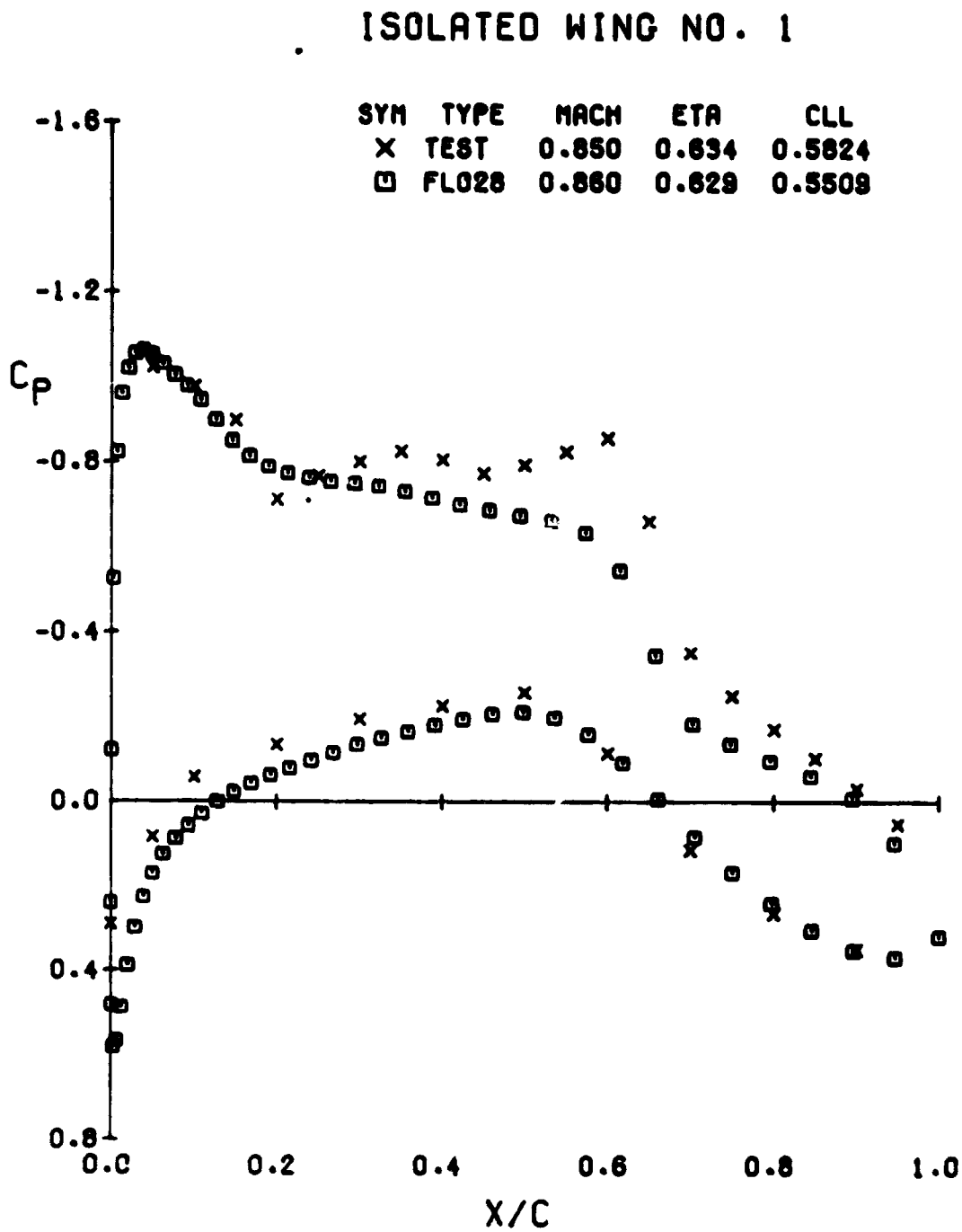

(C) ETA = 0.634

FIGURE 8.- CONTINUED

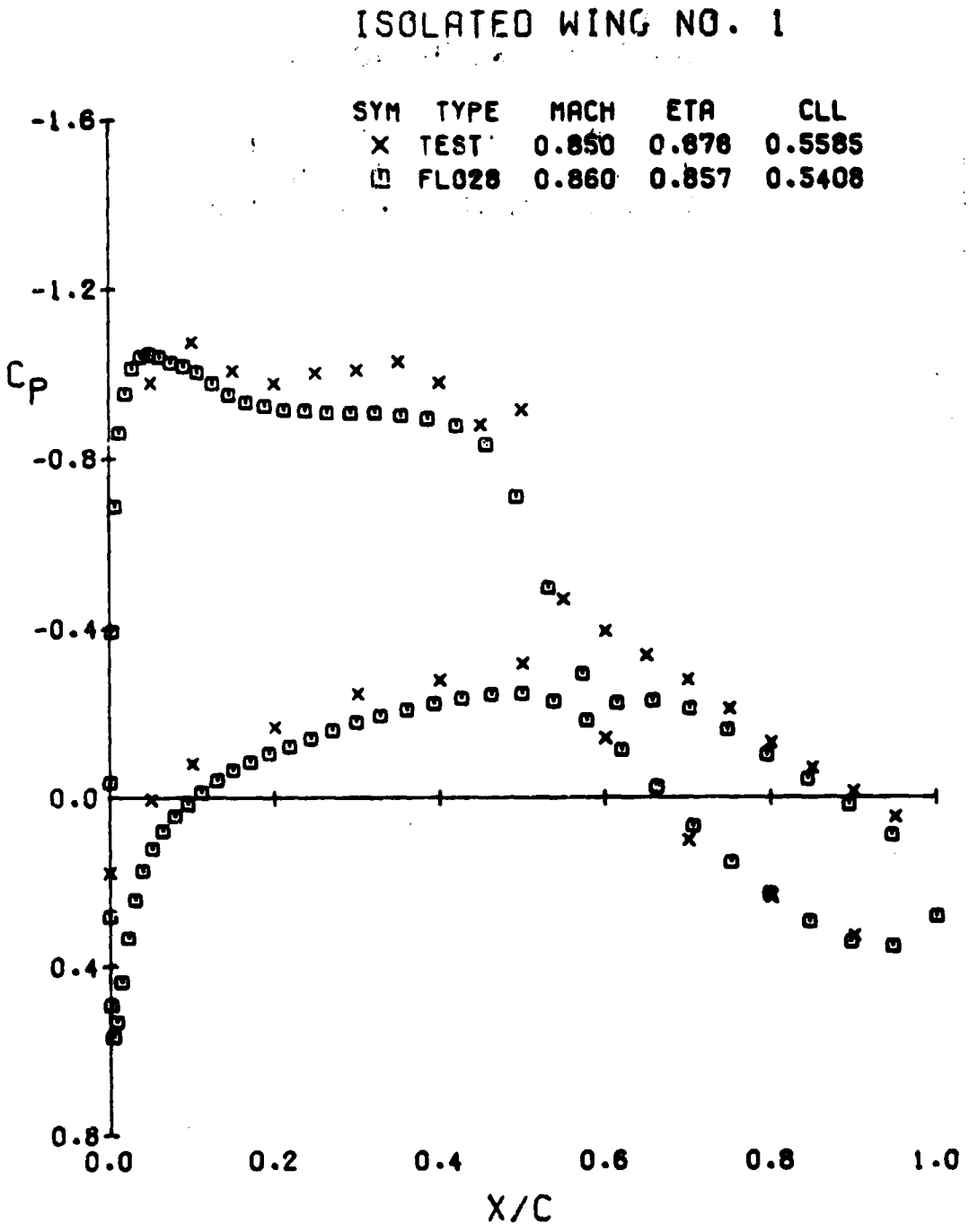

(D) ETA = 0.878

FIGURE 8.- CONCLUDED

FIGURE 9.- A-7 TRANSONIC WING-BODY GEOMETRY

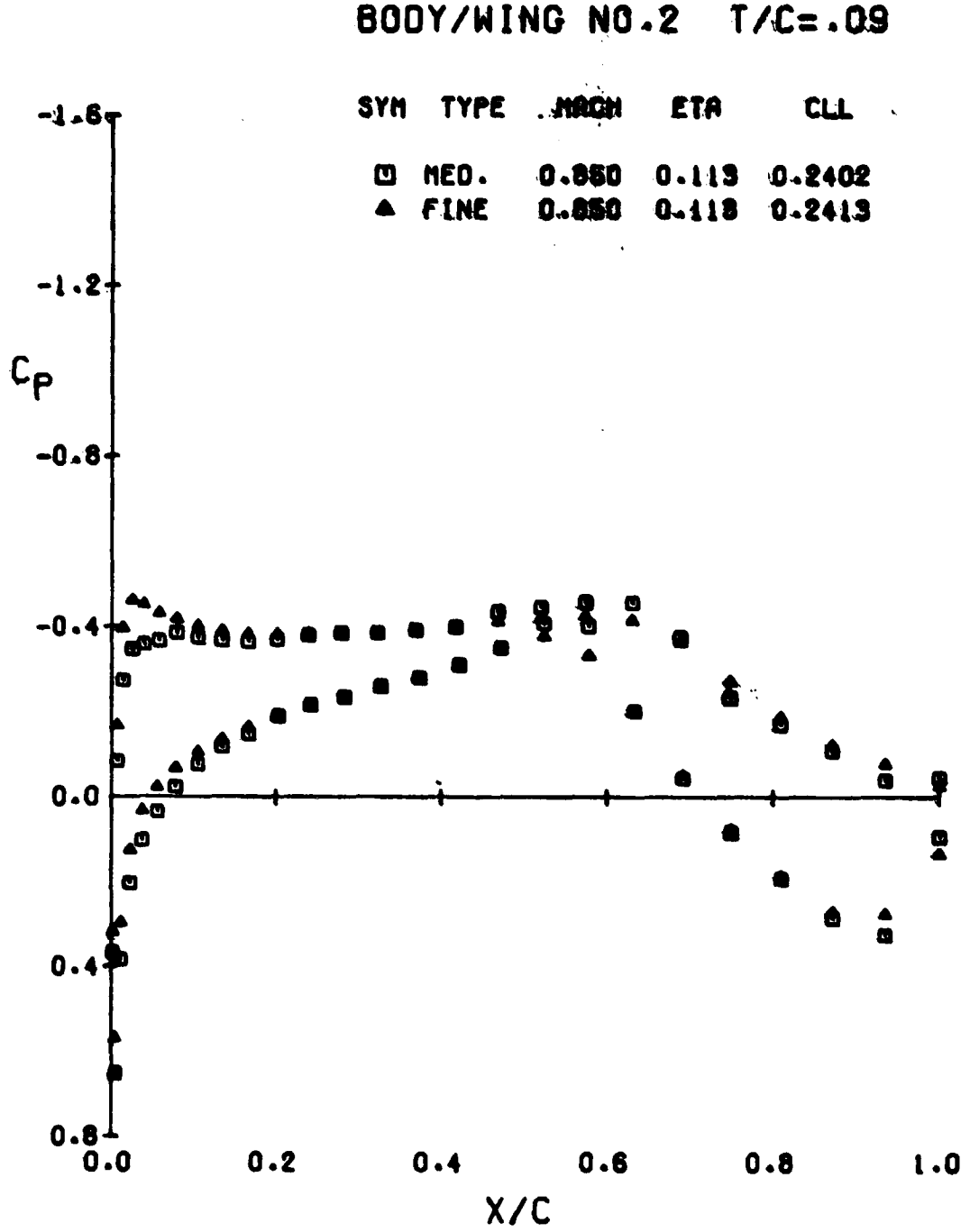

(A) ETA = 0.113

FIGURE10.- COMPARISON OF MEDIUM AND FINE GRID SOLUTIONS

FLO30 MED = 80X12X16 FINE = 160X24X32

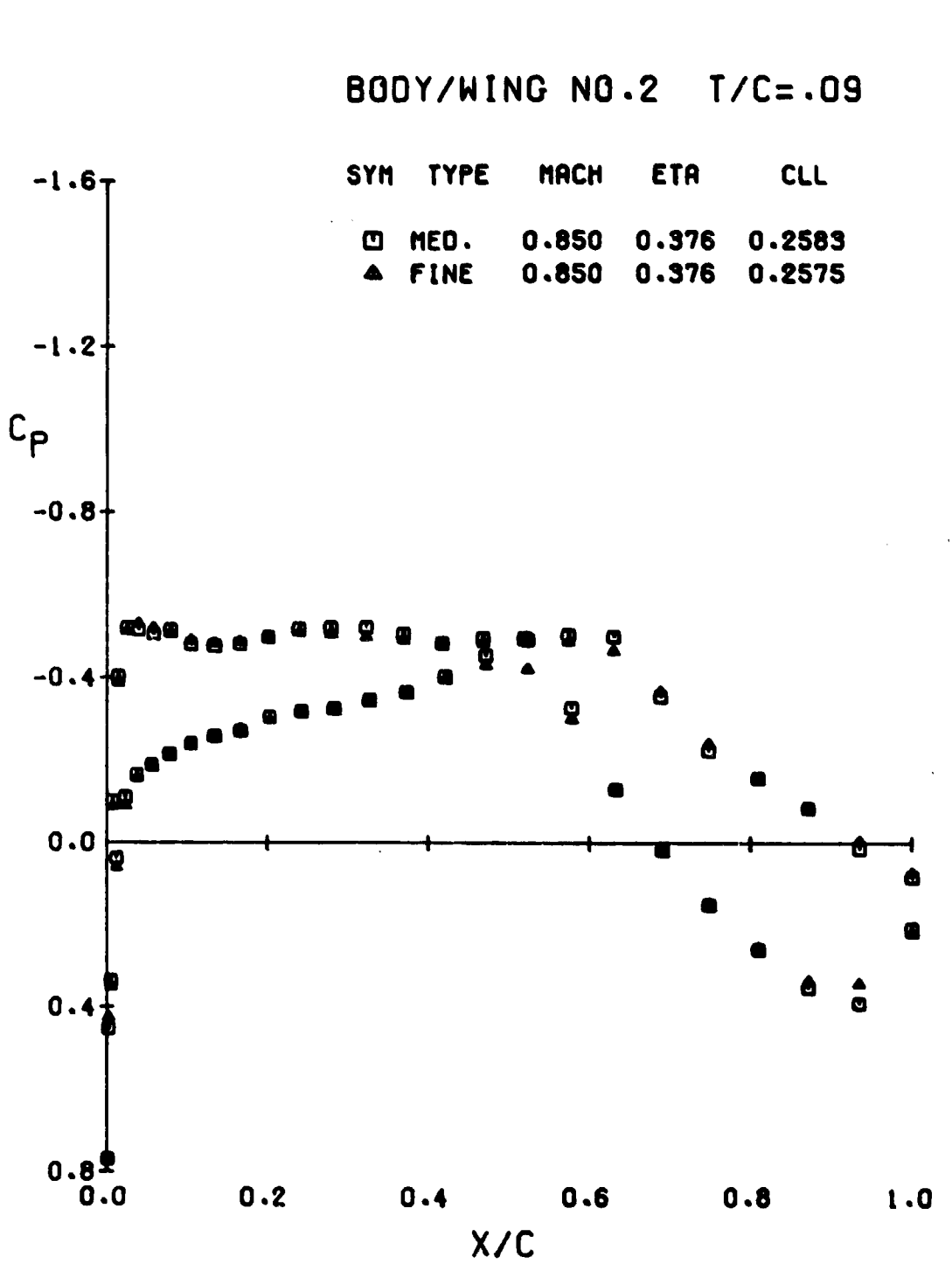

(B) ETA = 0.376

FIGURE10.- CONTINUED

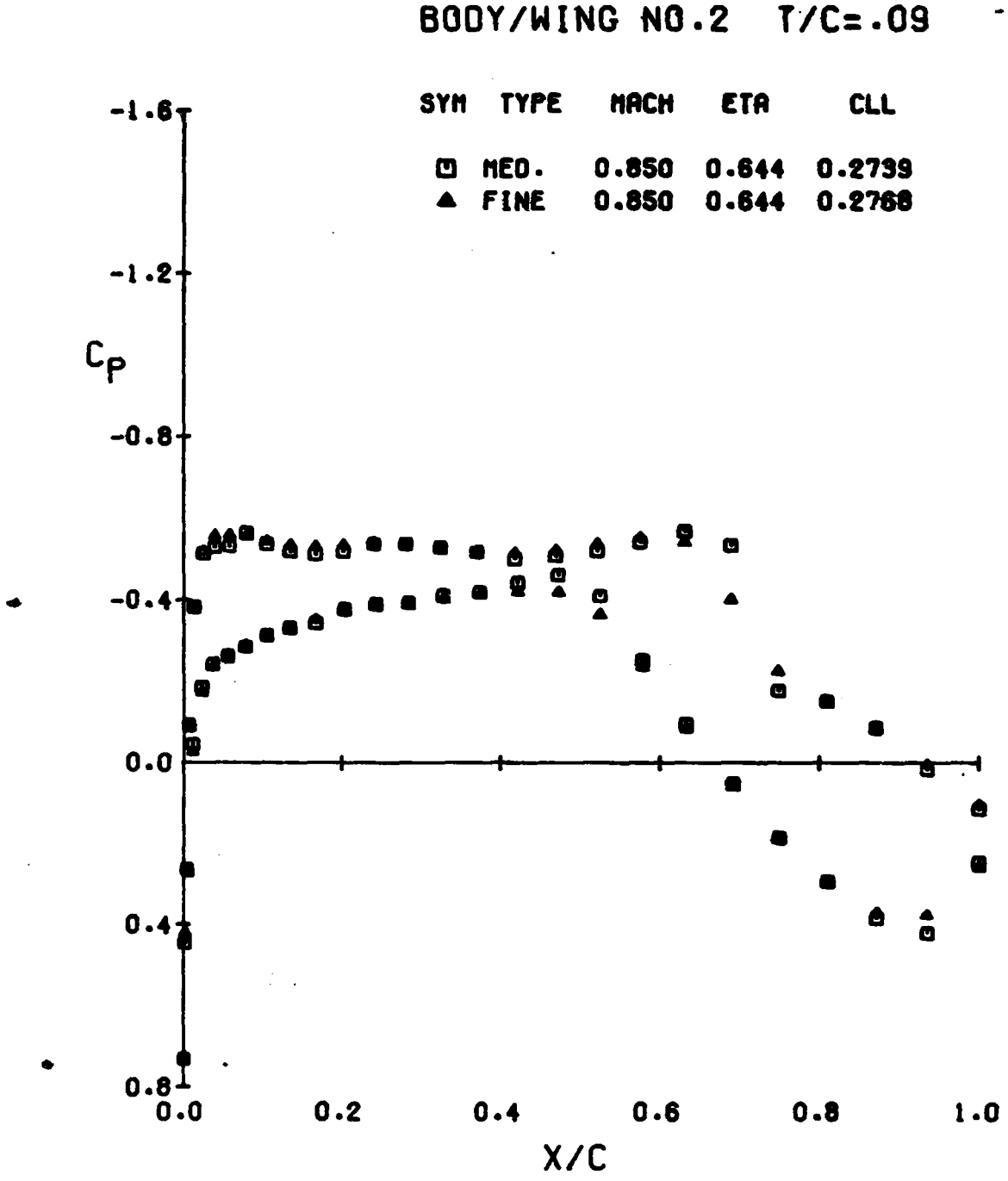

(C) ETA = 0.644

FIGURE10.- CONTINUED

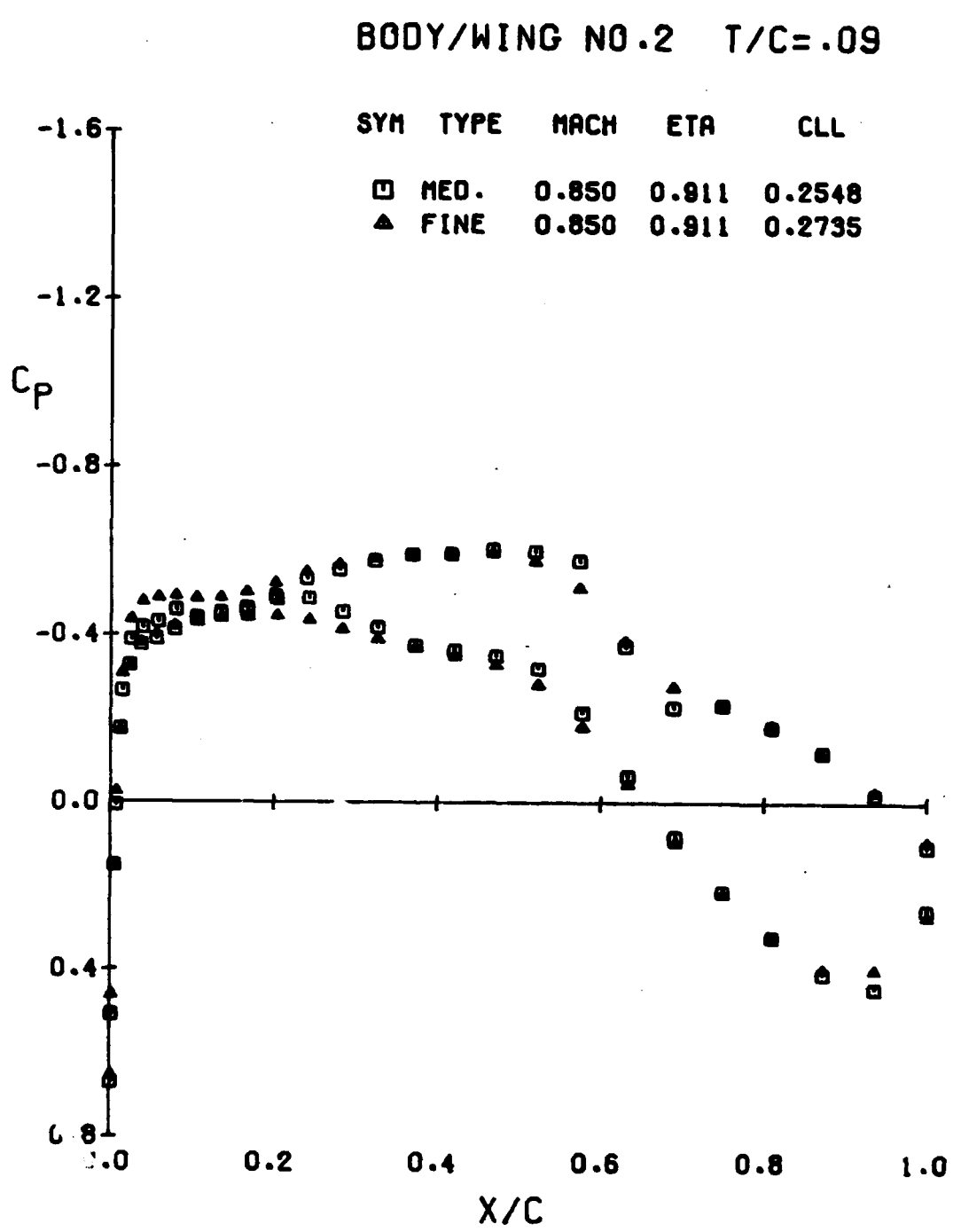

(D) ETA = 0.911

FIGURE10.- CONCLUDED

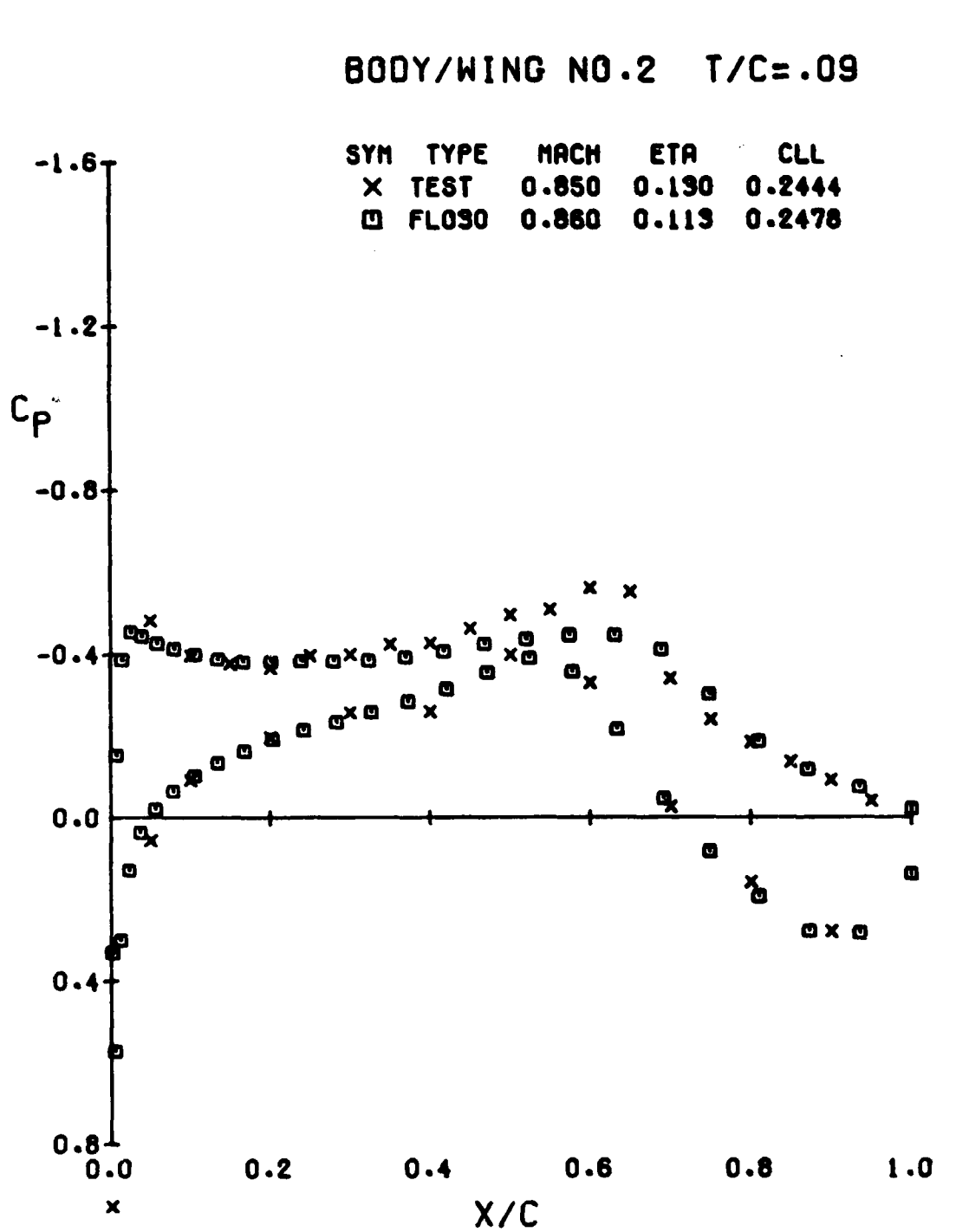

(A) ETA = 0.130

FIGURE11.- COMPARISON OF FLO30 WING/BODY PRESSURES WITH EXPERIMENT

ALPHA = 4.48 CL(EXP) = .282

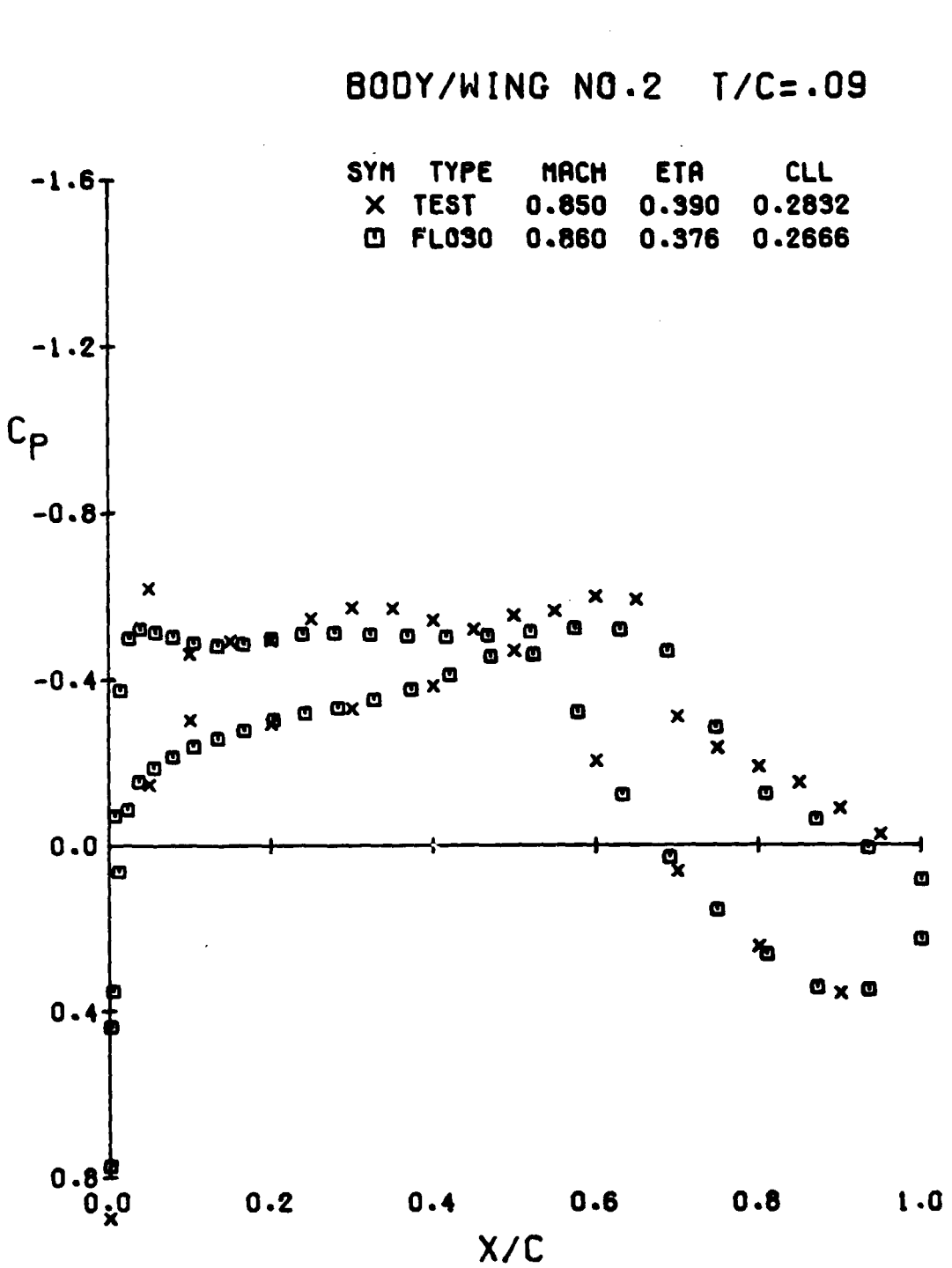

(B) ETA = 0.390

FIGURE11.- CONTINUED

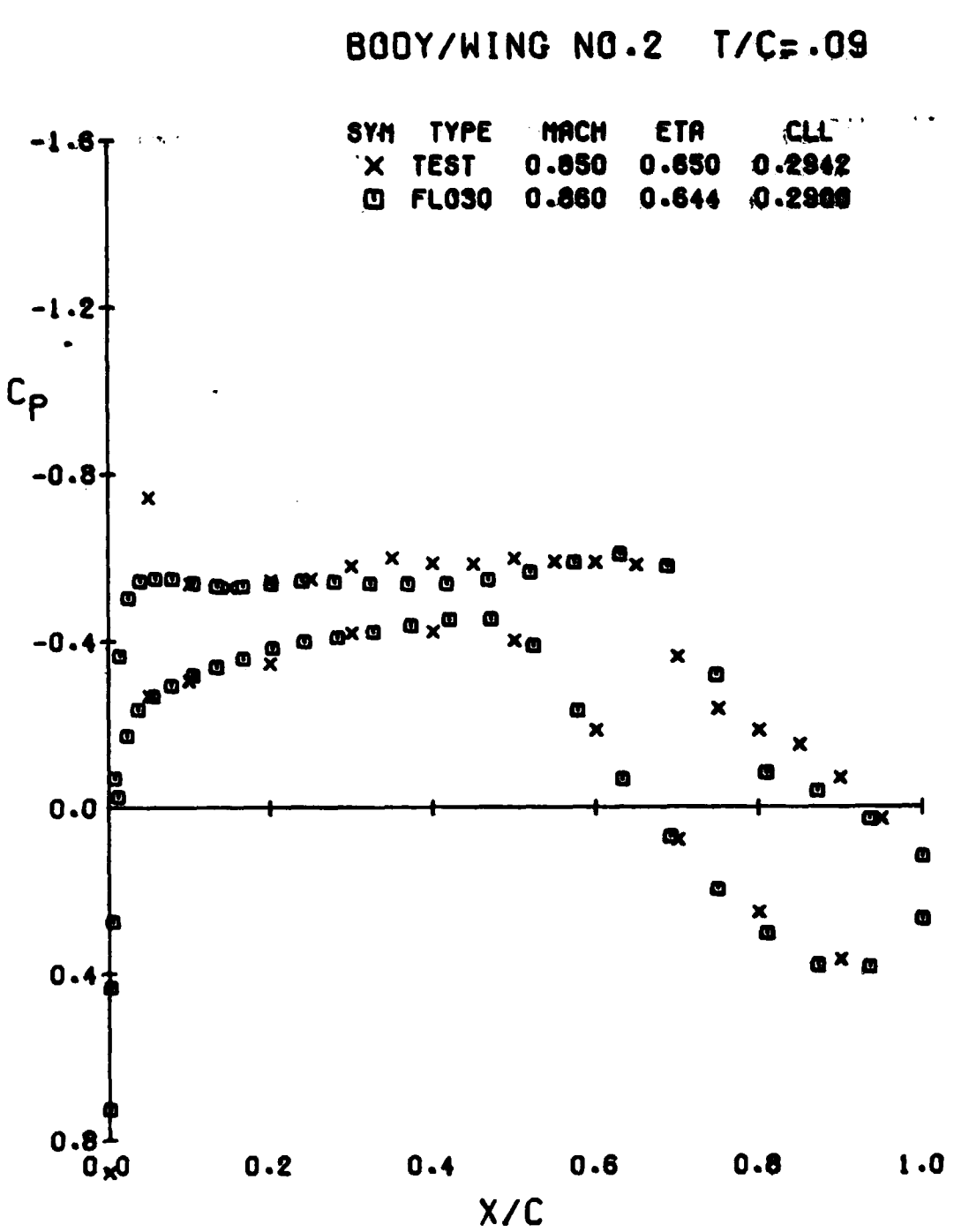

(C) ETA = 0.650

FIGURE11.- CONTINUED

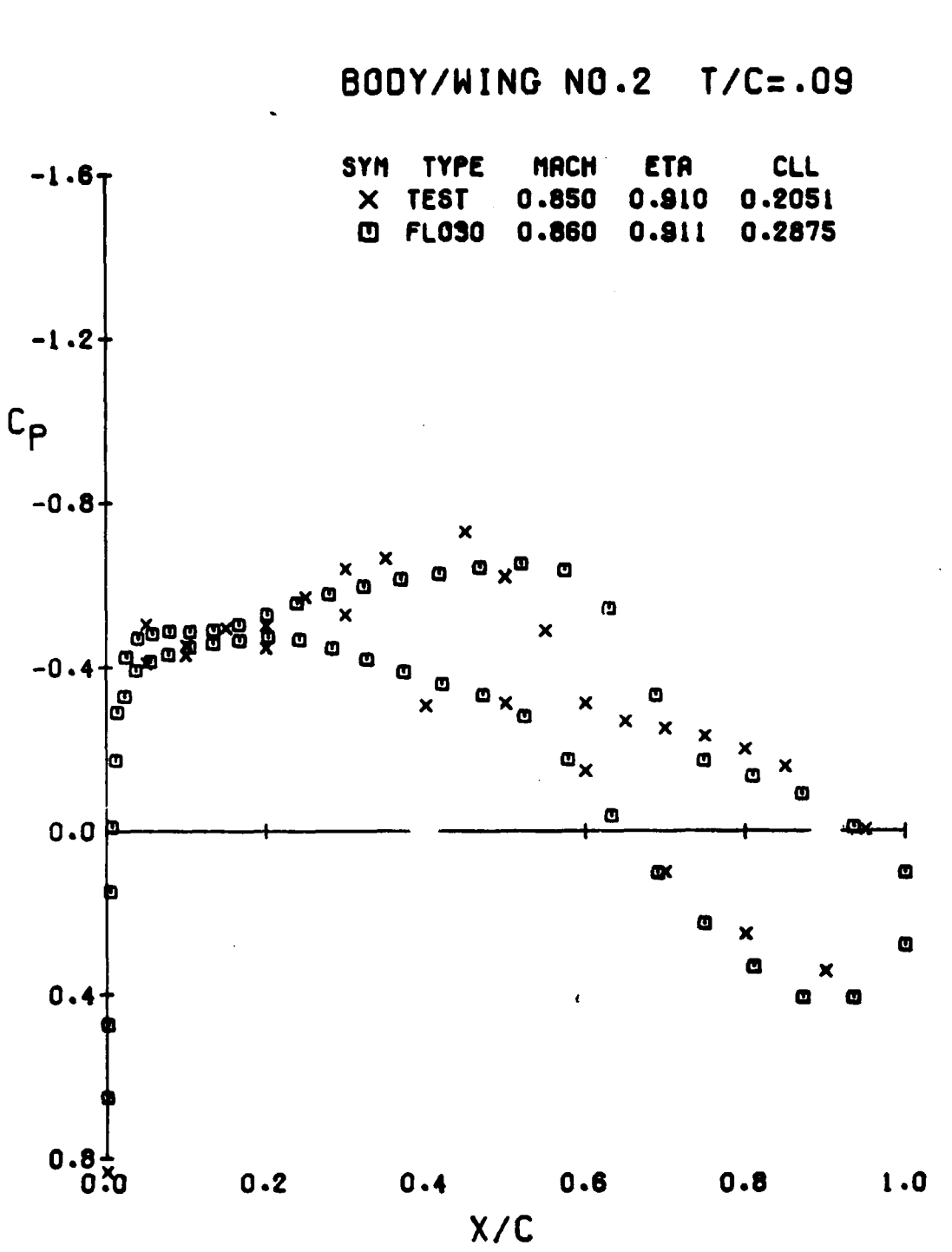

(D) ETA = 0.910

FIGURE11.- CONCLUDED

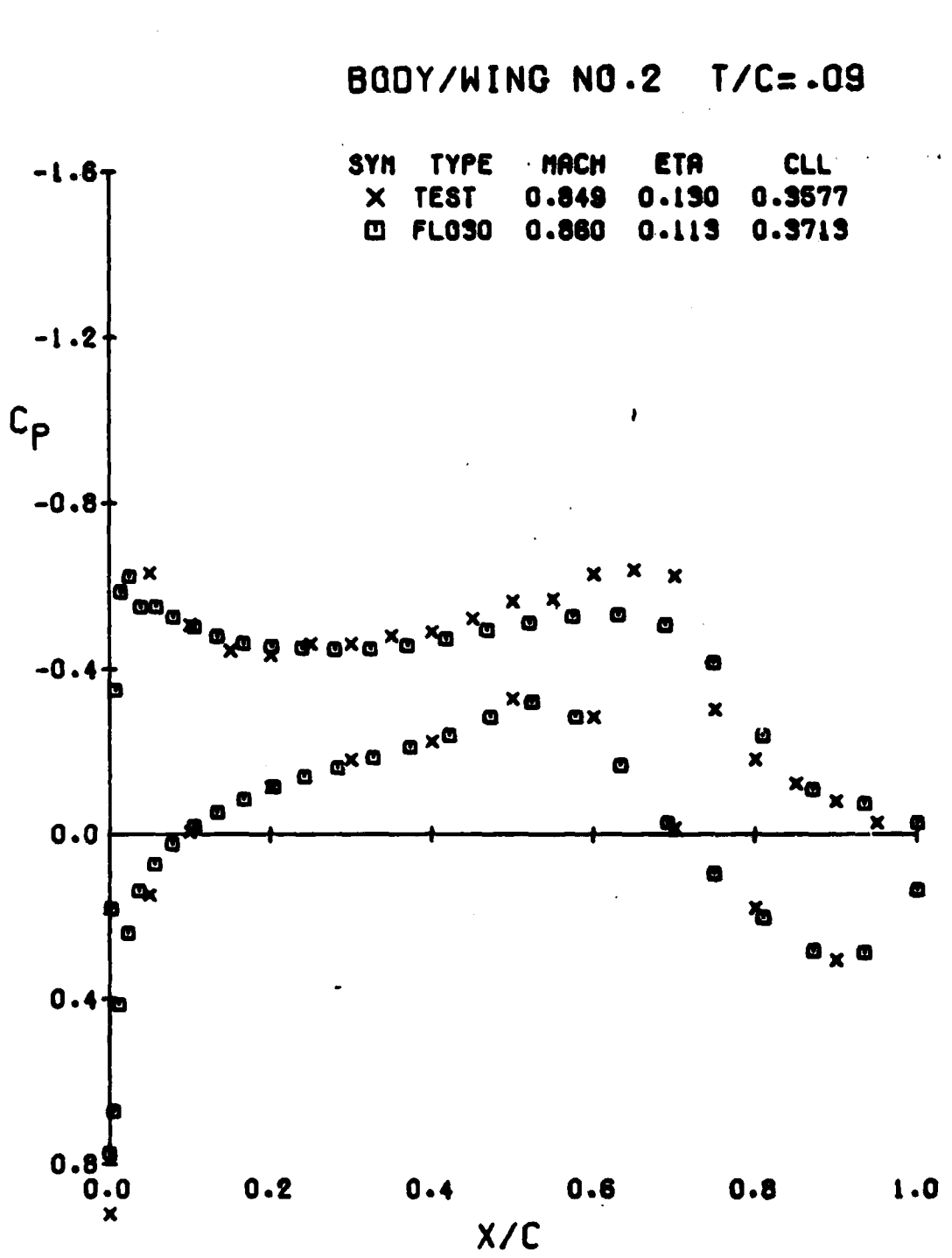

(A) ETA = 0.130

FIGURE12.- COMPARISON OF FL030 WING/BODY PRESSURES WITH EXPERIMENT

ALPHA = 5.62 CL(EXP) = .416

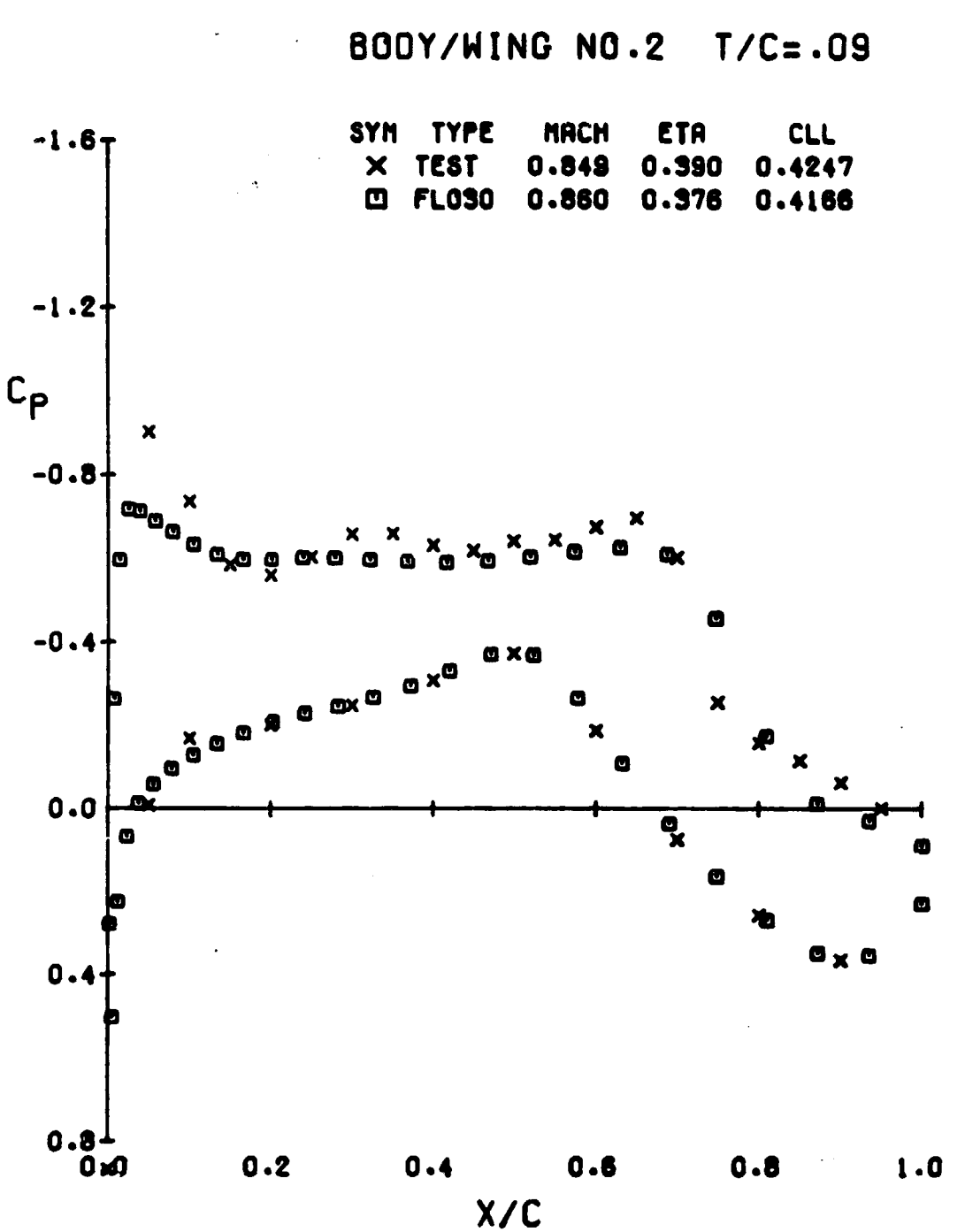

(B) ETA = 0.390

FIGURE12.- CONTINUED

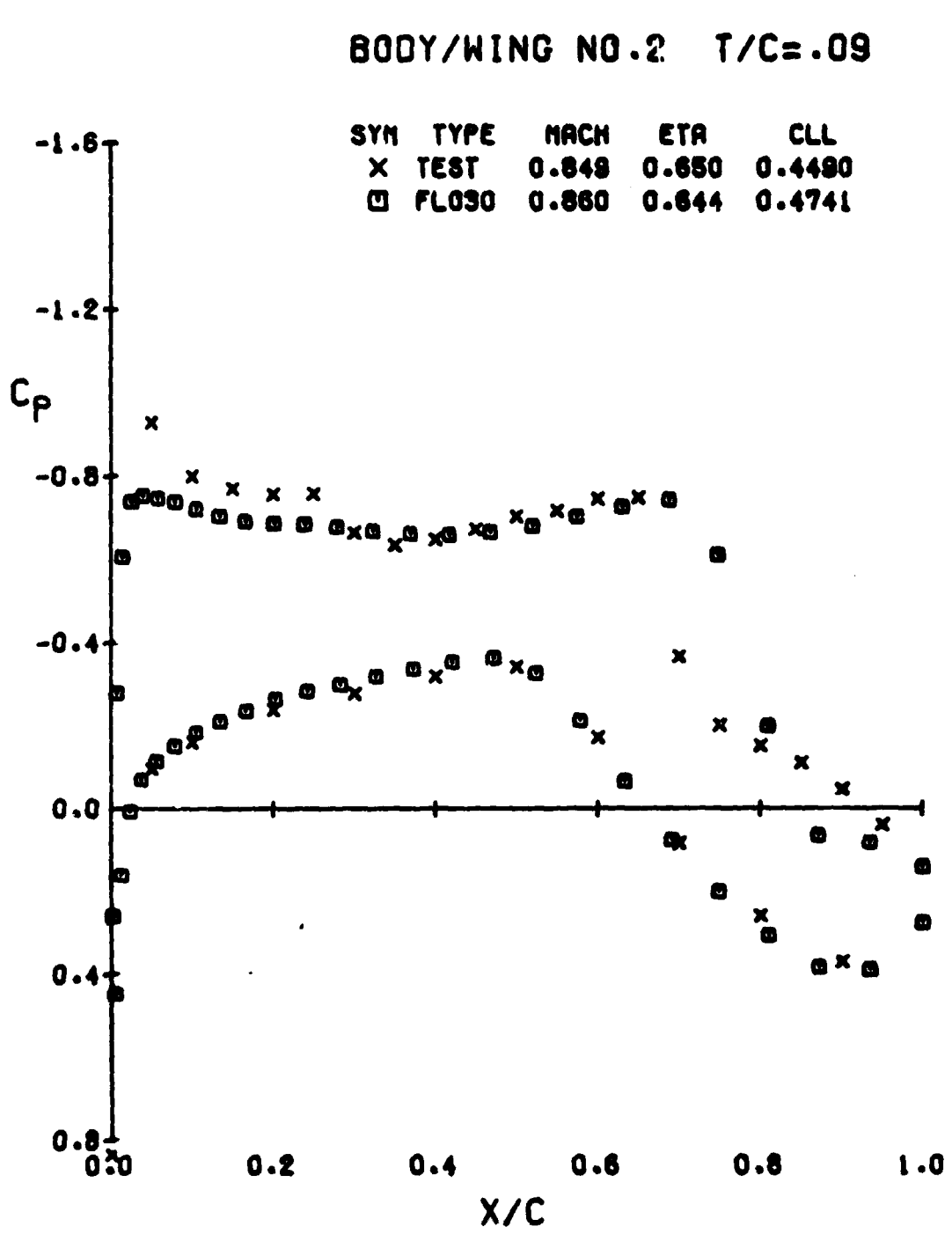

(C) ETA = 0.650

FIGURE12.- CONTINUED

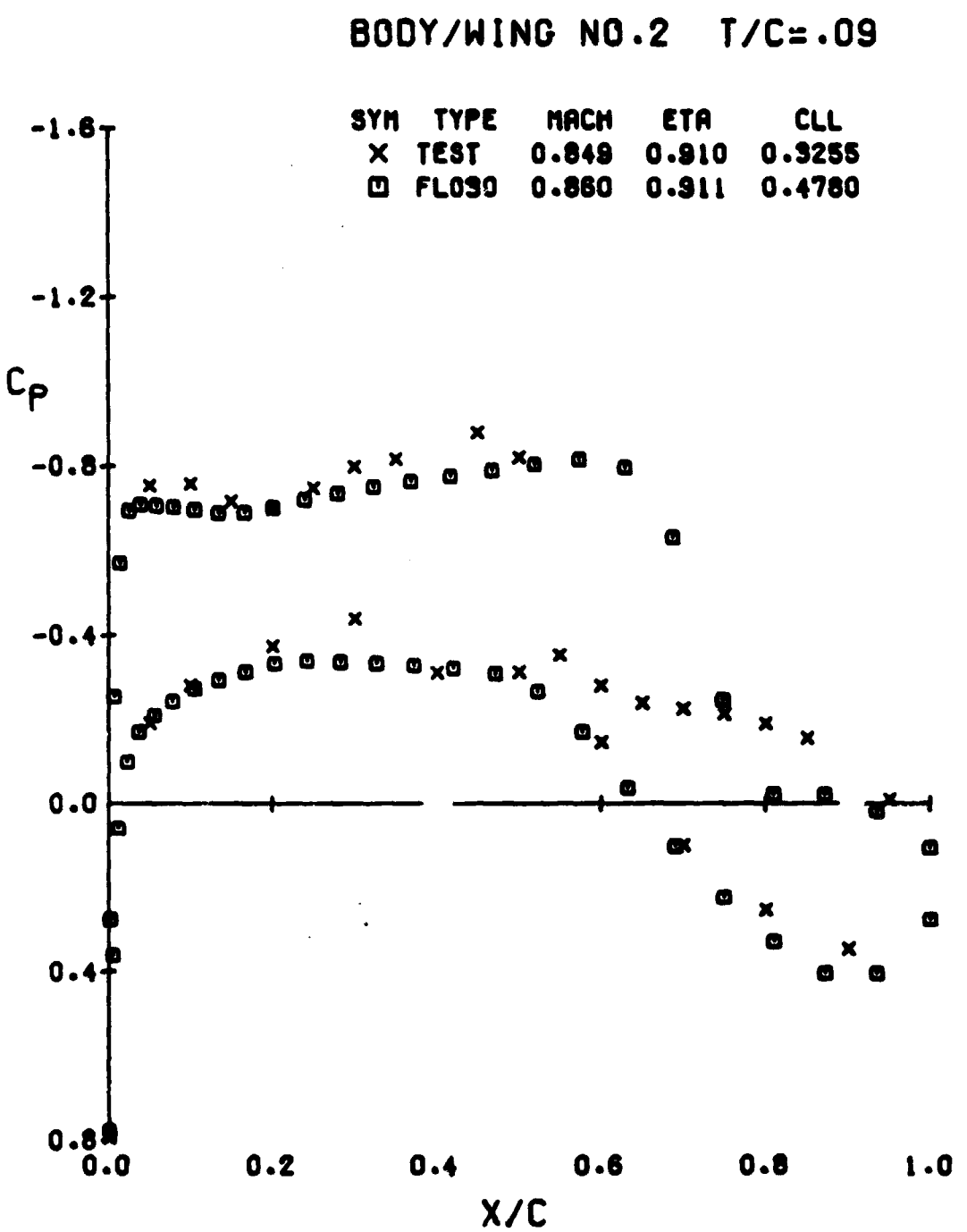

(D) ETA = 0.910

FIGURE12.- CONCLUDED

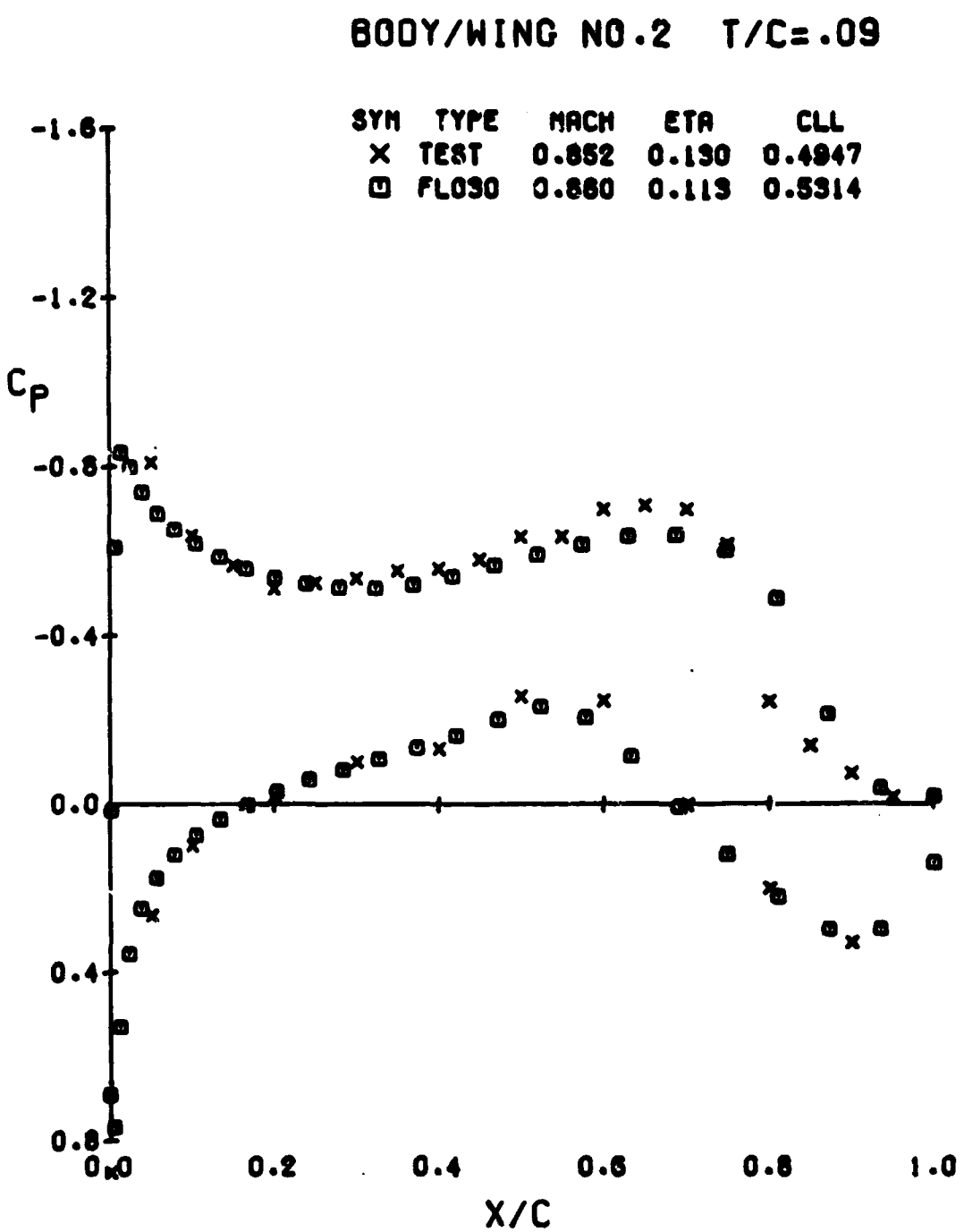

(A) ETA = 0.130

FIGURE13.- COMPARISON OF FLO30 WING/BODY PRESSURES WITH EXPERIMENT

ALPHA = 6.8 CL(EXP) = .57

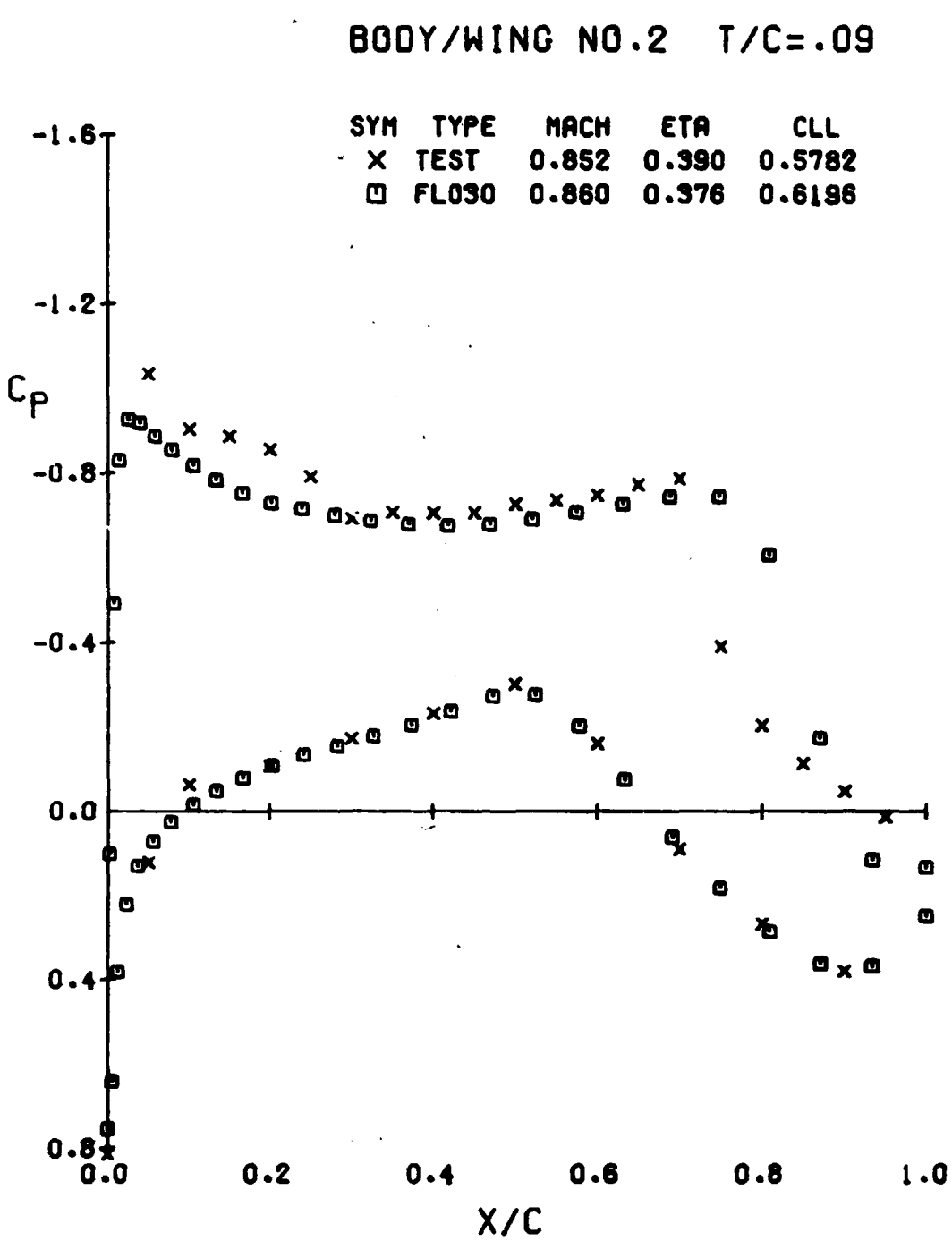

(B) ETA = 0.390

FIGURE 19.- CONTINUED

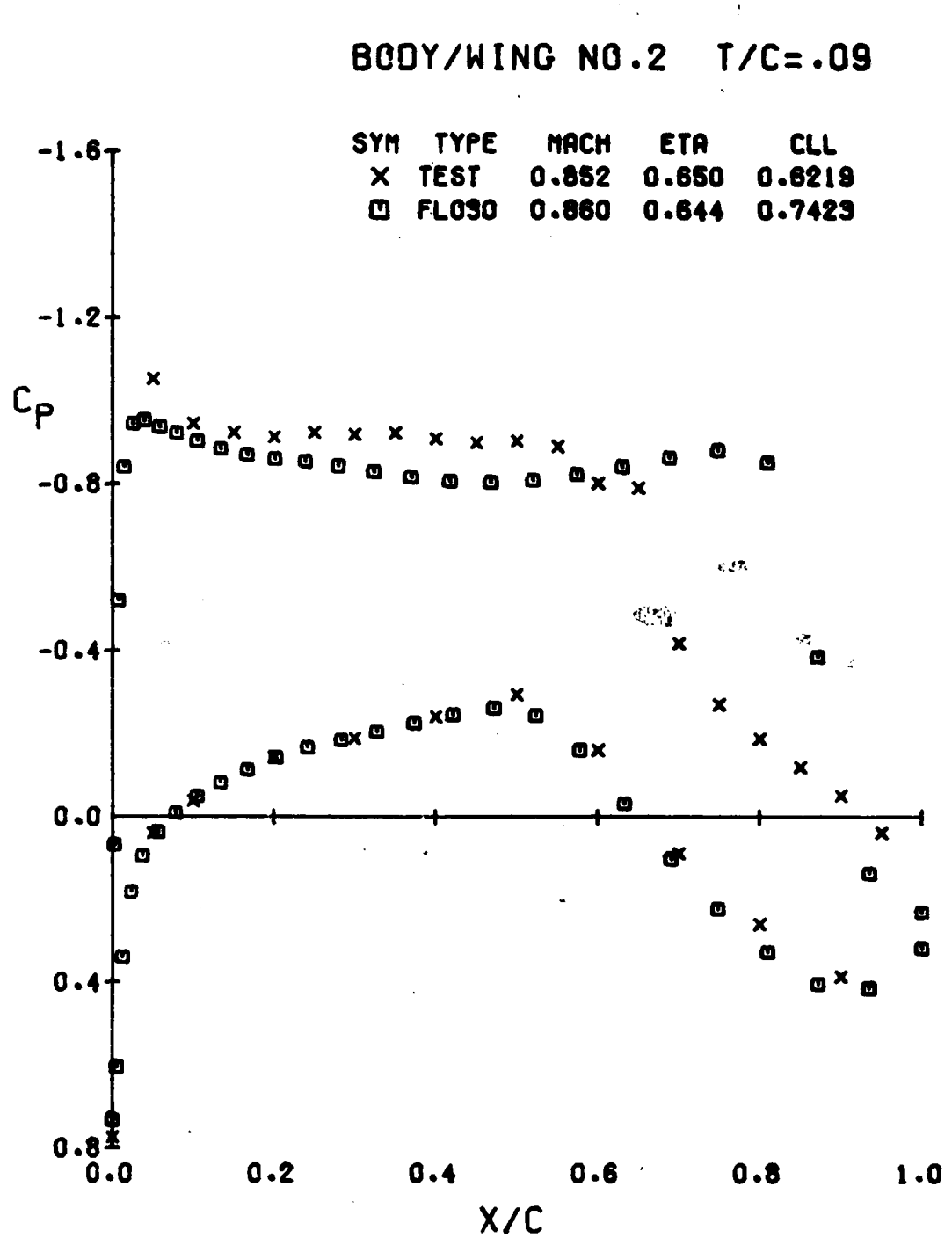

(C) ETA = 0.650

FIGURE13.- CONTINUED

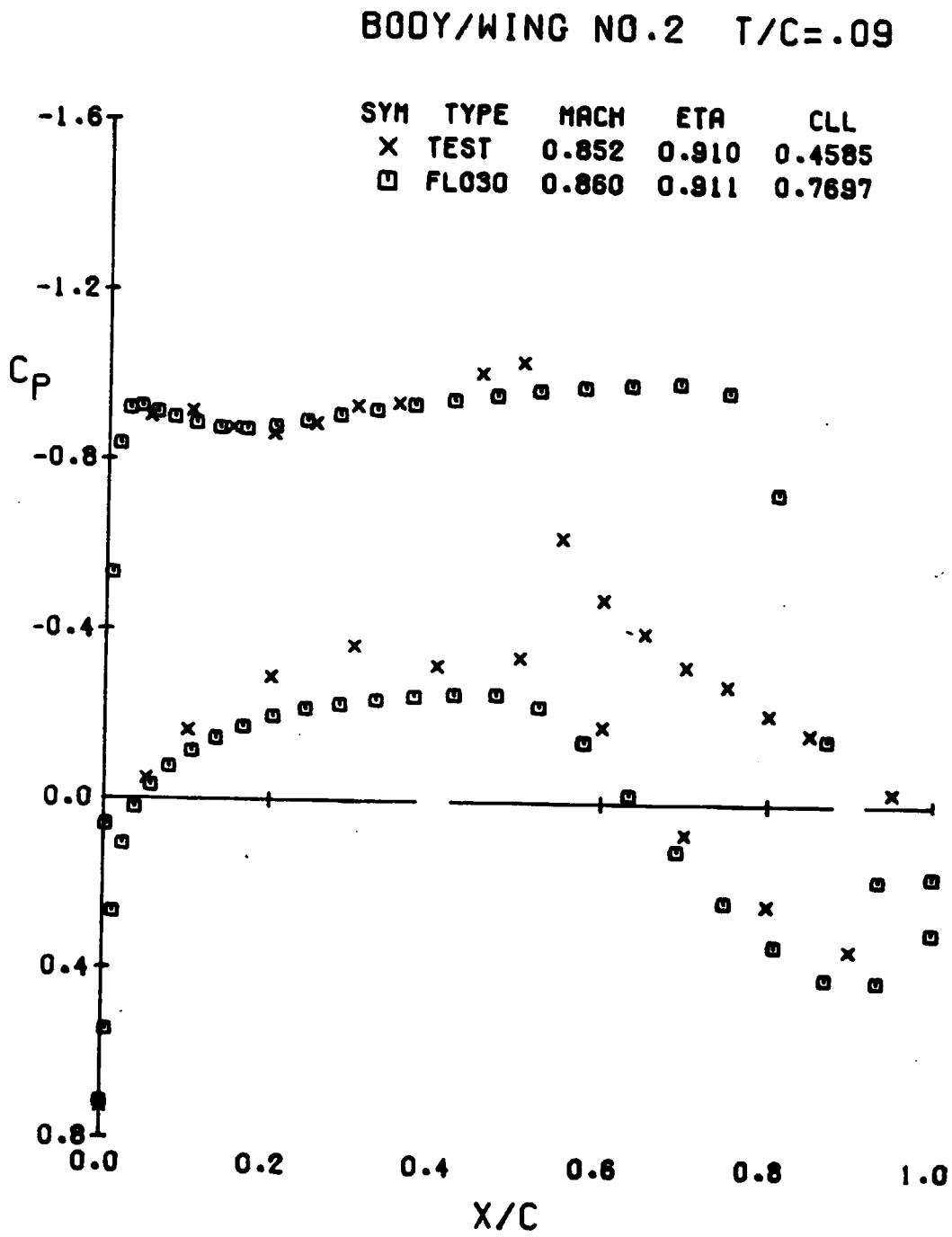

(D) ETA = 0.910

FIGURE13.- CONCLUDED

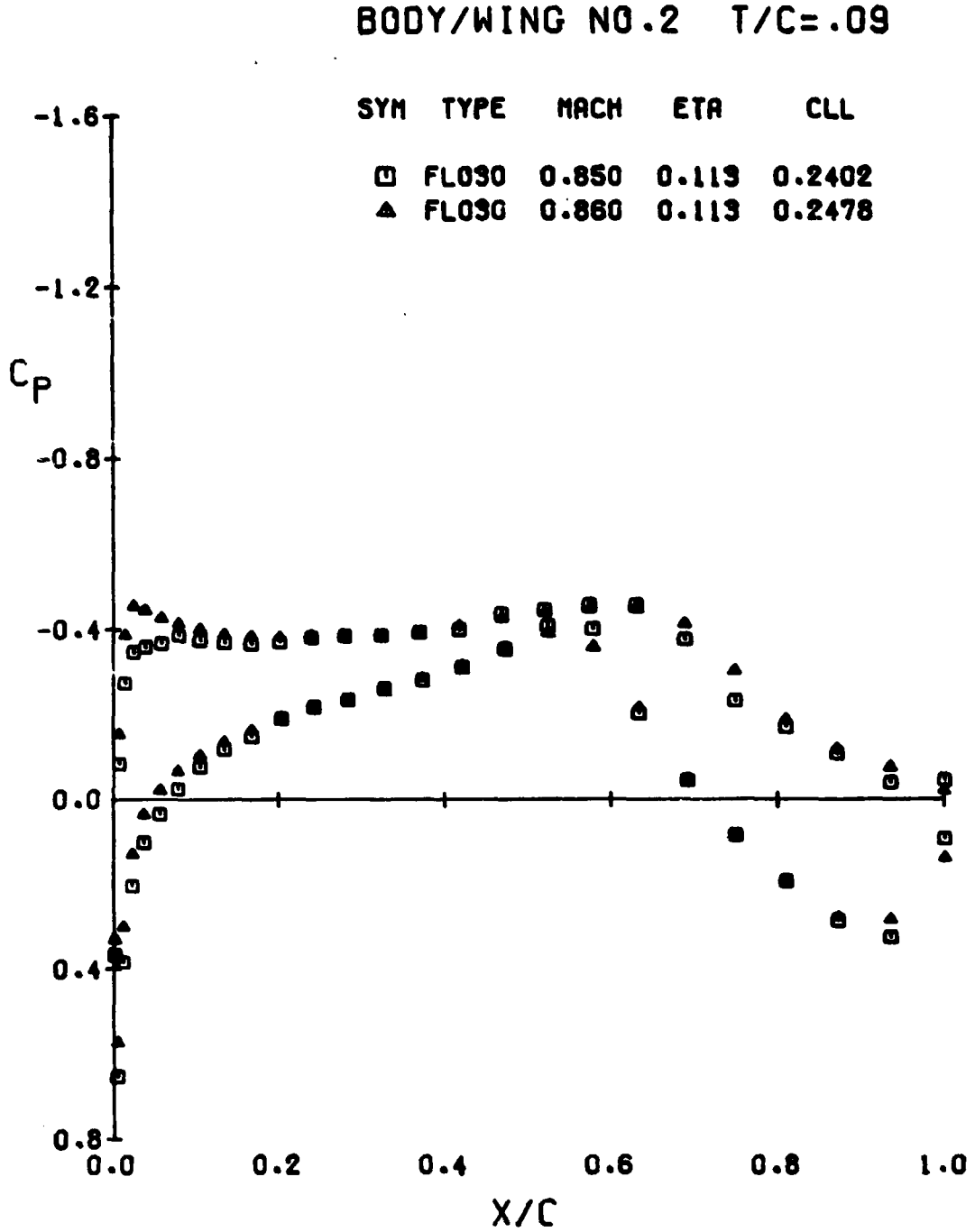

(A) ETA = 0.113

FIGURE14.- EFFECT OF 0.01 MACH NUMBER CHANGE ON PREDICTED PRESSURES CAUGHEY FLO3O TRANSONIC ANALYSIS

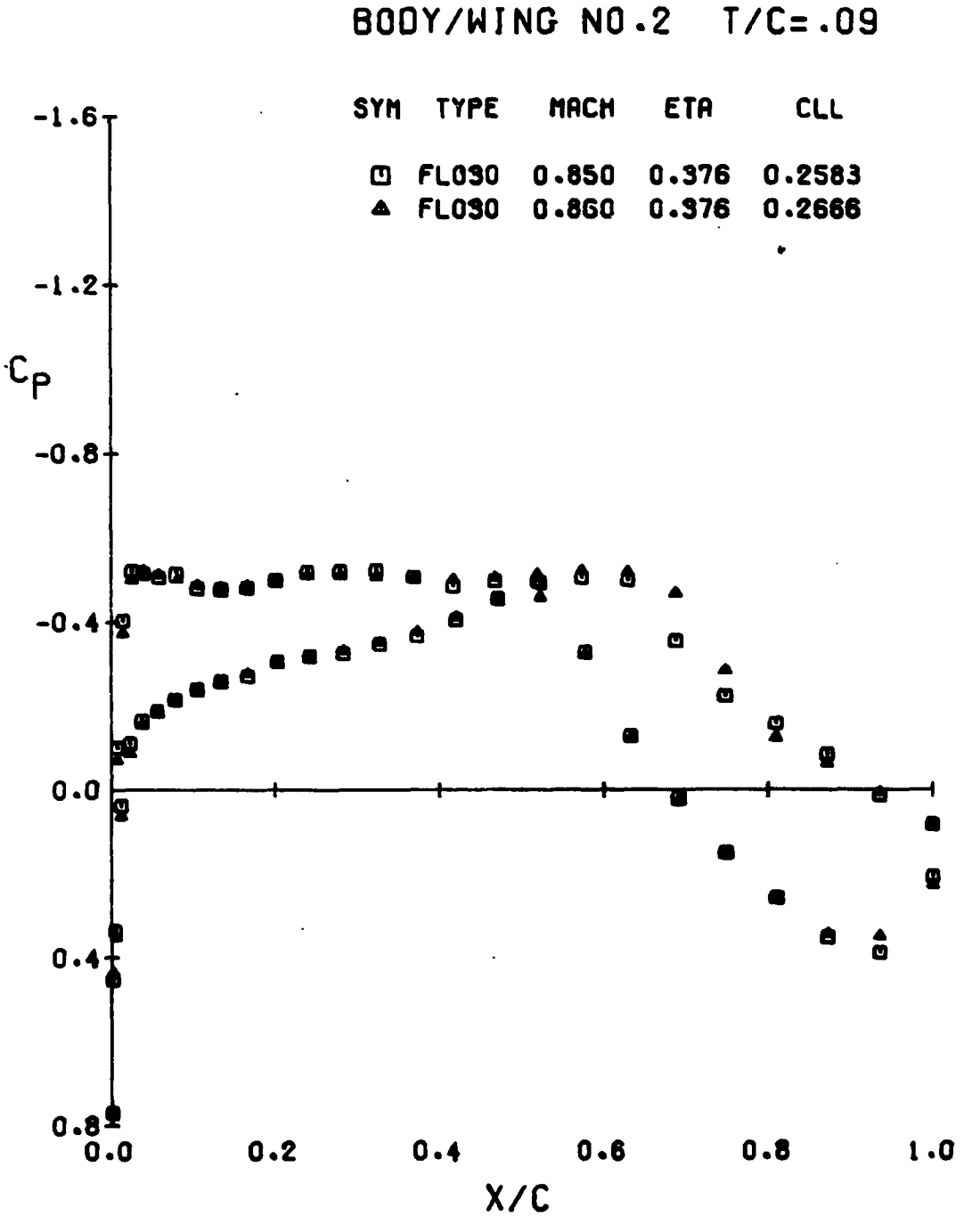

(B) ETA = 0.376

FIGURE14.- CONTINUED

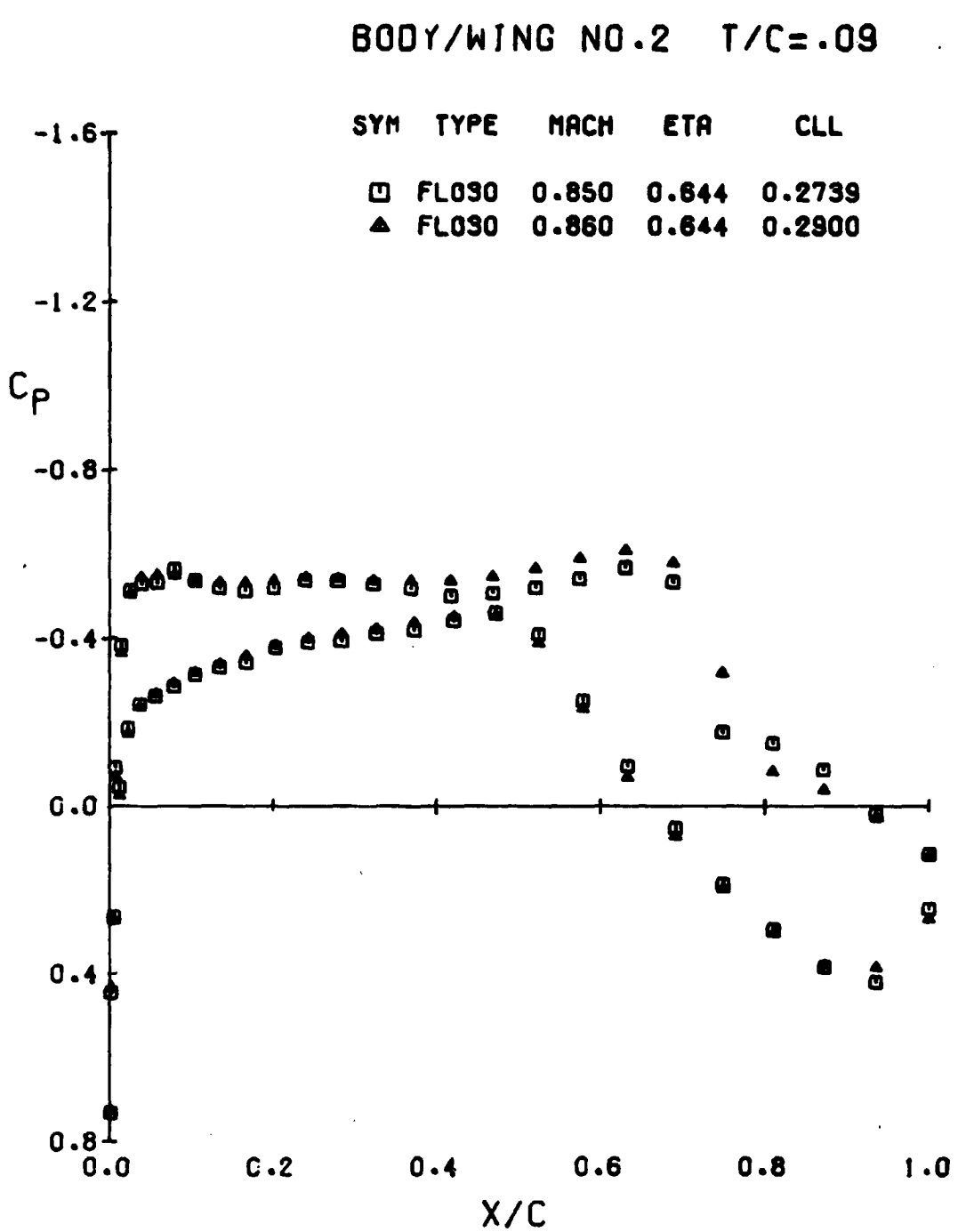

(C) ETA = 0.644

FIGURE14.- CONTINUED

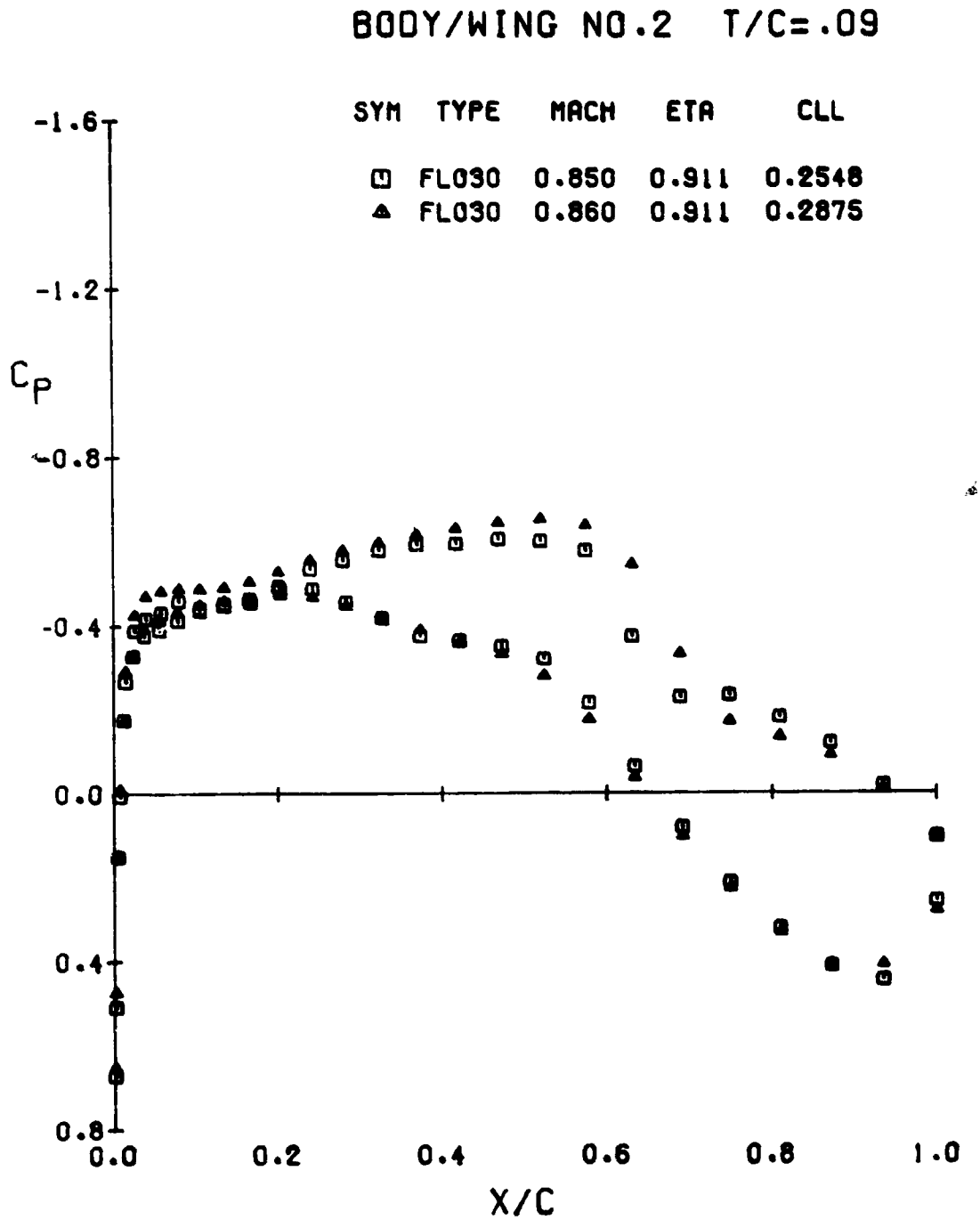

(D) ETA = 0.911

FIGURE14.- CONCLUDED

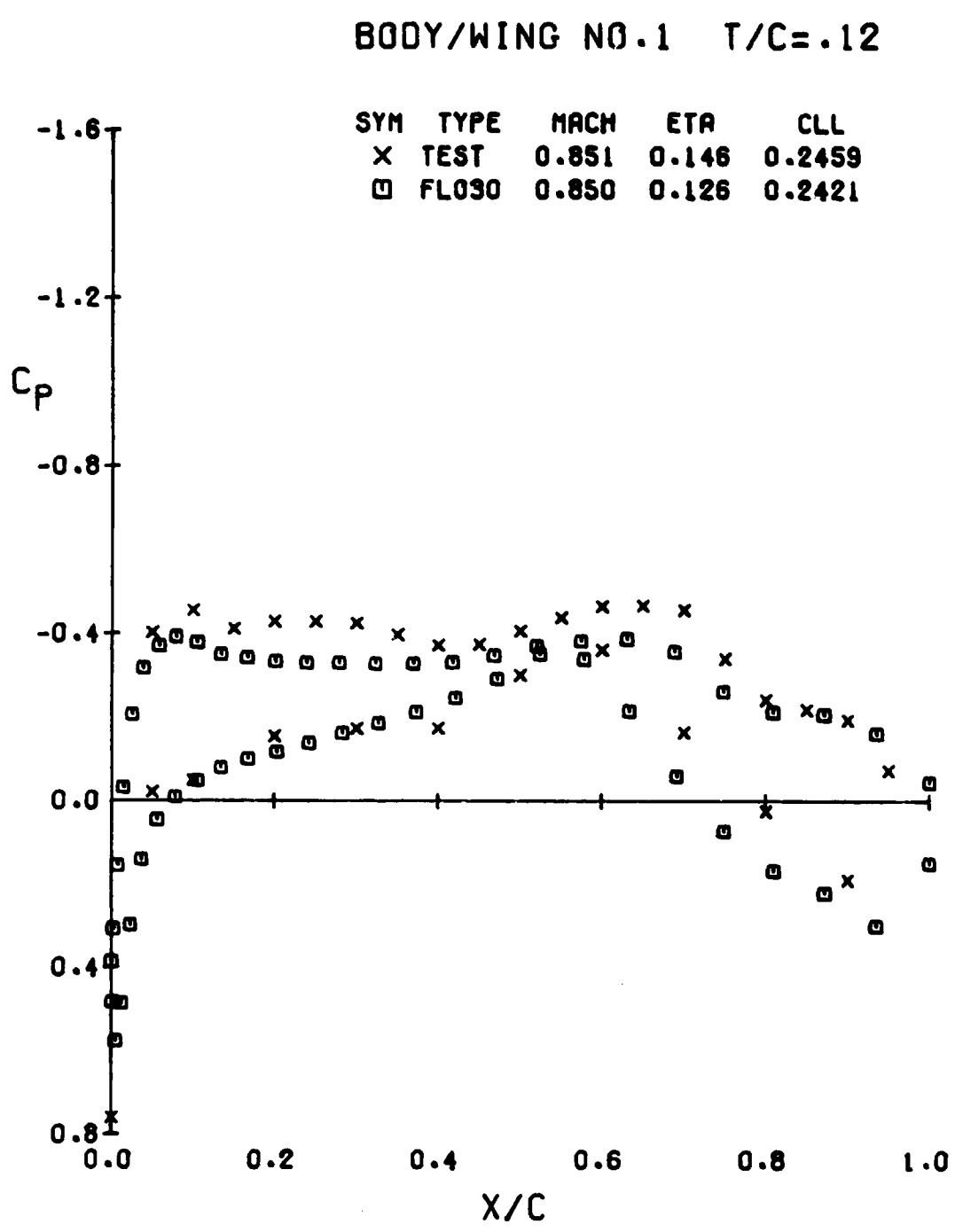

(A) ETA = 0.146

FIGURE15.- COMPARISON OF FL030 WING/BODY PRESSURES WITH EXPERIMENT

ALPHA = 4.68 CL(EXP) = .34

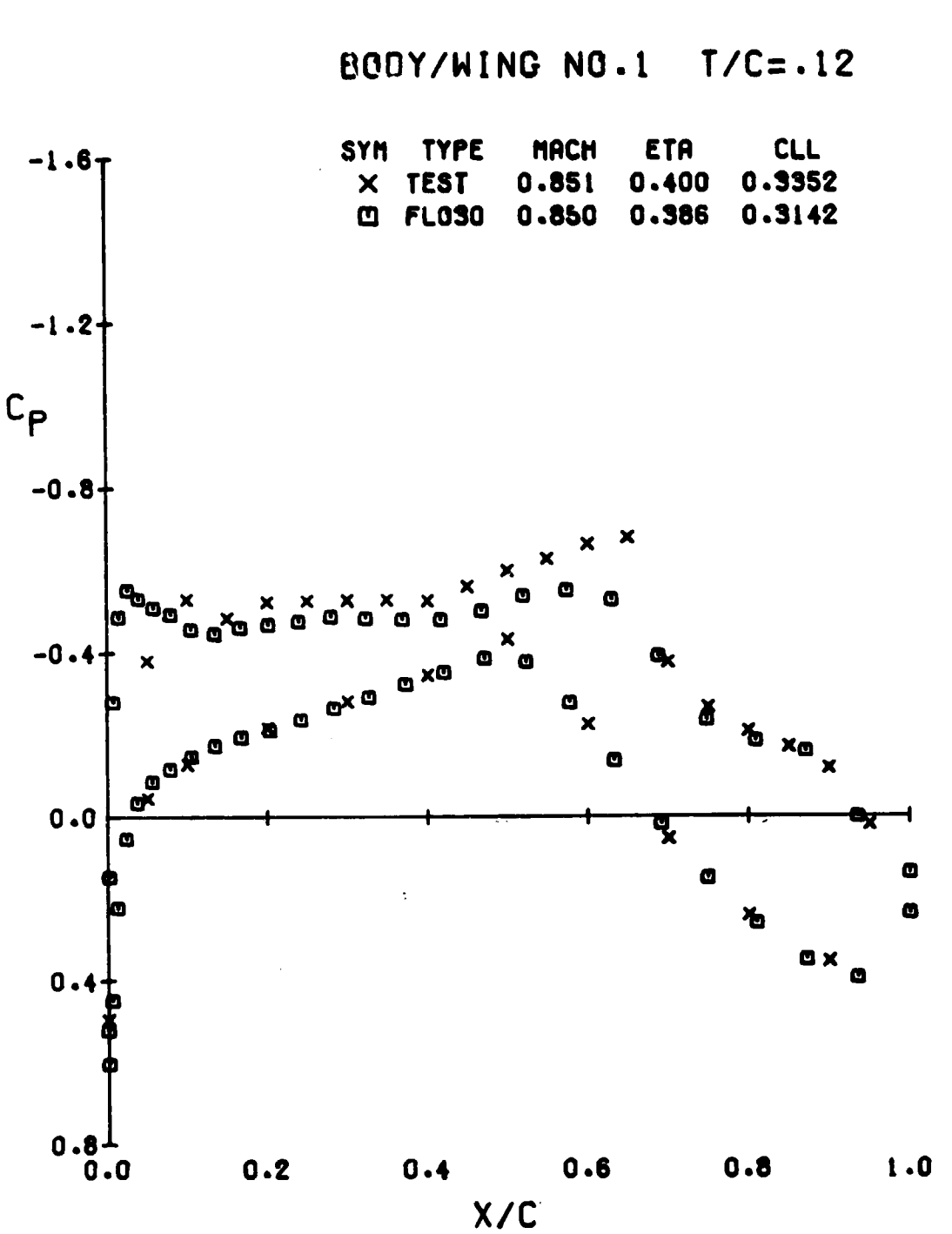

(B) ETA = 0.400

FIGURE15.- CONTINUED

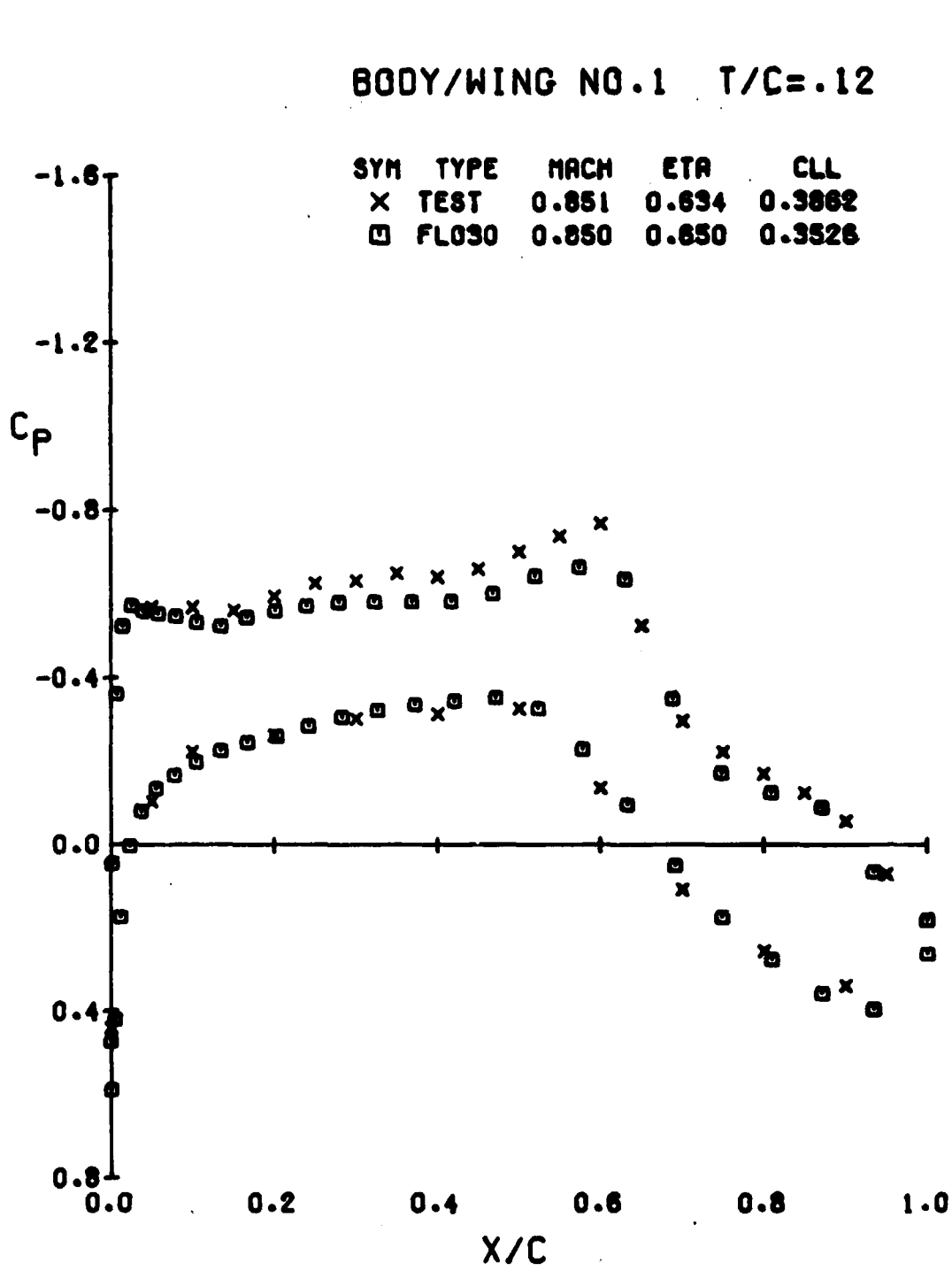

(C) ETA = 0.634

FIGURE15.- CONTINUED

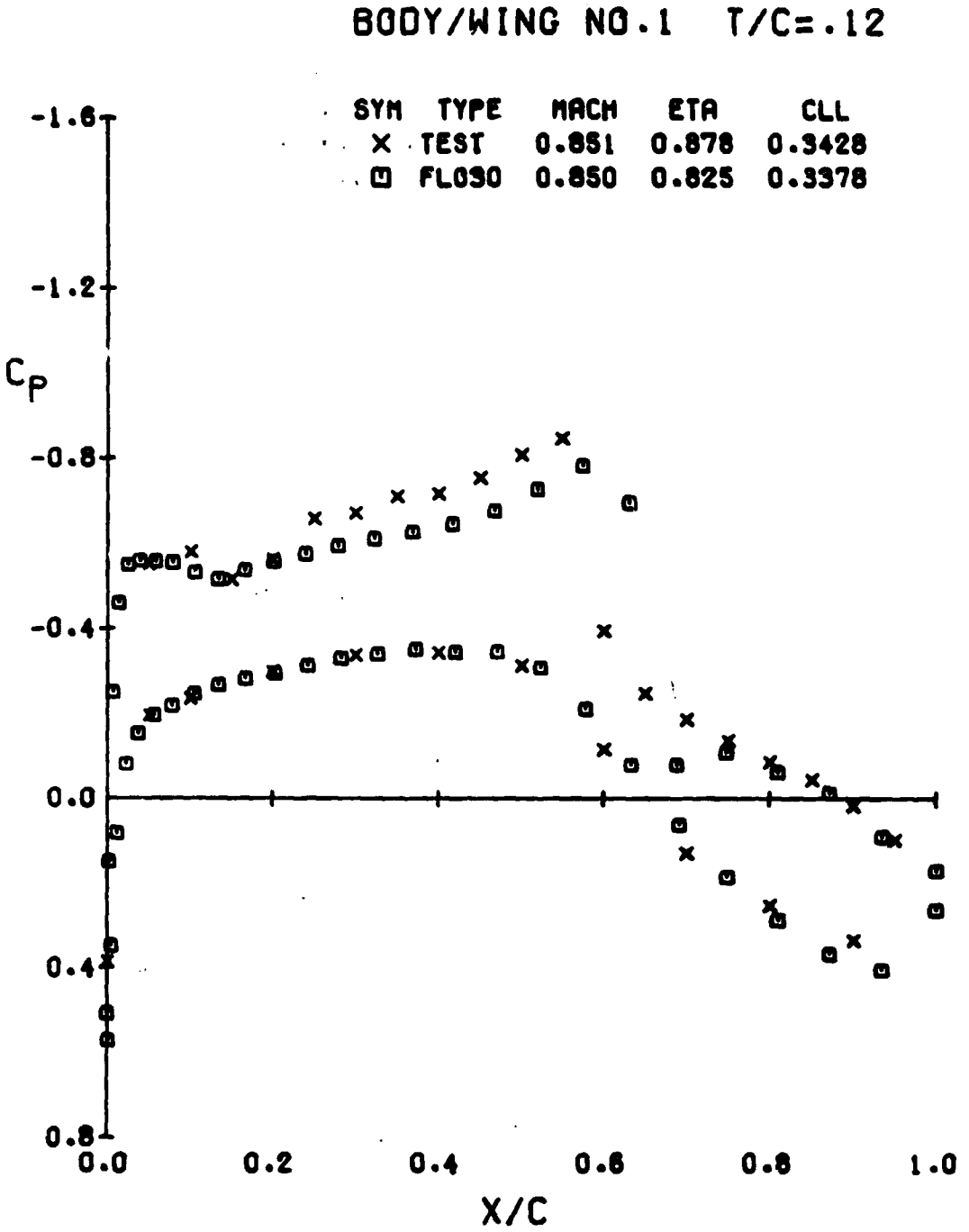

(D) ETA = 0.878

FIGURE15.- CONCLUDED

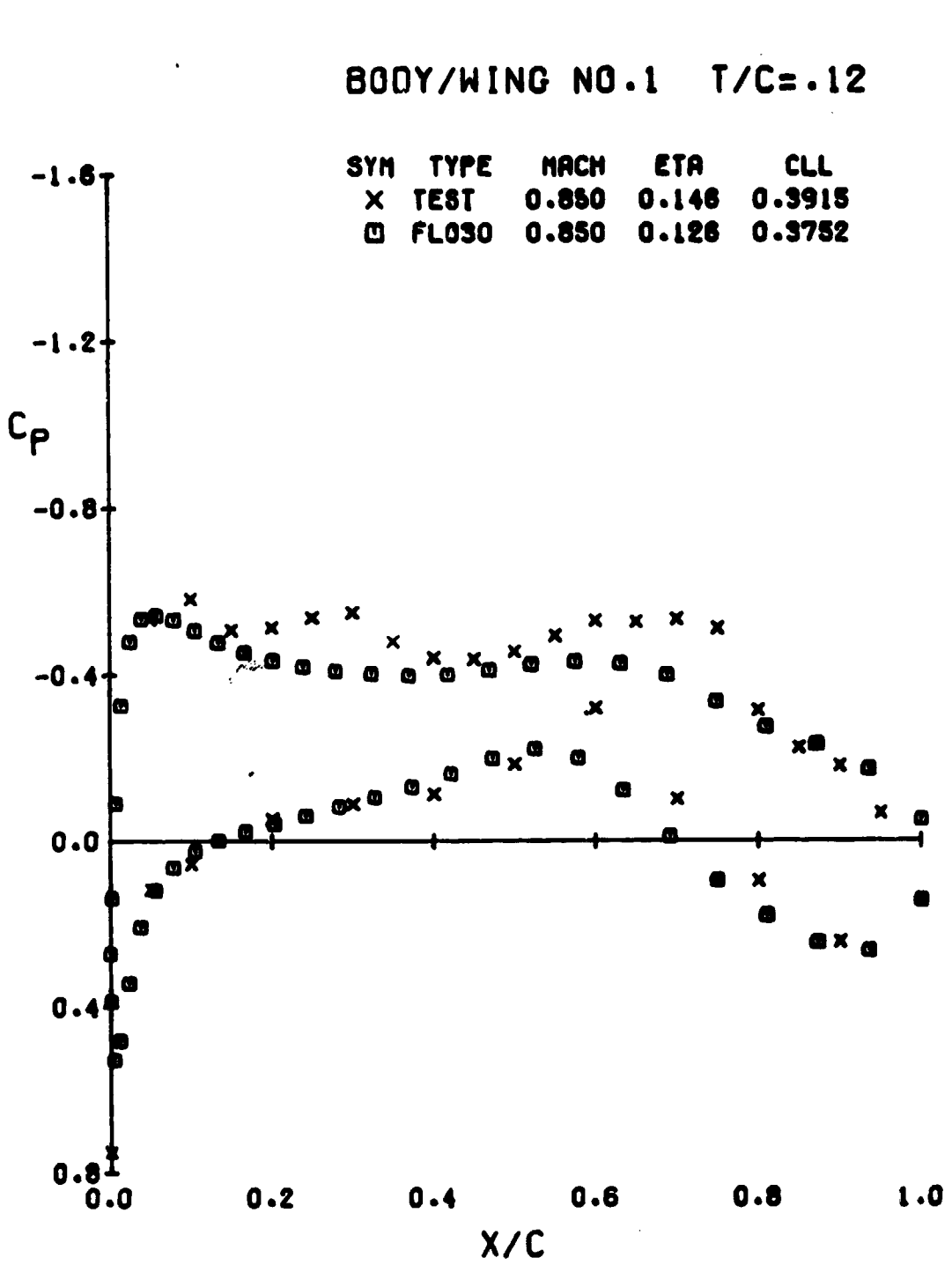

(A) ETA = 0.146

FIGURE16.- COMPARISON OF FLO30 WING/BODY PRESSURES WITH EXPERIMENT

ALPHA = 6.52 CL(EXP) = .515

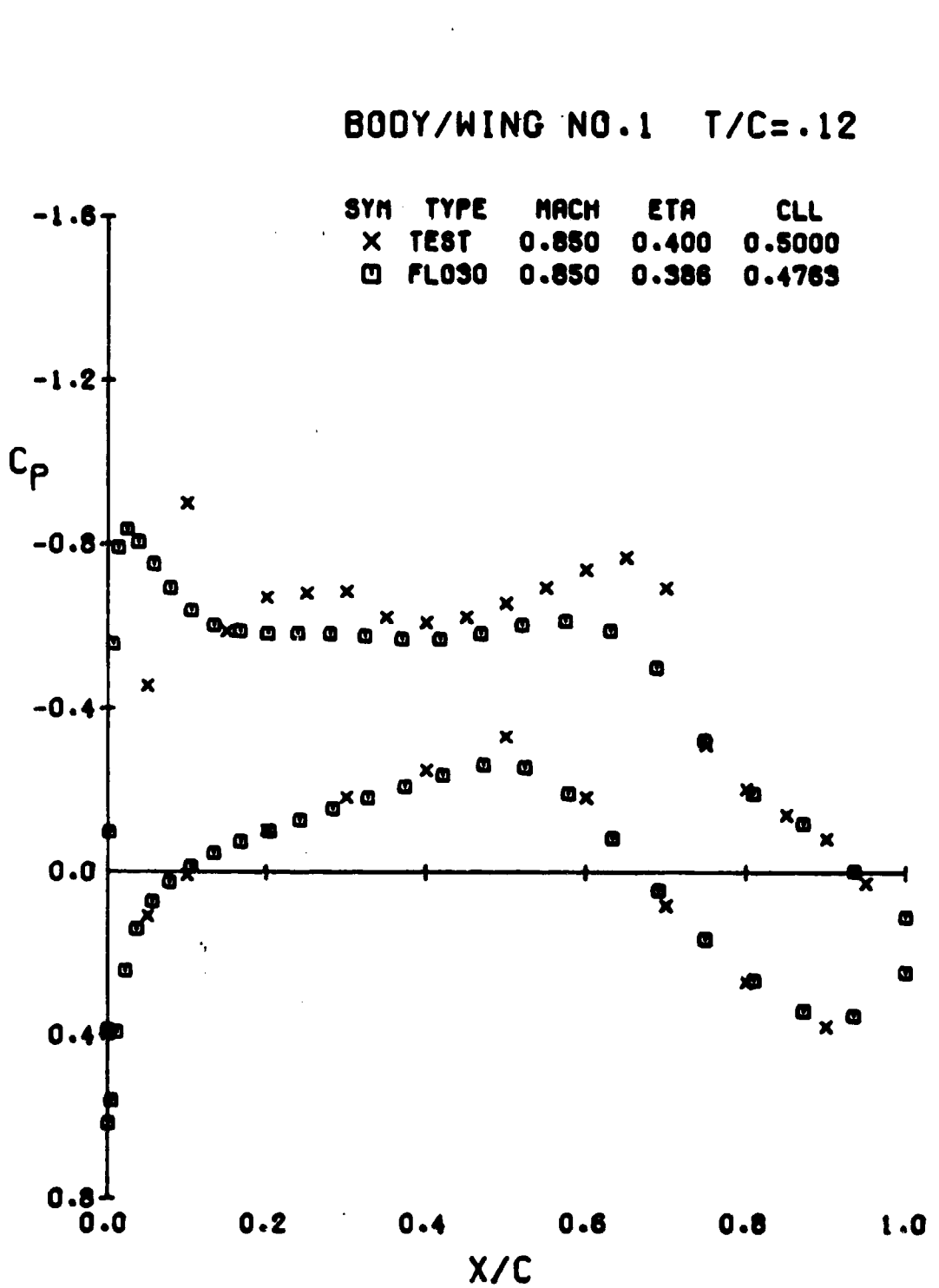

(B) ETA = 0.400

FIGURE16.- CONTINUED

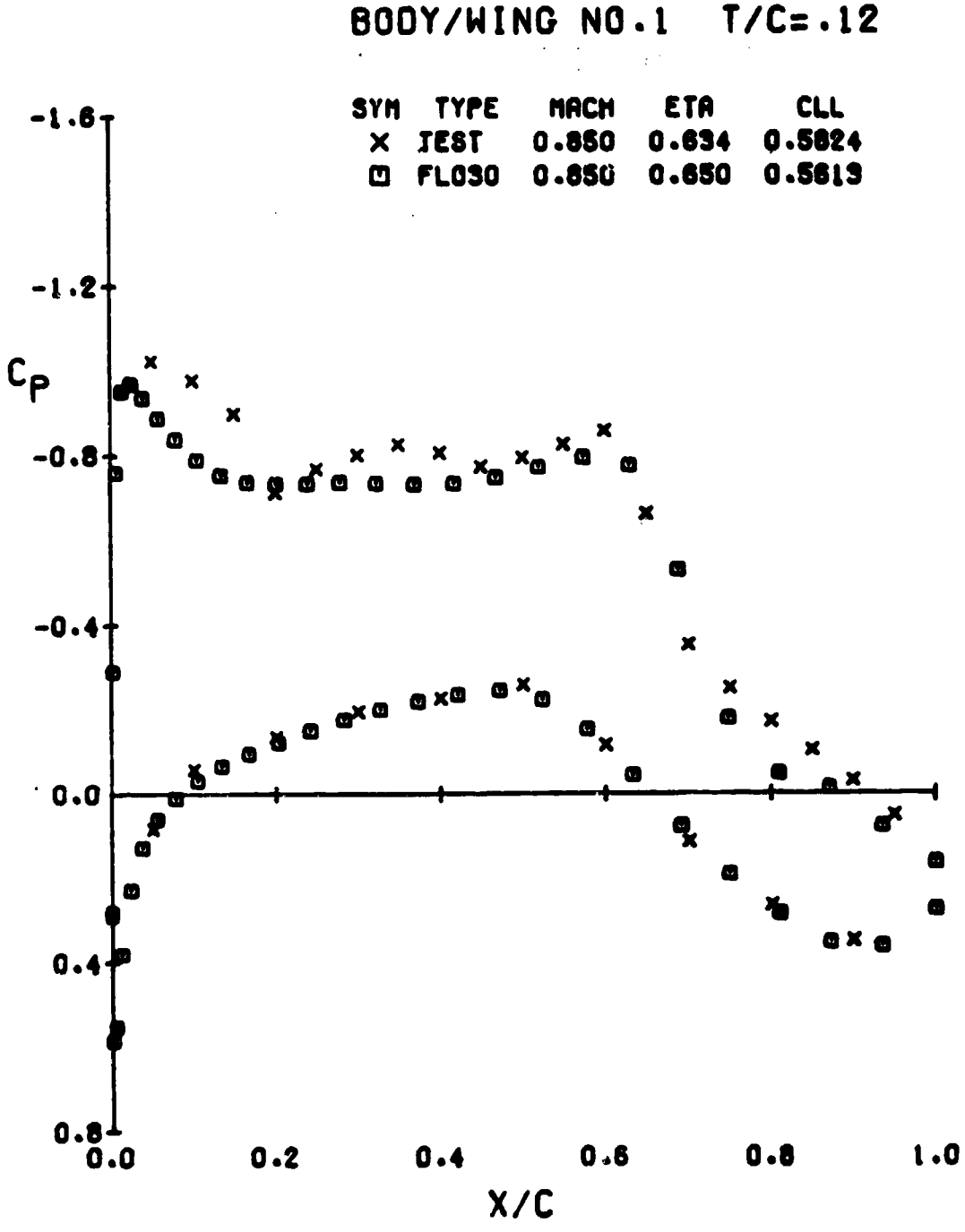

(C) ETA = 0.634

FIGURE16.- CONTINUED

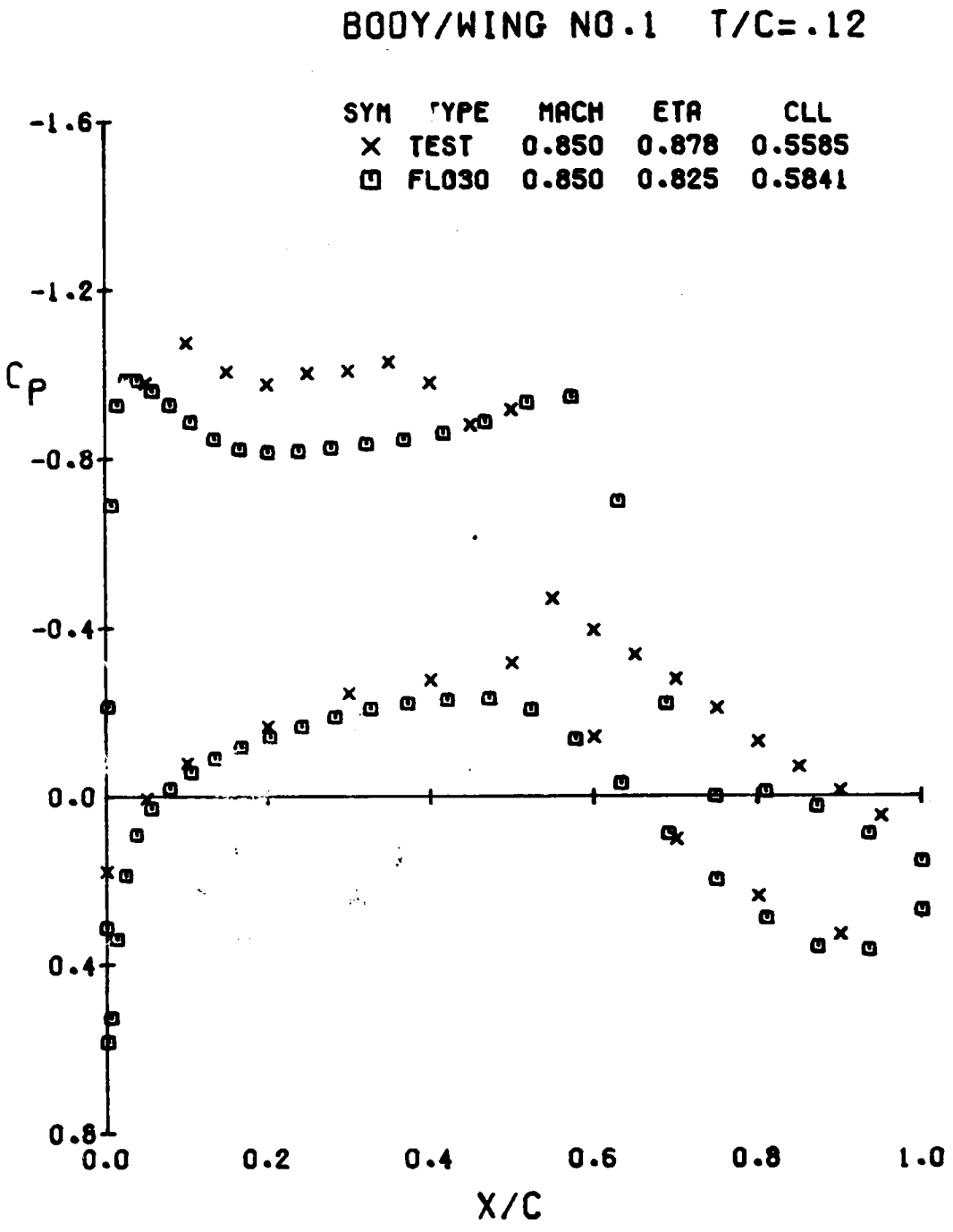

(D) ETA = 0.878

FIGURE16.- CONCLUDED

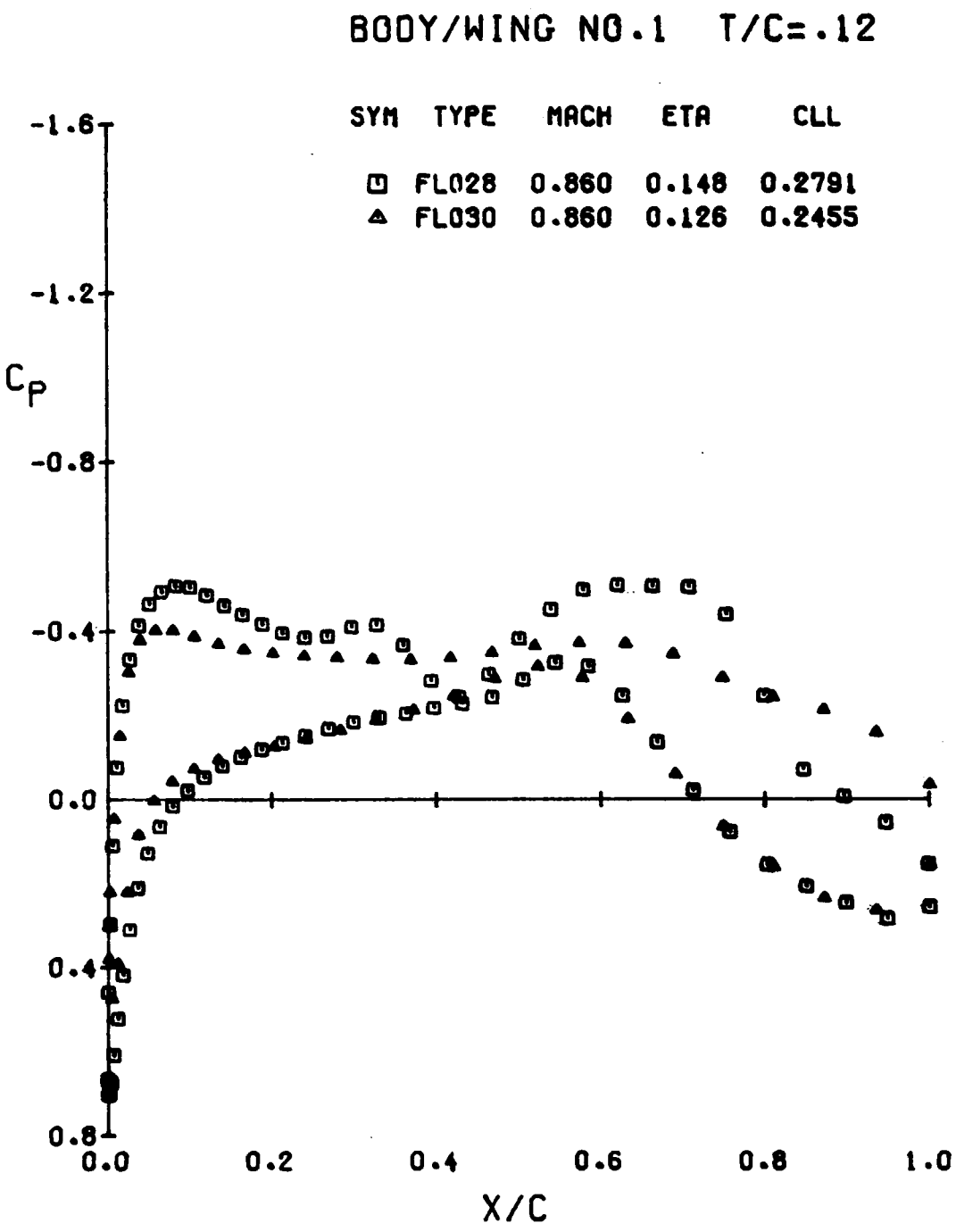

(A) ETA = 0.148

FIGURE17.- COMPARISON OF FL028 AND FL030 SOLUTIONS

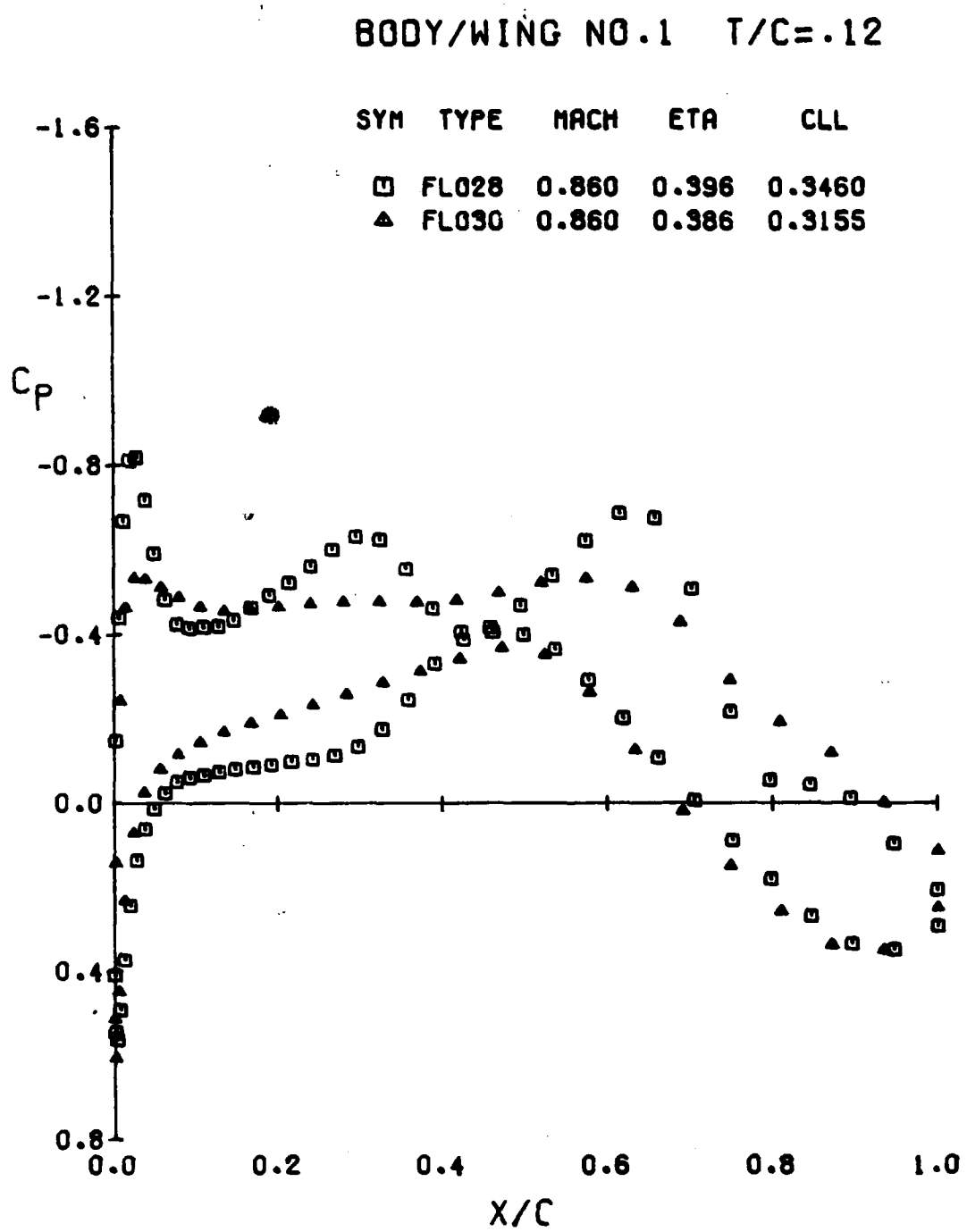

(B) ETA = 0.396

FIGURE17.- CONTINUED

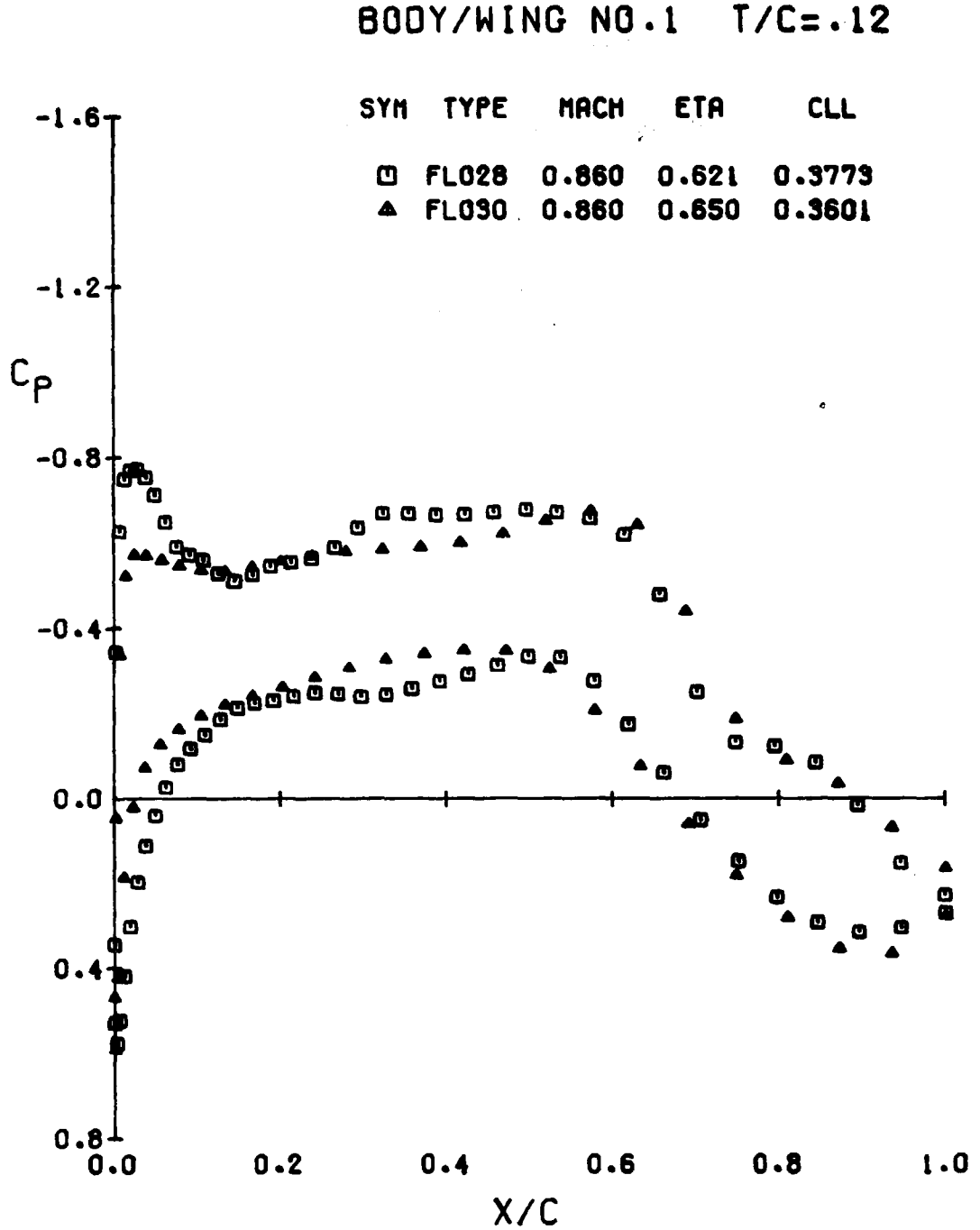

(C) ETA = 0.621

FIGURE17.- CONTINUED

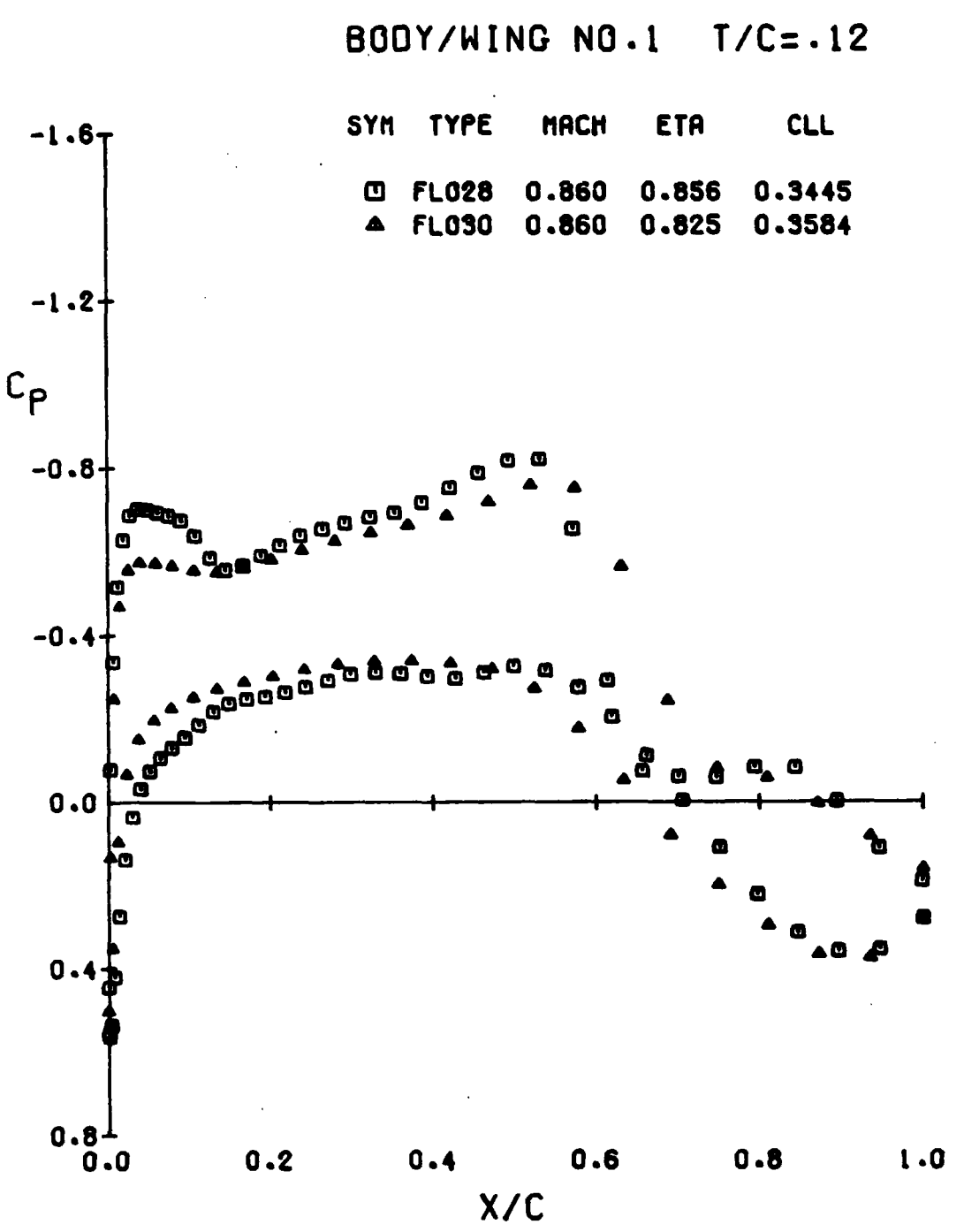

(D) ETA = 0.856

FIGURE17.- CONCLUDED

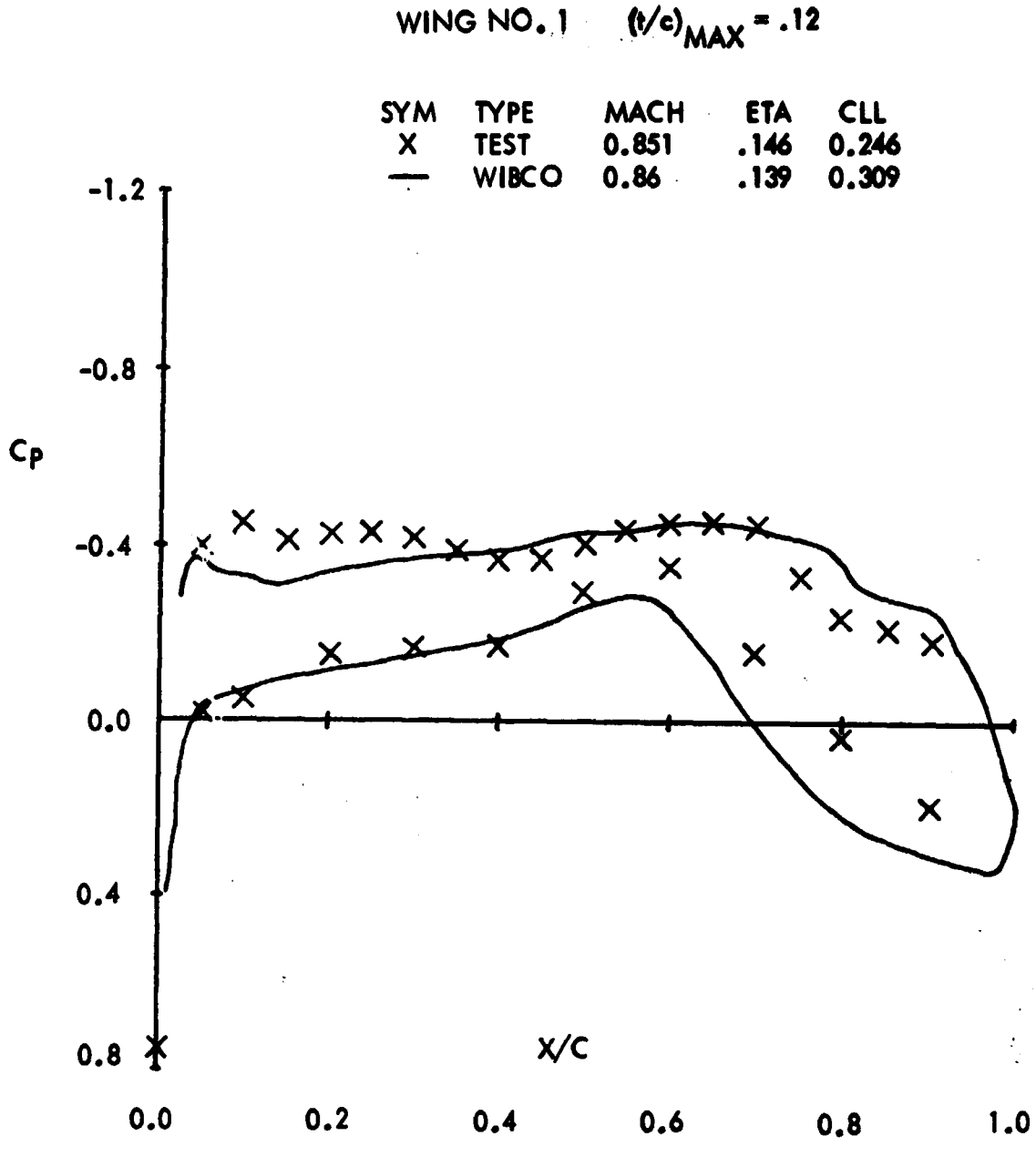

(A) ETA = 0.146

FIGURE 18. - COMPARISON OF WIBCO WING/BODY PRESSURES WITH EXPERIMENT

ALPHA = 4.68 C_L = .34

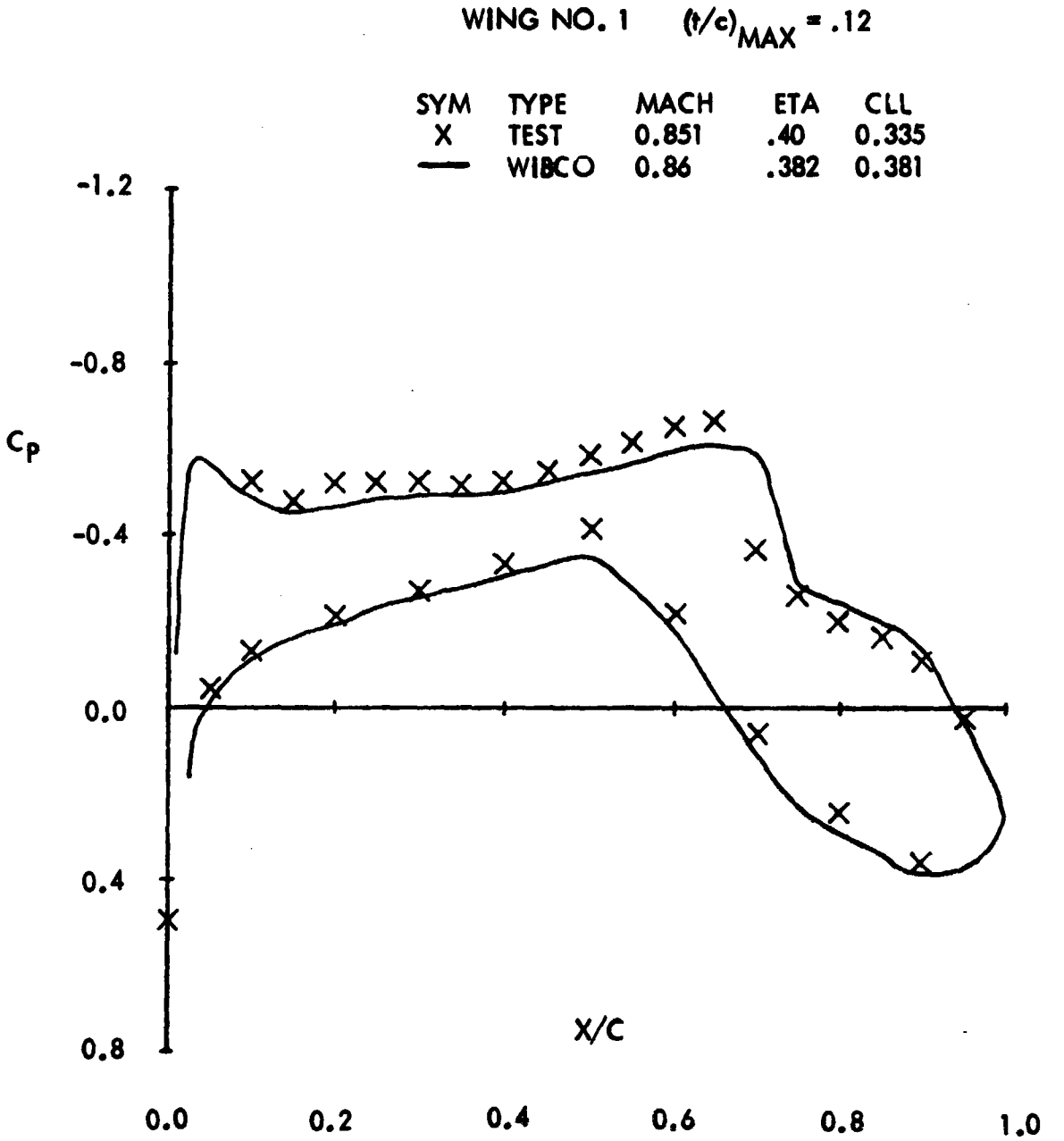

(B) ETA = 0.40

FIGURE 18. - CONTINUED

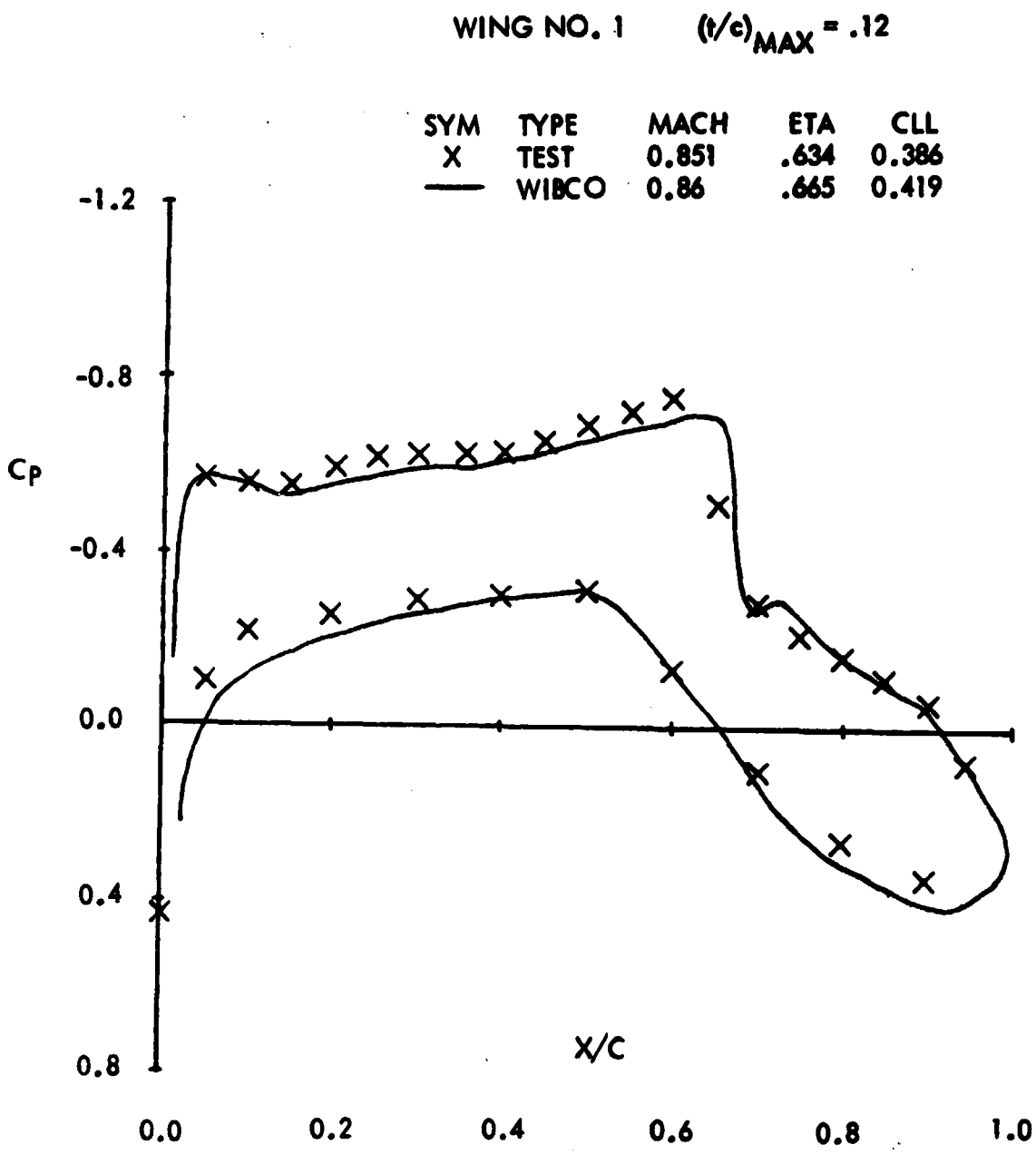

(C) ETA = 0.634

FIGURE 18. - CONTINUED

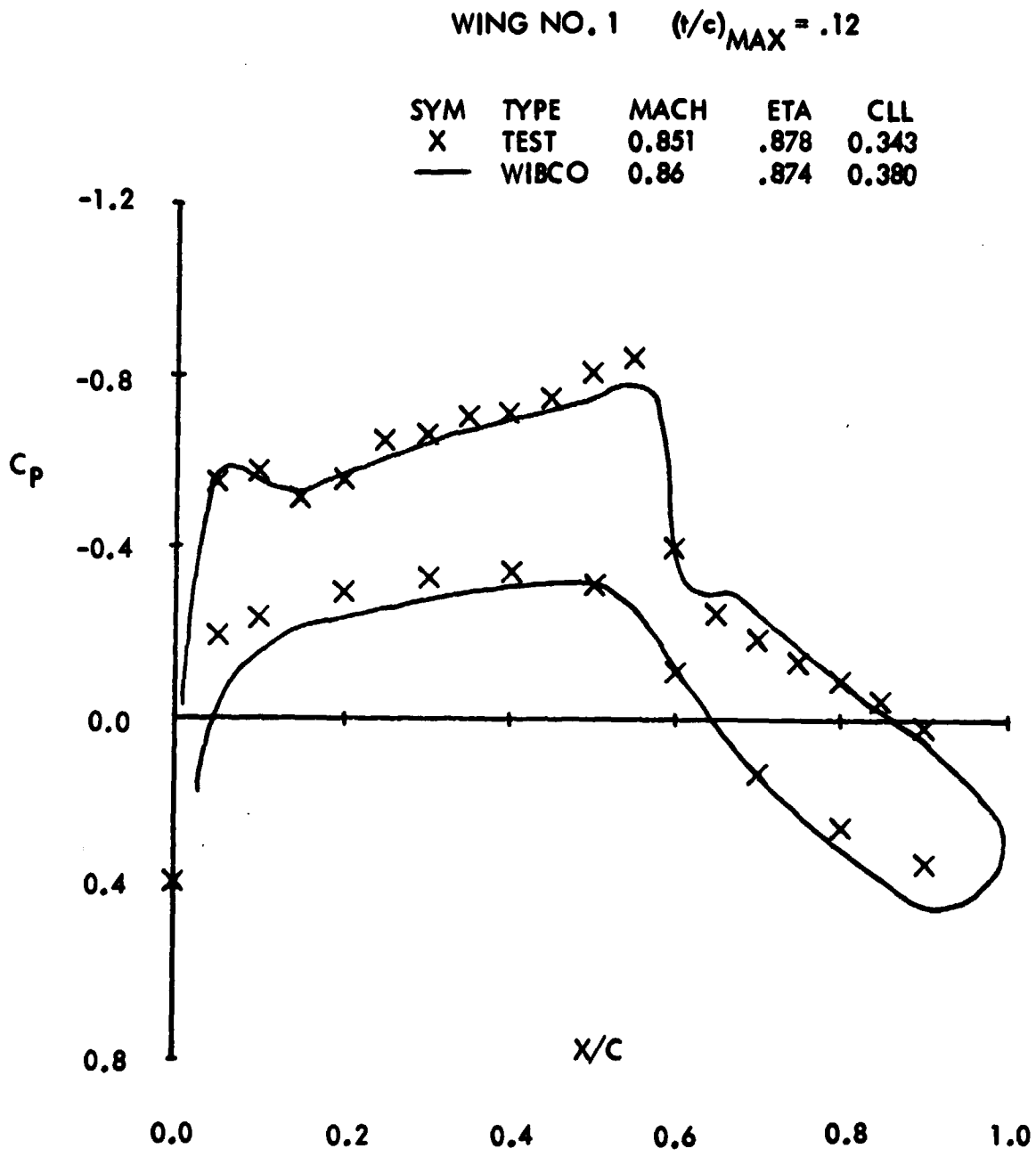

(D) ETA = 0.878

FIGURE 18. CONCLUDED

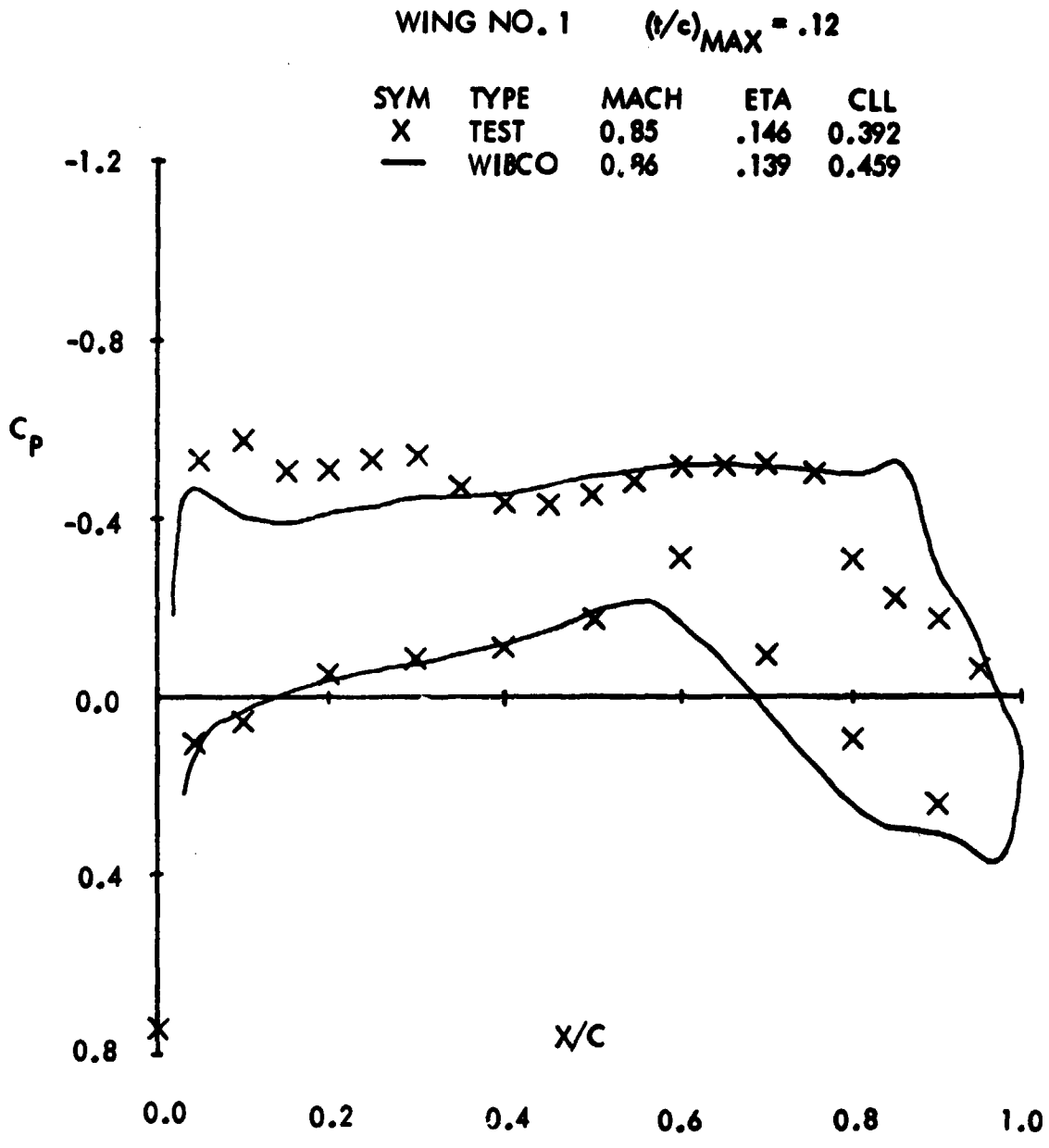

(A) ETA = 0.146

FIGURE 19. - COMPARISON OF WIBCO WING/BODY PRESSURES WITH EXPERIMENT

ALPHA = 6.52 C_L = .52

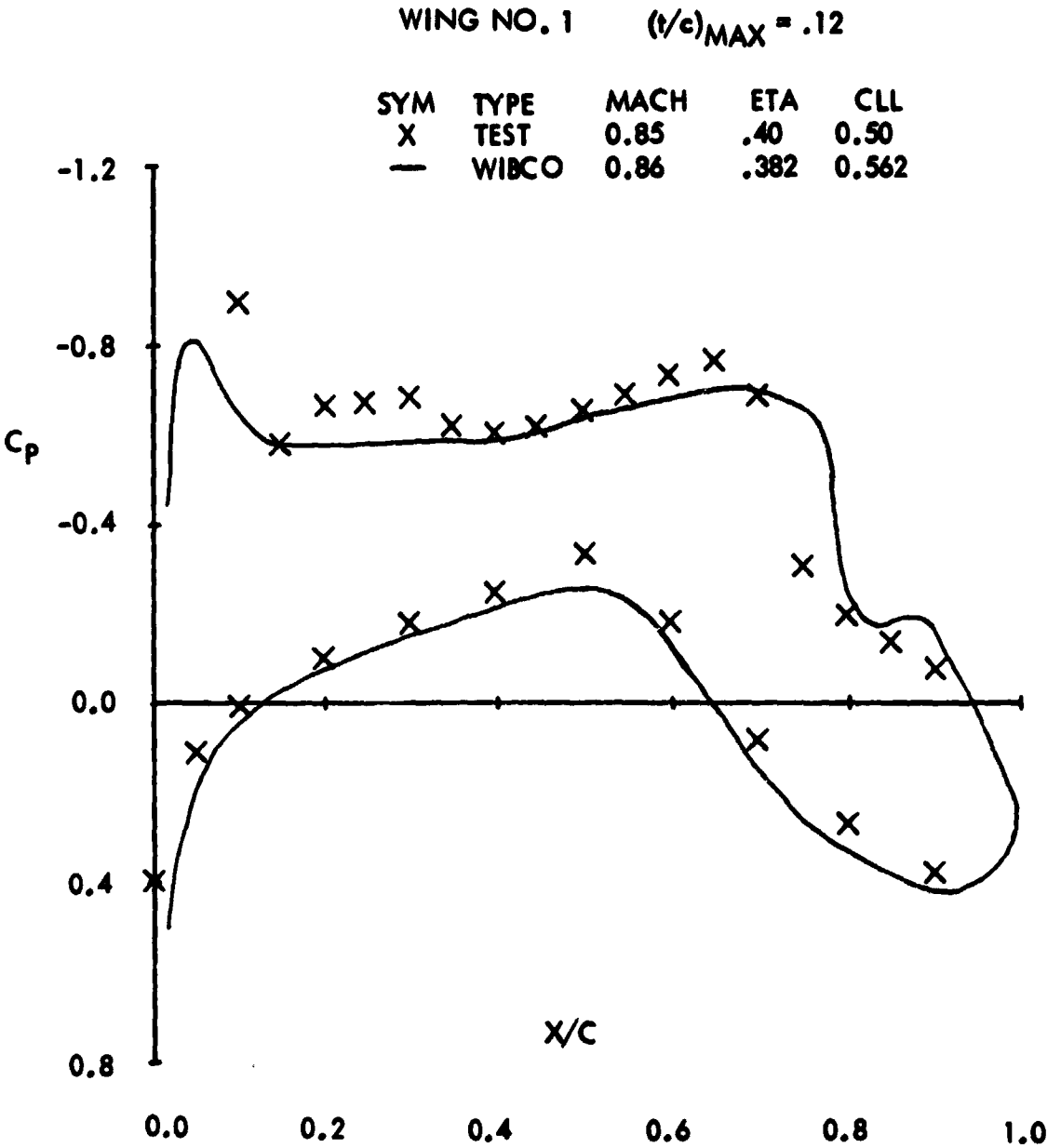

(B) ETA = 0.40

FIGURE 19. - CONTINUED

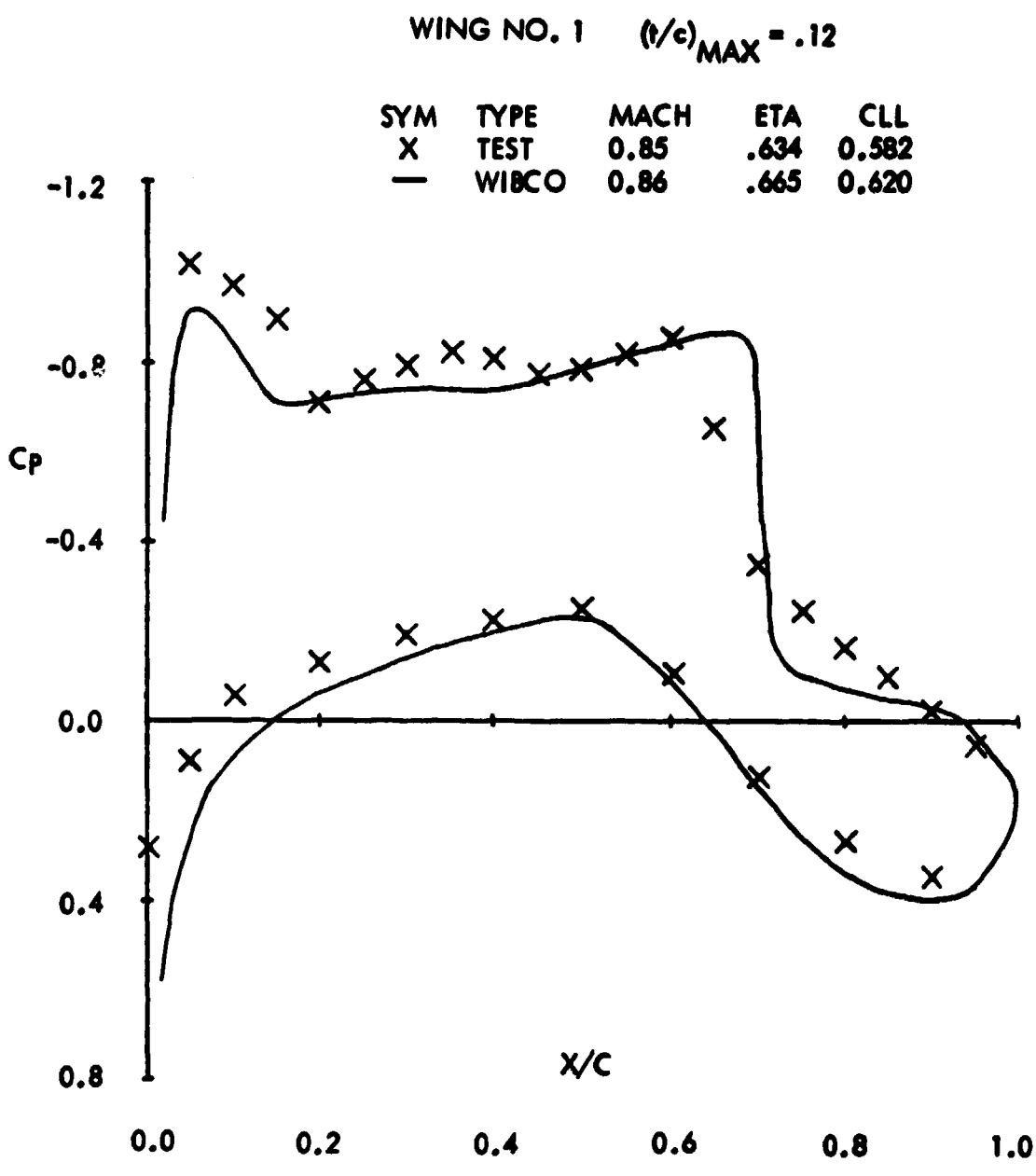

(C) ETA = 0.634

FIGURE 19. - CONTINUED

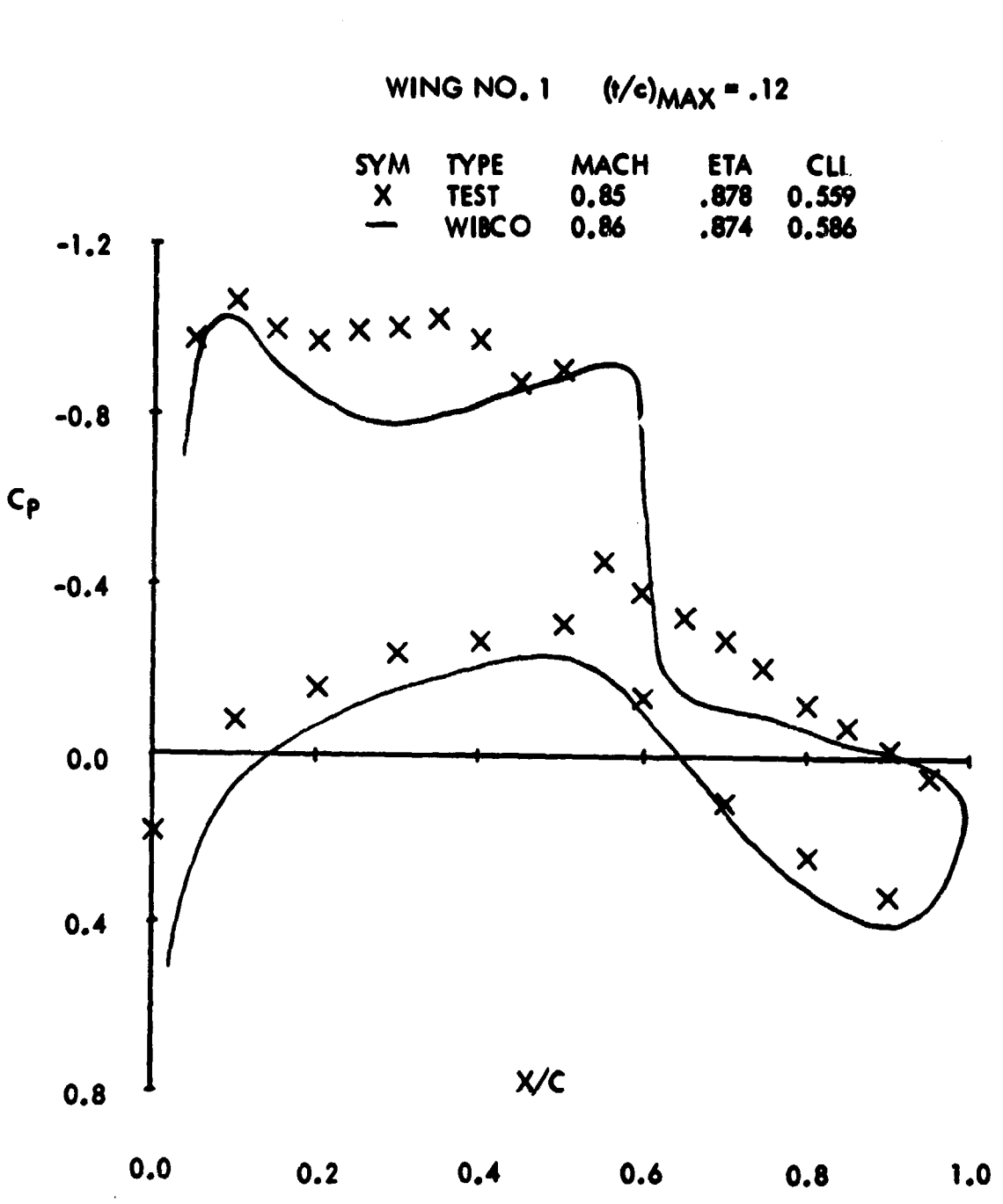

(D) ETA = 0.878

FIGURE 19. - CONCLUDED

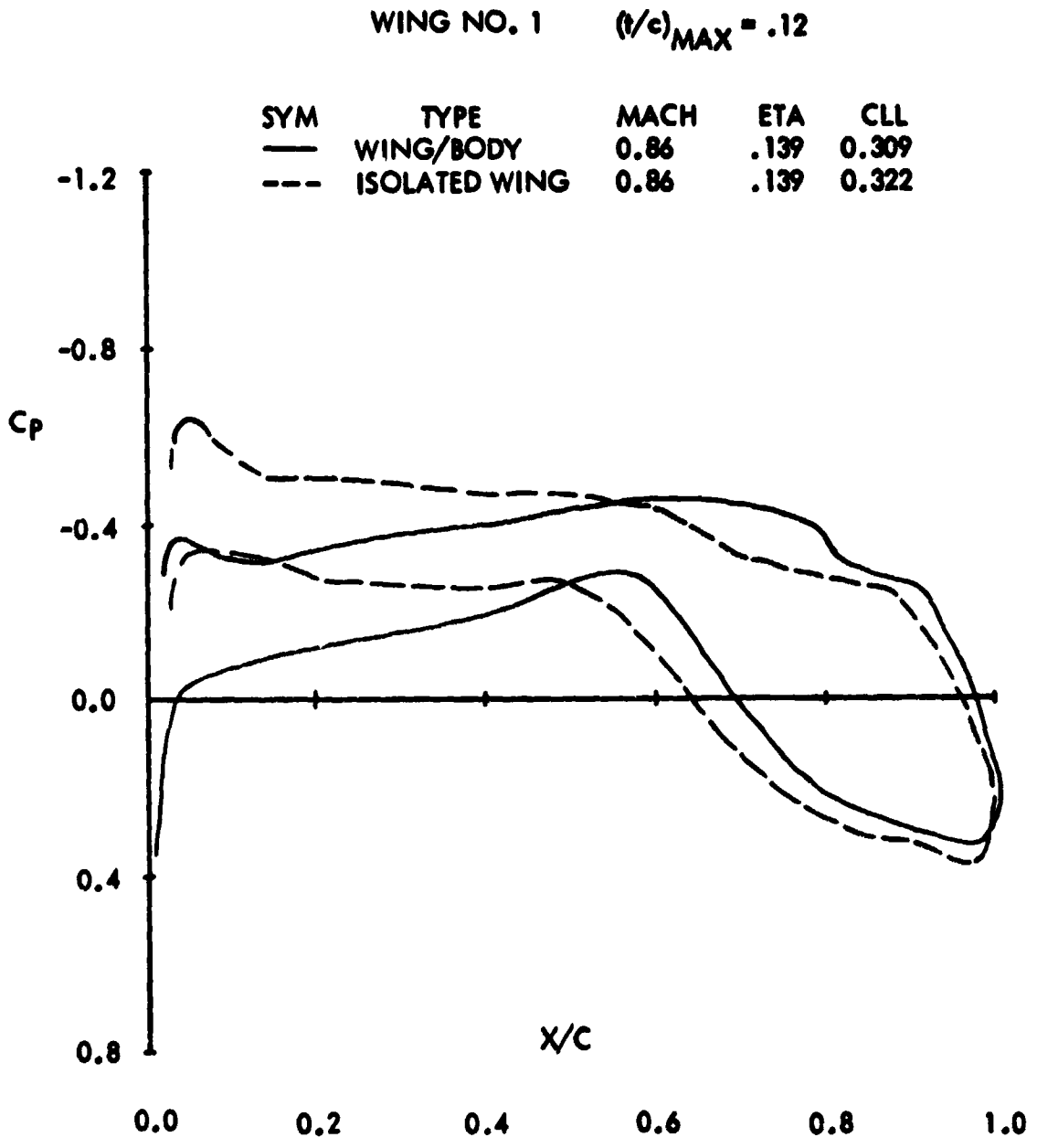

(A) ETA = 0.146

FIGURE 20. - COMPARISON OF WIBCO WING/BODY AND ISOLATED WING PRESSURES

ALPHA = 4.68

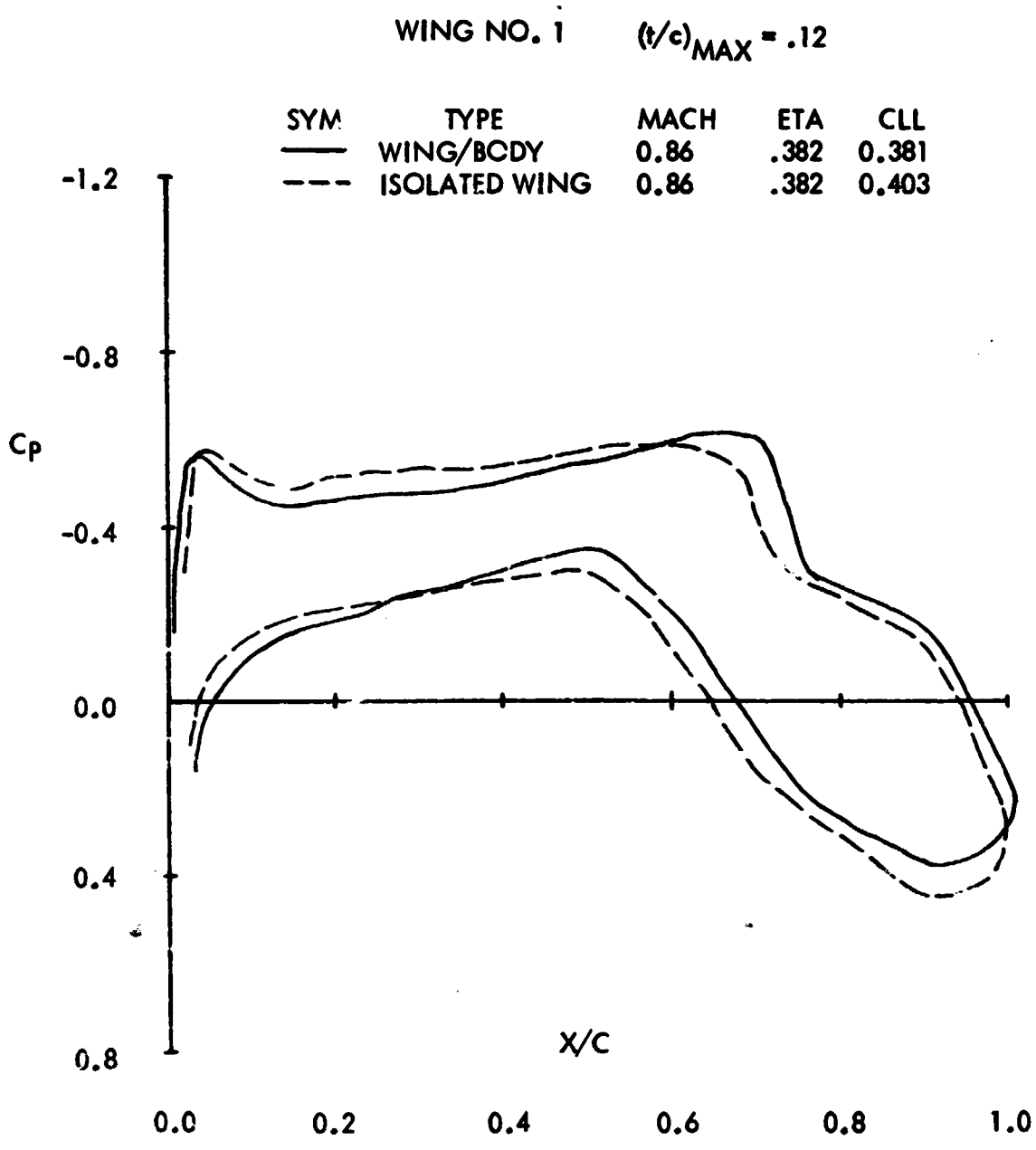

(B) ETA = 0.40

FIGURE 20. - CONTINUED

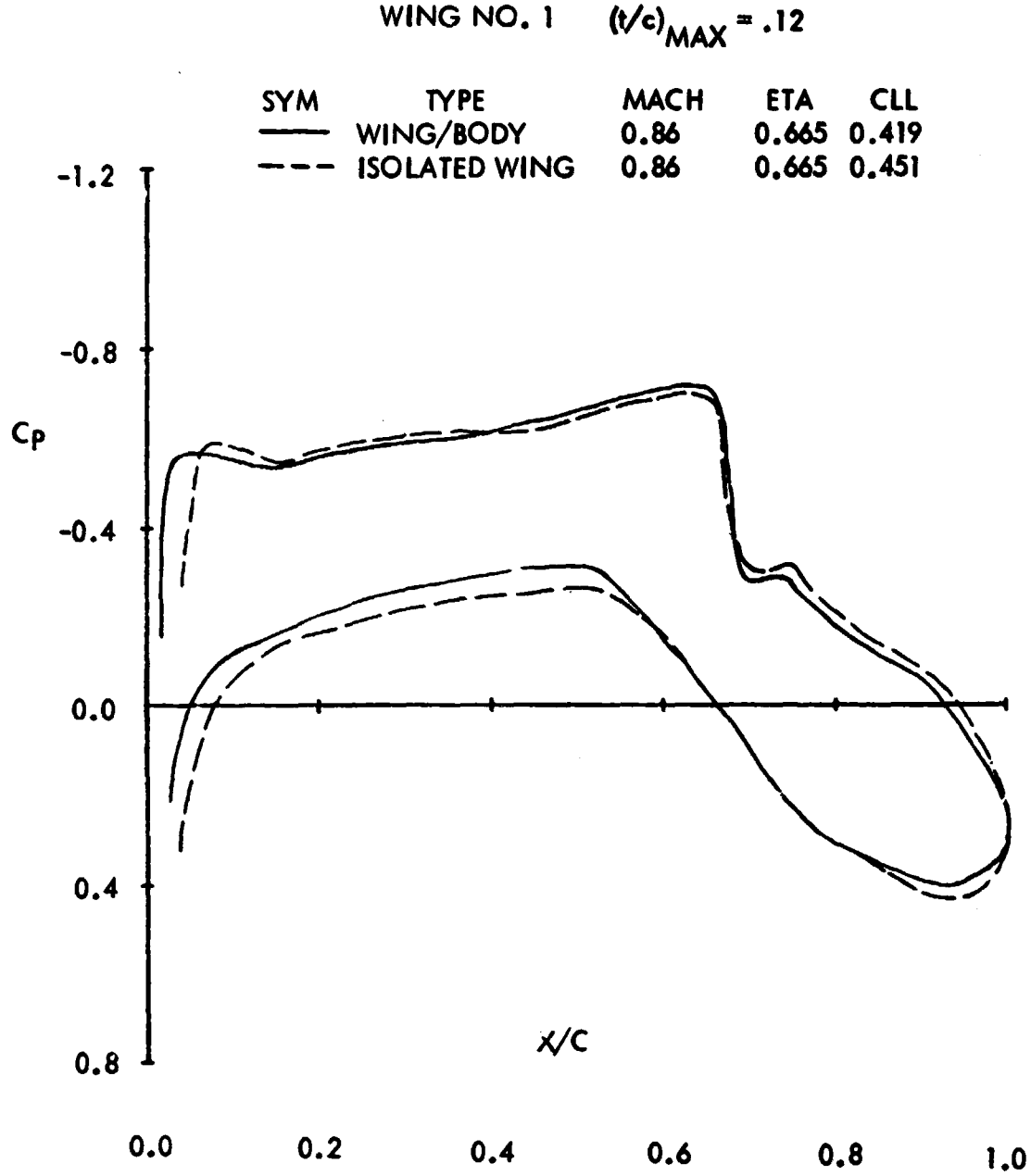

(C) ETA = 0.634

FIGURE 20. - CONTINUED

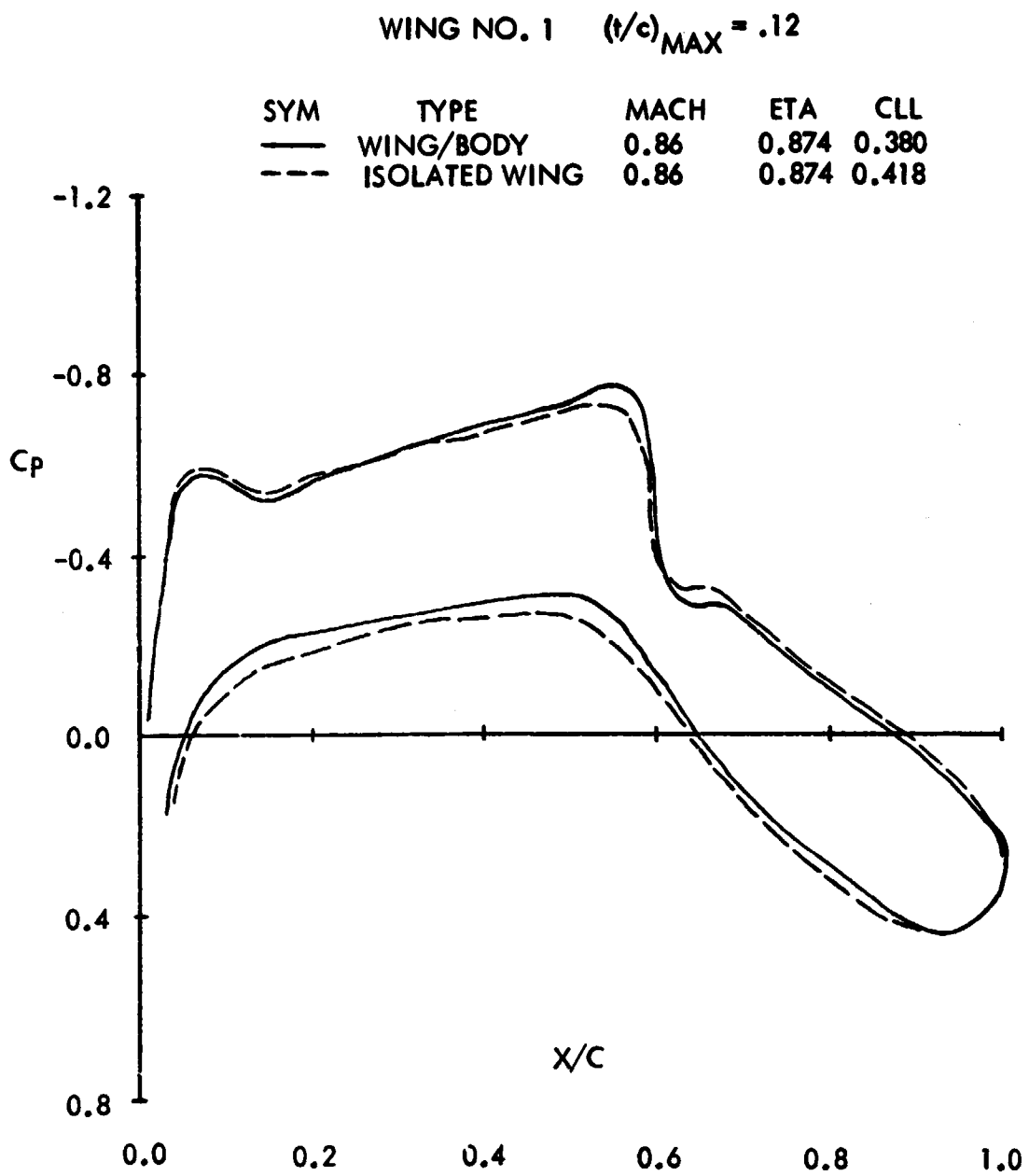

(D) ETA = 0.878

FIGURE 20. - CONCLUDED